



<https://theses.gla.ac.uk/>

Theses Digitisation:

<https://www.gla.ac.uk/myglasgow/research/enlighten/theses/digitisation/>

This is a digitised version of the original print thesis.

Copyright and moral rights for this work are retained by the author

A copy can be downloaded for personal non-commercial research or study, without prior permission or charge

This work cannot be reproduced or quoted extensively from without first obtaining permission in writing from the author

The content must not be changed in any way or sold commercially in any format or medium without the formal permission of the author

When referring to this work, full bibliographic details including the author, title, awarding institution and date of the thesis must be given

Enlighten: Theses

<https://theses.gla.ac.uk/>
research-enlighten@glasgow.ac.uk

SIMULATION OF RENDEZVOUS
OF A MAN IN DEEP SPACE

by .

Daniel Pablo Méndez

Thesis presented for the degree of
M.Sc. to the Faculty of Engineering

The University of Glasgow

Department of Aeronautics
and Fluid Mechanics

March 1971

Having then a large number of simulations with different initial conditions, and with simulated operators of a wide range of ability, we analyse the relations between the different variables affecting the process (i.e. specific variables of the manoeuvre such as initial distance of the operator from the target, acceleration provided by the thruster,... etc., and specific variables of the human operator such as his errors of observation, reaction time,...etc.). Likewise we study their influence on the process and check the results with the ones obtained in the analog simulation.

As far as this formalized treatment resembles human behaviour, we find that there is an optimum (in the sense of minimum fuel consumption) value of acceleration around 0.5 times the rendezvous distance per sec^{-2} . Besides, it seems that the human being is more handicapped by his implementation errors (in pointing the thruster) than by his visual observation errors.

ProQuest Number: 10647401

All rights reserved

INFORMATION TO ALL USERS

The quality of this reproduction is dependent upon the quality of the copy submitted.

In the unlikely event that the author did not send a complete manuscript and there are missing pages, these will be noted. Also, if material had to be removed, a note will indicate the deletion.



ProQuest 10647401

Published by ProQuest LLC (2017). Copyright of the Dissertation is held by the Author.

All rights reserved.

This work is protected against unauthorized copying under Title 17, United States Code
Microform Edition © ProQuest LLC.

ProQuest LLC.
789 East Eisenhower Parkway
P.O. Box 1346
Ann Arbor, MI 48106 – 1346

Daniel Pablo
Aeronautics & Fluid Mech. Dept.

Thesis presented for M.Sc. degree

SIMULATION OF RENDEZVOUS OF A MAN IN DEEP SPACE

SUMMARY

We study here the rendezvous of an isolated man in deep space with a predetermined target (say, his parent vehicle) with the purpose of determining the main factors which influence the process. We assume that he utilizes (effectively) monocular vision as the only mean of observation, and that he is equipped with some thruster which, when necessary, he can direct either along the line of sight or at right angles to it.

Two simulations, by analogue and digital computer, have been devised to study this manoeuvre. The analog computer is used to represent (on an oscilloscope screen) the appearance of the target and star background during the course of the manoeuvre. Its main purpose is to obtain an insight into such a manoeuvre and to observe the strategies and performance of a real human being in such a process.

The digital simulation consists of a program which formalises human behaviour in this rendezvous manoeuvre. We use it to provide a fast and ready method of obtaining a large number of simulations under different well defined circumstances.

Thesis
3537
Copy 2

ACKNOWLEDGEMENTS

The author is deeply grateful for the help, interest and encouragement of Professor T.R.F. Nonweiler of the Aeronautics and Fluid Mechanics Dept. of Glasgow University, and wishes to state how deeply he values the help and friendship received.

The author express his gratitude to Mr. P.H. Tanner for his suggestions.

This study was made possible through the sponsorship of the European Space Research Organization and Glasgow University. The author is very happy to acknowledge their generous support.

LIST OF CONTENTS

Symbols	iii
Summary.....	1
Statement of Problem.....	3
Previous Work.....	6
Procedure.....	8
PART I: Digital Simulation	
I.1. Introduction.....	13
I.2. Image Point Model.....	16
I.3. States and Decisions..	21
I.4. Decision Boundaries...	29
I.5. Reaction Time.....	35
I.6. Application of Thrust.	37
I.7 The Program.....	38
PART II: Analog Simulation	
II.1. Introduction.....	43
II.2. Target Trace.....	45
II.3. Star Field.....	48
II.4. Equations of Motion..	51
II.5. Control Voltages.....	53
II.6. Oscilloscope Display.	54
II.7 Presentation of Data..	58
PART III : Results.....	61
References.....	94
Appendix A: Analog Patch Panel and Simulation Records.....	95
Appendix B: General Image Point Motion	98
Appendix C: Digital Sample Size.....	101
Appendix D: Digital Program.....	103

SYMBOLS

The origin of coordinates will be the center of the parent vehicle, and in consequence all the variables are referred to this moving system. Unless otherwise specified, distances, velocities and accelerations are those of the operator with respect to the vehicle.

$B_{\dot{\theta}}$ = Upper boundary for $\dot{\theta}$ in the decision diagram.

$B_{\dot{\varphi}}$ = Upper boundary for $\dot{\varphi}$ in the decision diagram.

F_1 = Transverse thrust.

F_2 = Thrust to approach the target

F_3 = Thrust to recede from the target

R_o = Target apparent size voltage

V_e = Voltage needed to reach the edge of the oscilloscope screen.

a = Operator's acceleration provided by the thruster.

a_r = Radial acceleration

a_{θ} = Transverse acceleration

$b_{\dot{\theta}}$ = Lower boundary for $\dot{\theta}$ in the decision diagram

$b_{\dot{\varphi}}$ = Lower boundary for $\dot{\varphi}$ in the decision diagram

f_1 = Coefficient for radial control decision

f_2 = Coefficient for transverse control decision

- \underline{r} = Radius vector of the operator's position
 r_o = Rendezvous distance (Distance from the target
at which rendezvous is considered achieved)
 r_i = Modulus of the initial radius vector (initial
separation)
 r_m = minimum distance from the target to the corresponding
operator's free linear trajectory.

 t_o = Maximum reaction time of the operator
 t_f = Minimum thrust time (level of uncertainty of
thrust time)

 \underline{v} = Operator's vector velocity
 v_o = Rendezvous velocity (Maximum value allowed for
the radial and transverse components of the
operator's final velocity)

 \underline{v}_i = Operator's velocity at the beginning of the manoeuvre

 v_r = Radial component of operator's velocity
 v_θ = Transverse component of operator's velocity

 x_o = Generating voltage of the target appearance
 x_i = Star abscissa voltage

 y_o = Generating voltage of the target appearance
 y_i = Star ordinate voltage

- α_0 = Size of the vehicle
 β = Initial angle between operator's radius vector
and velocity
 φ = Solid angle subtended by the vehicle from the
operator's position
 θ = Angle between \underline{r} and the line of sight of any star
on the plane determined by \underline{r} and \underline{v}
 θ_0 = Rate threshold, in general
 θ_{ot} = Rate threshold in the frontal plane
 θ_{or} = Rate threshold in depth
 ρ = Relation (Total time employed in the manoeuvre to
time the impulse has been applied)
 σ = Standard deviation of the error (either visual ob-
servation or aiming)
 σ_1 = Standard deviation of the visual observation errors
 σ_2 = Standard deviation of the thrust aiming errors

SUMMARY

We study here the rendezvous of an isolated man in deep space with a predetermined target (say, his parent vehicle) with the purpose of determining the main factors which influence the process. We assume that he utilizes (effectively) monocular vision as the only mean of observation, and that he is equipped with some thruster which, when necessary ; he can direct either along the line of sight or at right angles to it.

Two simulations, by analogue and digital computer, have been devised to study this manoeuvre. The analog computer is used to represent (on an oscilloscope screen) the appearance of the target and star background during the course of the manoeuvre. Its main purpose is to obtain an insight into such a manoeuvre and to observe the strategies and performance of a real human being in such a process.

The digital simulation consists of a program which formalises human behaviour in this rendezvous manoeuvre. We use it to provide a fast and ready method of obtaining a large number of simulations under different well defined circumstances.

Having then a large number of simulations with different initial conditions, and with simulated operators of a wide range of ability, we analyse the relations between the different variables affecting the process (i.e. specific variables of the manoeuvre such as initial distance of the operator from the target, acceleration provided by the thruster,... etc., and specific variables of the human operator such as his errors of observation, reaction time,...etc.). Likewise we study their influence on the process and check the results with the ones obtained in the analog simulation.

As far as this formalized treatment resembles human behaviour, we find that there is an optimum (in the sense of minimum fuel consumption) value of acceleration around 0.5 times the rendezvous distance per sec^{-2} . Besides, it seems that the human being is more handicapped by his implementation errors (in pointing the thruster) than by his visual observation errors.

STATEMENT OF PROBLEM

The rendezvous of an isolated human being in deep space with a determined target (for instance his parent vehicle), will be of prime importance in many future space missions, such as the assembling of space stations.

Therefore is highly desirable to study the ability of a human operator to carry out such a task with the minimum amount of equipment (i.e. only a small thrust booster).

We presume that the operator is able to perform the manoeuvre with the aid of (effectively) monocular vision as his only source of information; no automatic means of observation or control are supposed to be employed.

The best way to provide a reliable knowledge of this rendezvous process is by simulation. A complete simulation of the manoeuvre would be desirable as a training aid, but clearly this is an aim beyond the bounds of the present investigation; it would also involve a study of the possible inter-relations between the diverse variables affecting the process and their separate influence on it; and this is our aim here.

These variables could be subdivided into:

- a) Specific variables of the manoeuvre, such as,
 - Initial distance of the operator from the target.
 - Initial velocity of the operator relative to the target.
 - Initial angle of this velocity vector with the line of sight.
 - Acceleration provided by the thruster.
 - Size of the target.
 - Rendezvous distance.
 - Rendezvous velocity limit.

- b) Specific variables of the human operator, such as,
 - Minimum observable rates of angular velocity of the target against the star background and its apparent rate of increase in size (called here the angular discrimination thresholds -transverse and radial- of human vision).
 - Standard deviation of the errors of visual observation of these angular rates.
 - Standard deviation of the errors of implementation (i.e. of directing the thruster unit -the thrust being assumed constant-).
 - Maximum reaction time of the operator (by convention taken to include observation, decision, alignment of thruster and thrust initiation).

As a particular aim of such a study, we may endeavour to discover if there is an optimum value of booster thrust (acceleration) which minimises the propellant consumption. Additionally, of course, there is the general problem of "optimizing" the strategy, or decision process, of the operator in the rendezvous manoeuvre.

PREVIOUS WORK

Before proceeding we shall very briefly refer to accounts of the "state of the art" in the large national space programs, in so far as these bear on our problem.

There are some simulation studies of the capability of the human being for extravehicular tasks in weightless condition (refs. 4 and 6).

In the Gemini project, there were used Neutral-Buoyancy Simulation Techniques, Air-Bearing Training Equipment and an Inertia Coupling Training-Air Model, for understanding manned extravehicular operations in space (refs. 2,5 and 8).

The preparation for Gemini IX extravehicular activity included a 6-degree of freedom simulator (Manned Aerospace Flight Simulator) useful at target distances below 250 feet. It was used for training with the AMU (Astronaut Manoeuvring Unit) (refs. 2 and 3). Other Gemini Simulations used a small thruster (Hand Held Manoeuvring Unit--HHMU-) (refs. 2 and 3).

These studies seem to have been very useful in training operators for accomplishing extravehicular activity tasks.

Extravehicular capabilities of the human being were demonstrated in the course of several spatial missions,

and the HHMU was evaluated briefly, but successfully, on two different Gemini missions (ref.2)

Most of this work has been directed towards evaluating the performance of a tethered human being in performing tasks in the close proximity of his parent vehicle. It has been very valuable in determining the many difficulties and limitations presented by the problem. However, none of this work has involved large translations, and therefore it is of little direct relevance to our study.

PROCEDURE

A simulator is more acceptable the more it resembles the true conditions, but unfortunately it is then also more expensive.

We have been contend to use the relatively simple resources of digital and analogue computers as simulators. The analog computer is used to represent, on an oscilloscope screen, a rough approximation to the visual impression of the rendezvous manoeuvre. The digital computation seeks to formalize the reactions of the human operator during the process and to output the measures of performance, with the intention of enlarging and completing the information from the analog simulation.

Despite the inherent simplification of the problem, the analog simulation is used to acquire a first and direct acquaintance with the most important characteristics of the process, and to obtain a better knowledge of the strategy utilized by the man in this manoeuvre (this knowledge has been applied in programing the digital simulator). The analog simulator serves, as well, as a checking model for particular cases of the digital program. Ultimately it could be used as a very simple training device.

The digital simulator program is a fast and cheap way for obtaining a large number of simulations under very different assumed conditions and with many sorts of simulated "human

operators".

Undoubtedly, the human behaviour is very difficult to simulate. Among the many possible and useful models which could be built up, we have developed one which consists schematically of a sequence of calculation of the variables the man is observing (which are "humanized" by introducing some error), and of application of the subsequent human control action. This sequence of "cause" and "effect" is essentially the one that a human being would follow in such a process. The main difficulty arises when we try to establish which particular action (and what duration of it) corresponds to each combination of the observable variables. Therefore the program has, certainly, the weak points of every simple program trying to simulate reactions of a human being, i.e. the lack of the extensive range of strategies that every man may employ and the absence of a learning process in its widest sense.

Further, in our particular case, one knows little of the effect of weightlessness on human behaviour, with respect to the coordination of motion and attitude.

No doubt, the model we have devised in this digital simulation could be improved substantially. However, several models of the decision process have been tried, and the one which we shall detail here seems to be the most satisfactory.

The method used in obtaining results from this digital program consists on running simulations under different initial data parameters, i.e. the specific parameters of the manoeuvre, and these of the human operator. Each particular simulation is repeated several times for statistical purposes. After these repeated runs, the program will output some average data of the simulation (such as the total time employed in the manoeuvre, and impulse consumption), and the standard deviations of these data .

The structure of the results was checked, when possible, by means of the analog simulator. Nevertheless, a wider dispersion of the analog results must be expected because the analog simulation implies a real human operator. He will be continuously changing his strategy whereas, in the digital simulation the dispersion of the results is due entirely to the effect of the simulated human errors, but not to the changes of strategy.

In both simulations, analog and digital, we have assumed that the applied thrust during the manoeuvre, is directed either along the line of sight (so as to cause the operator to approach or to recede from the target), or at right angles of it.

We assume only two degrees of freedom in the analog simulation (translations in a plane) and three degrees of freedom in the digital simulation (translations in space).

As a consequence, the equations of motion (polar coordinates) in the analog simulation are reduced to

$$\begin{aligned}a_r &= \ddot{r} - r\dot{\theta}^2 \\ a_\theta &= r\ddot{\theta} + 2\dot{r}\dot{\theta}\end{aligned}$$

In the digital simulation we use cartesian coordinates.

In both cases no field of force exists and the only acceleration is the one provided by the thruster.

The two methods of simulation are described in detail in separate parts of this work, and finally the results obtained are discussed in a separate section.

Part I. DIGITAL SIMULATION

- I.1. Introduction
- I.2. Image Point Model
- I.3. States and Decisions
- I.4. Decision Boundaries
- I.5. Reaction Time
- I.6. Application of Thrust
- I.7. The Program

I.1. INTRODUCTION

The simulation consists of a program designed to calculate the position and attitude of the man with respect to the target vehicle.

The man is supposed to observe (by means effectively of monocular vision) the following quantities:

ψ = solid angle subtended by the vehicle.

$-\dot{\theta}$ = apparent angular velocity of the parent vehicle against the star background.

From these, he infers a value of $\dot{\psi}$, and his angular velocity about the vehicle ($+\dot{\theta}$).

According to the particular combination of values of these variables, in effect he may take action in one of the following ways: he may

- apply a transverse thrust, that is a thrust directed towards $-v_{\theta}$, so as to reduce $\dot{\theta}$, or
- apply a radial thrust either to approach or to move away from the vehicle (in other words, to control $\dot{\psi}$), or
- he may wait.

The process is finished by reaching the rendezvous conditions ($|r| \leq r_0$ and $|v| \leq v_0$) or upon exceeding a specified maximum time.

Two sources of error are introduced (to simulate "human error"):

--- errors of observation: The simulation does not operate with the true values of Ψ , $\dot{\Psi}$ and $\dot{\Theta}$, but with randomised values selected to have a gaussian distribution whose mean value is the true value, and whose standard deviation is a parameter adjusted by program data.

---- errors of implementation: It is assumed that the man applies the thrust with some randomised error in direction, normally distributed. Its most probable value is taken to be the true direction. (The precise method of applying the error is discussed later).

Trying to develop a program which displays a close resemblance to human response suggest something like the block diagram of fig. I-1.

There is a period of time occupied by each decision which the man takes. This time could be subdivided into two parts: one dealing with the time spent in observation and decision, and the other spent in preparing for the appropriate action (i.e. to apply a thrust). Because of this passage of time, the position and attitude of the man with respect to the vehicle must be updated. The decision must depend only on the observed current values of the variables Ψ , $\dot{\Psi}$ and $\dot{\Theta}$. This suggests that

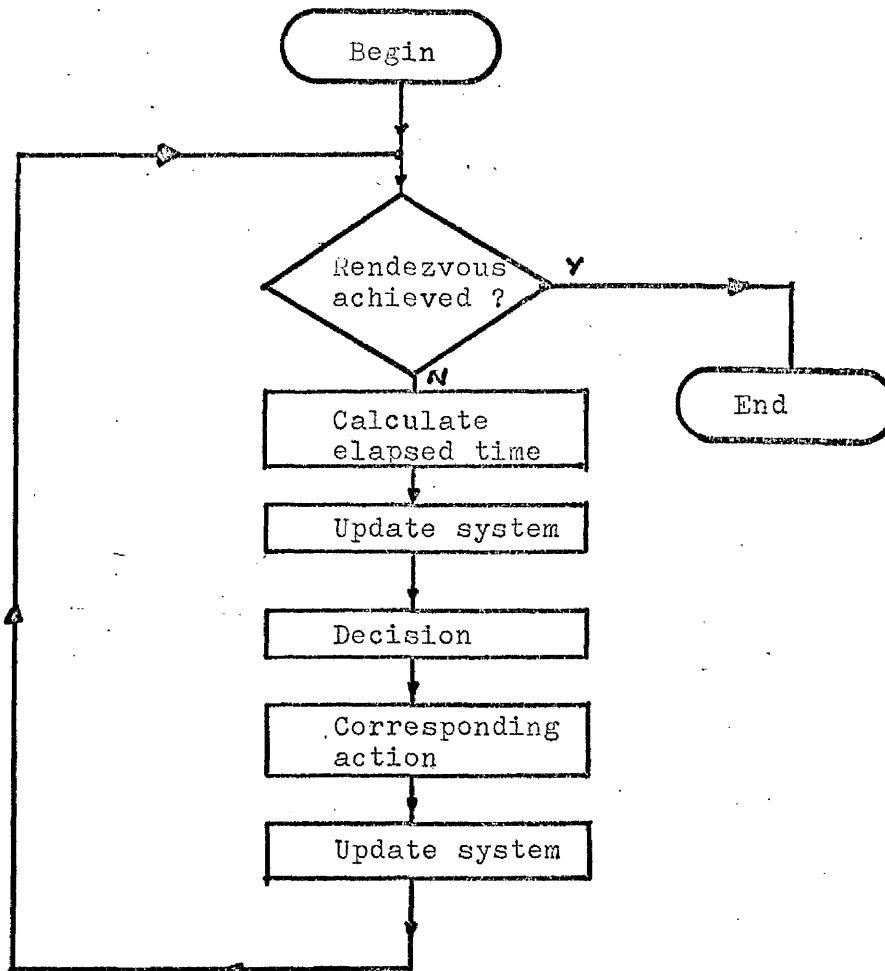


Fig. I-1. First approach simulation flow-chart.

it would be useful to study the problem in terms of the coordinates of a point represented by the values of φ , $\dot{\varphi}$ and $\dot{\theta}$ and to study what decision corresponds to every position of this so called "image point".

I.2. IMAGE POINT MODEL

We suppose that what the man is doing is to provide a mean of control so that:

- $\dot{\psi}$ is not too big. Otherwise the approach would be too quick.
- $\dot{\psi} > 0$, so that he does not recede from the vehicle.
- $|\dot{\theta}|$ is kept within reasonable bounds.

We interpret this as implying that the process of human control will seek to keep the "image point" within a volume close to the ψ axis (in the "phase-space" given by $\psi, \dot{\psi}, \dot{\theta}$). The cross-sectional dimensions of this volume can be expected to increase with ψ .

A successful rendezvous will be achieved only if the image point passes through a rectangular "window" ABCD (see fig. I.2.), whose corners have the coordinates:

	$\dot{\psi}$	$\dot{\theta}$	ψ
A	0	0	α_0/r_0
B	0	v_0/r_0	α_0/r_0
D	$\alpha_0 v_0/r_0^2$	0	α_0/r_0

as $v \leq v_0$ at $r \leq r_0$.

Here α_0 represents vehicle size, r_0 is the rendezvous distance, and v_0 is the limiting approach speed at rendezvous.

In order to try to appreciate the problems involved, let us consider some examples of the motion in terms of that of the image point.

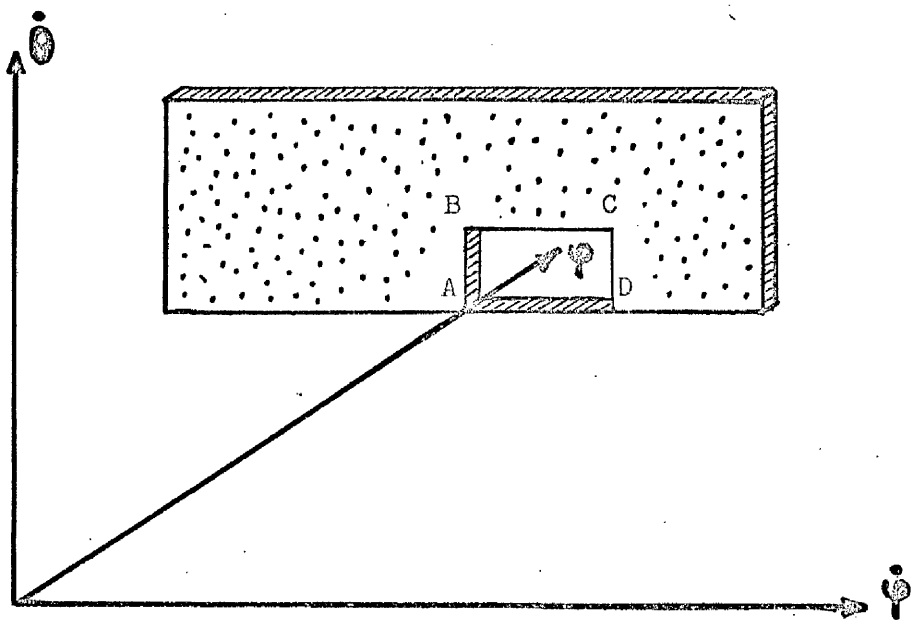


Fig. I-2. Rendezvous window.

I.2.1. Motion of the image point

a) Radial motion at constant speed.

If the transverse component of the velocity is zero, then

$$\dot{\theta} = 0 \quad (1)$$

and consequently

$$\dot{\psi} = - \frac{\alpha_0}{r^2} K \quad (2)$$

Since $\psi = \alpha_0 / r$, we obtain

$$\dot{\psi} = \frac{K}{\alpha_0} \psi^2 \quad (3)$$

The equations (1) and (3) show that in this circumstance the motion of the image point is in the plane $\dot{\theta} = 0$ and follows a parabola of the family indicated by (3). The image point moves in the direction of increasing ψ if the man is approaching the vehicle, and to decreasing ψ in the opposite case. (See fig. I.3).

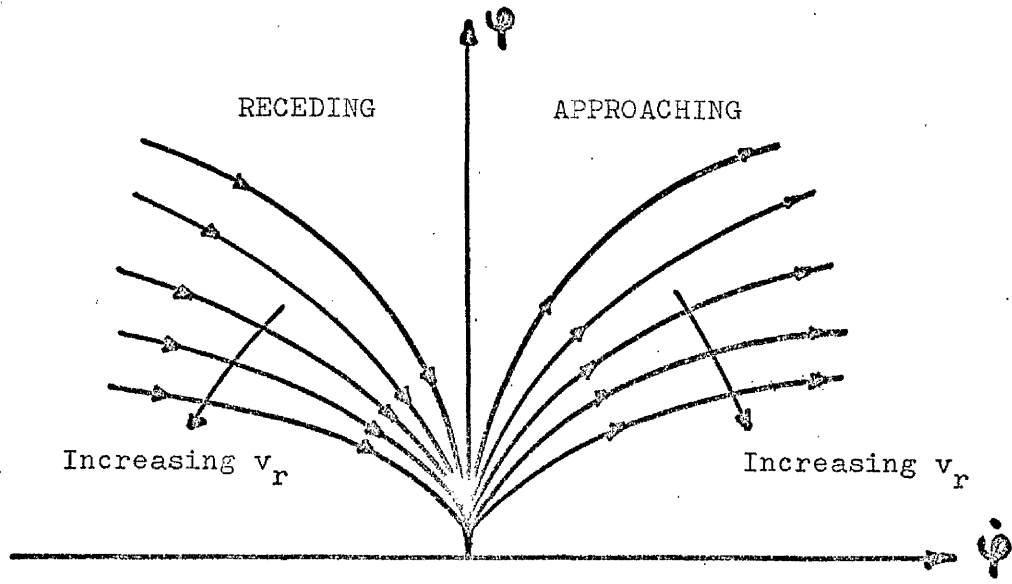


Fig. I.3. Motion of the image point. Constant radial speed

b) General motion at constant velocity

Let the man have a velocity v and move without applying any force, and let us call the perpendicular distance between the velocity vector and the vehicle r_m .

Since

$$v_r = v \sqrt{1 - \frac{r_m^2}{r^2}}$$

is

$$\dot{\psi} = \pm \frac{\alpha_0}{2} v \sqrt{1 - \frac{r_m^2}{r^2}} \quad (4)$$

The plus sign denoting approach, and the minus sign recession from the vehicle.

Eliminating r by expressing it as a function of ψ (i.e. $r = \alpha_0 / \psi$) and calling

$$\varphi_m = \frac{\alpha_0}{r_m}$$

we find the relation

$$\dot{\psi} = \frac{v}{\alpha_0} \psi^2 \sqrt{1 - (\psi / \varphi_m)^2} \quad (5)$$

$\dot{\varphi}$ reaches a maximum for

$$\varphi = \varphi_m \cdot \sqrt{2/3} = 0.8164 \varphi_m \quad (6)$$

and the value of this maximum is

$$\dot{\varphi}_{\max.} = \frac{2v}{3\sqrt{3}\alpha_0} \cdot \varphi_m^2 = 0.3849 \varphi_m^2 \cdot \frac{v}{\alpha_0} \quad (7)$$

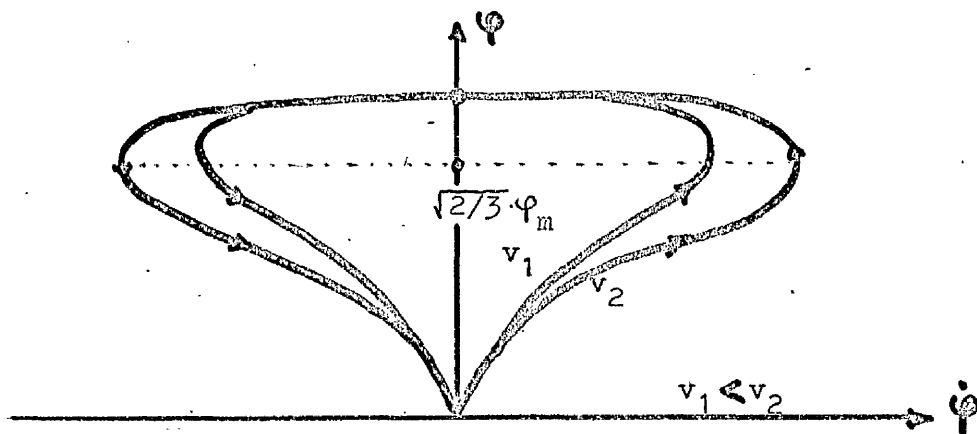


Fig. I.4. Motion of the image point on the plane $\dot{\theta}=0$. Constant speed

The projection of the image point on the plane $\dot{\theta} = 0$ follows a path like the represented on fig. I.4.

Under the same conditions, since

$$v_{\theta} = v \frac{r_m}{r}$$

we have

$$\dot{\theta} = \frac{v}{\alpha_0 \varphi_m} \varphi^2 \quad (8)$$

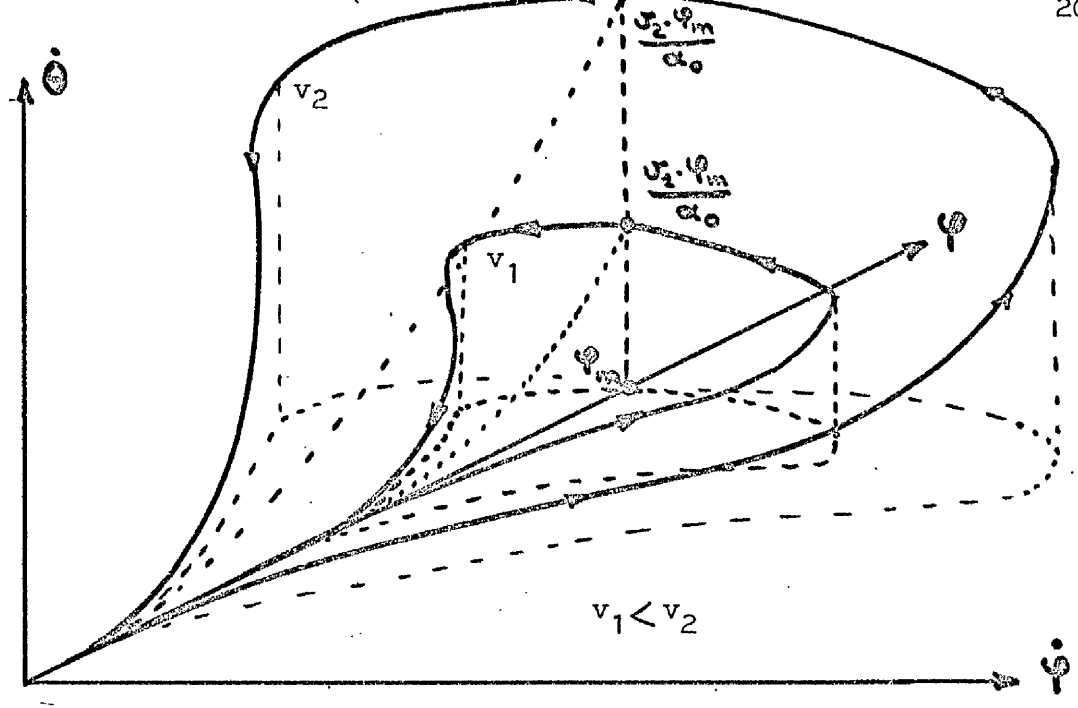


Fig. I.5. Tridimensional motion of the image point.

Eq. (8) indicates that the motion of the image point on the plane $\dot{\phi} = 0$ is a parabola, and fig. I.5. show the tridimensional nature of the motion.

I.3. STATES AND DECISIONS

For every value of the radial distance to the target vehicle r , that is for every value of Ψ , we shall now try to construct plausible decision-making process, which we can interpret by means of a diagram in the phase-space $(\dot{\theta}, \dot{\Psi})$, so as to indicate the action to be taken in order to keep control of the process and lead ultimately to a successful rendezvous.

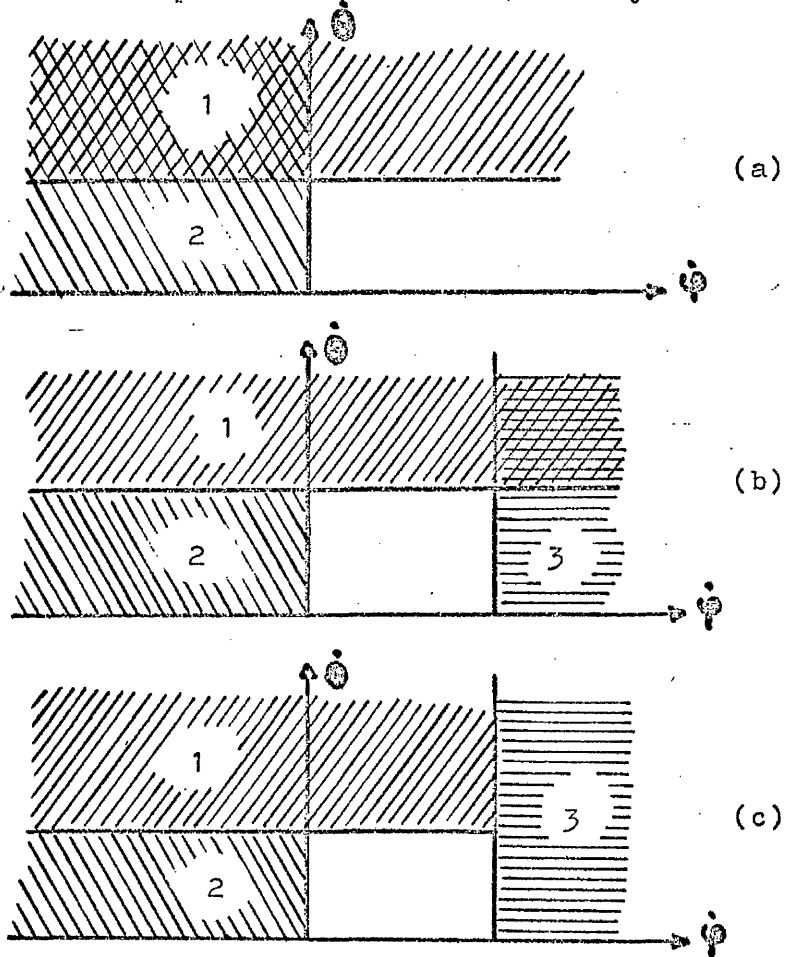


Fig. I.6. Fundamental actions.

If the image point lies in area 1 of fig. I.6.a, the value of $\dot{\theta}$ (i.e. the value of the transverse velocity) is greater than certain limit (this value will be specified later on). In that condition it will be appropriate to reduce the transverse component of the velocity by applying a transversal thrust.

If the point image lies in area 2 the value of $\dot{\psi}$ is less than zero which means that the apparent size of the vehicle is getting smaller, and consequently the man is moving away from it. Therefore it is necessary for him to apply a radial thrust towards the vehicle.

Note that area 1 overlaps area 2 in the half plane $\dot{\psi} < 0$. However, the analogue simulation, shows that in this region of overlap a human operator will generally prefer to apply transverse, rather than radial, thrust, and consequently we limit area 2 to bounded values of $\dot{\theta}$ outside the area 1, (see fig. I.6. b).

Area 3 (fig. I.6.b) corresponds to a large positive value of $\dot{\psi}$, implying that the approach is too rapid, with the inherent danger of loss of control or even crash. This area 3 again overlaps area 1, and as it represents a situation of possible danger which must be avoided at all costs, a human operator will prefer to remedy the situation by applying a radial, rather than a transverse, thrust. (Fig. I.6.c.)

We shall now try to show that if the reaction of the human being is quick enough, and the minimum impulse (a.t_f) is below

a certain limit, then the decision diagram of the figure will lead to successful rendezvous.

Calling

F_1 the transverse thrust,

F_2 the thrust towards $-r$,

F_3 the thrust towards $+r$,

and assuming that they are applied instantaneously and directed without error,

F_1 must decrease $\dot{\theta}$,

F_2 must increase $\dot{\psi}$,

F_3 must decrease $\dot{\psi}$,

and the motion of the image point on the plane $\varphi = \text{constant}$, after applying the respective thrust, will follow the direction of the arrows in fig. I.7.

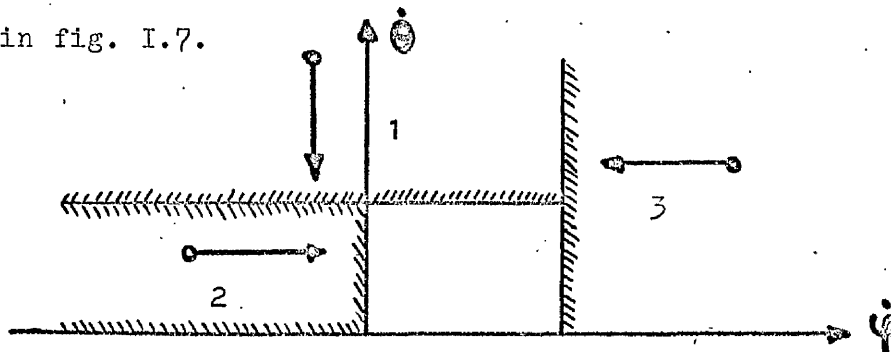


Fig. I.7. Initial direction of the image point movement by effect of the thrust.

In fact, the initial motion of the image point (see Appendix) can be determined by a study of the Taylor's first term for $\dot{\psi}$ and $\dot{\theta}$

$$\Delta \dot{\psi}_0 \approx \ddot{\psi}_0 \Delta t \quad (10)$$

$$\Delta \dot{\theta}_0 \approx \ddot{\theta}_0 \Delta t \quad (11)$$

Since $a_r = \ddot{r} - \theta^2 r \quad (12)$

$$a_\theta = r\ddot{\theta} + 2\dot{r}\dot{\theta} \quad (13)$$

expressing r and its derivatives as a function of ψ , we obtain

$$\Delta \dot{\psi}_0 \approx \left(\frac{2\dot{\psi}_0^2}{\dot{\psi}_0} - \dot{\psi}_0 \dot{\theta}_0^2 - a_r \frac{\psi_0^2}{\dot{\psi}_0} \right) \Delta t \quad (14)$$

$$\Delta \dot{\theta}_0 \approx \left(\frac{2\dot{\psi}_0 \dot{\theta}_0}{\dot{\psi}_0} + \frac{\psi_0}{\dot{\psi}_0} a_\theta \right) \Delta t \quad (15)$$

If $a_r = a_\theta = 0$, the remainder terms would detail the motion of the image point for operator's constant velocity (comprobate in fig.I.5.). A thrust applied according to the position of the image point on the phase-space decision diagram, would imply the displacements sketched in fig.I.8

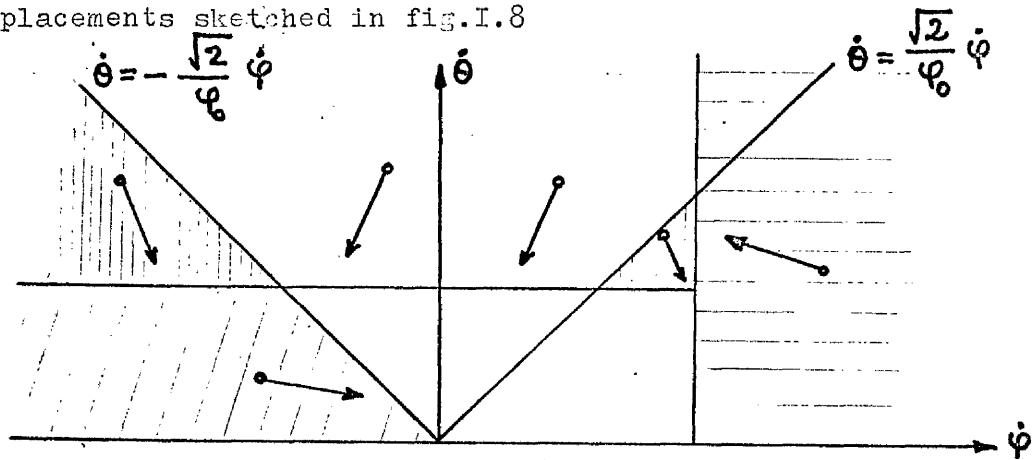


Fig.I.8. Effect of the thrust

We observe from fig. I.8. that whatever the initial position of the image point, the corresponding sequence of actions would ultimately cause the man to approach the vehicle.

In a real situation, we can expect there to be two further regions, 4 and 5, as shown in fig I.9., because if the point image lies persistently in one of these areas the human being

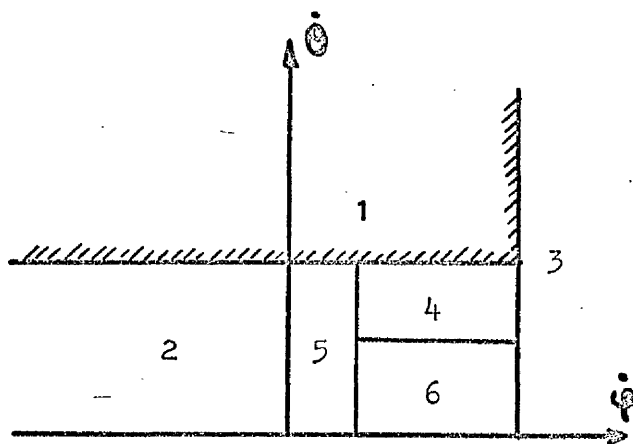


Fig.I.9. Decision diagram

would try to improve the control of the process, as there is nothing else urgent to do.

Area 5 corresponds to a very slow approach ($\dot{\psi}$ small and positive). A persistence in this area would be followed by a thrust towards the vehicle.

A situation in area 4 implies that the transverse component

of the velocity is still quite high although within reasonable bounds. A transverse thrust would be useful if the image point stays long within this area.

Area 5 has precedence over 4 because, if the model is to be realistic it must avoid the possibilities of oscillations or loops. These would happen if after applying an action (i.e. a thrust) the free motion of the image point reproduced the initial conditions. Of course this situation depends largely on the reaction

time of the operator and the minimum duration of the thrust, among other parameters. Nevertheless there can be discovered some possibilities of oscillation:

Let us assume that we take as decision diagram the one

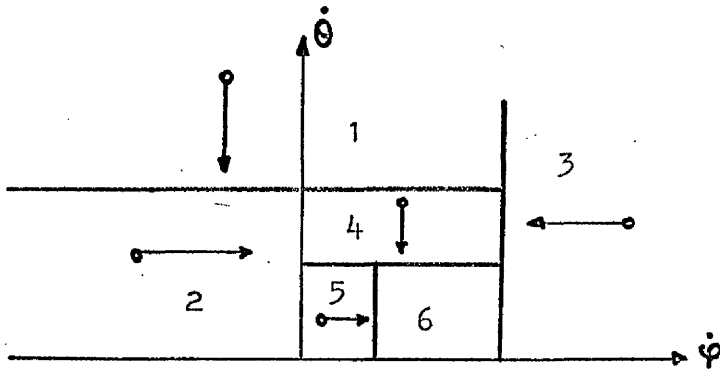


Fig. I.10. Initial effect of the thrust

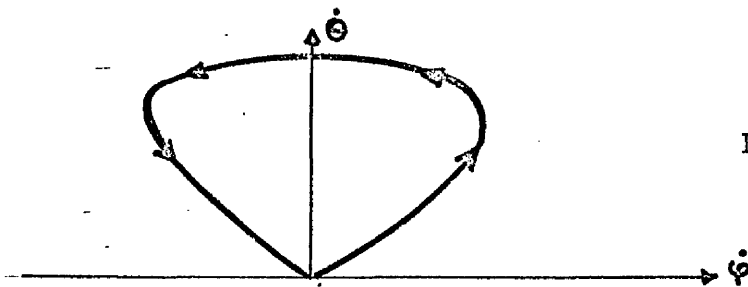


Fig. I.11. Motion of the image point on the plane of $\dot{\theta}$ and $\dot{\psi}$

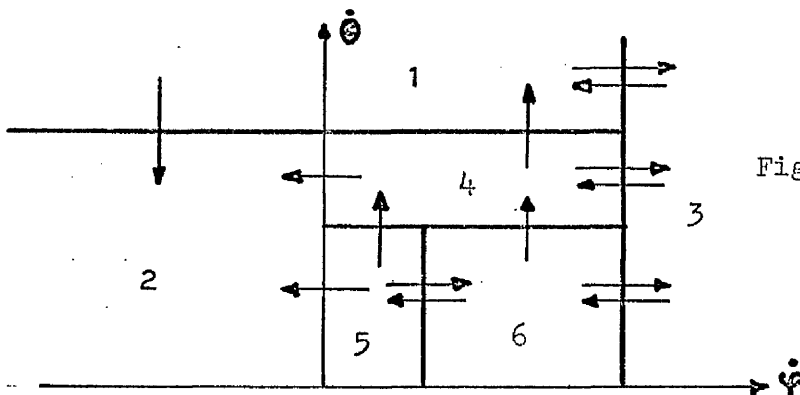


Fig. I.12. Possible motion of the image point across the boundaries

in fig.I.10., on which are represented the direction of the motion of the image point after applying the corresponding thrust. Bearing in mind the motion of the image point in the plane of $\dot{\theta}$ and $\dot{\psi}$ (fig.I.11), we observe that it may cross the borders of such decision diagram in the directions indicated in fig. I.12. by the arrows.

Oscillations can happen, if and only if, one of the directions shown on fig. I.10. is opposite to that indicated on fig.I.12. after crossing the appropriate boundary.

Therefore oscillations can take place near the following boundaries:

1 - 3	1 - 4	5 - 6
4 - 3	4 - 6	2 - 4
6 - 3	4 - 5	2 - 5

Fig.I.13. shows the directions of free motion (dotted arrows) and effect of thrust at the boundaries susceptible to oscillations.

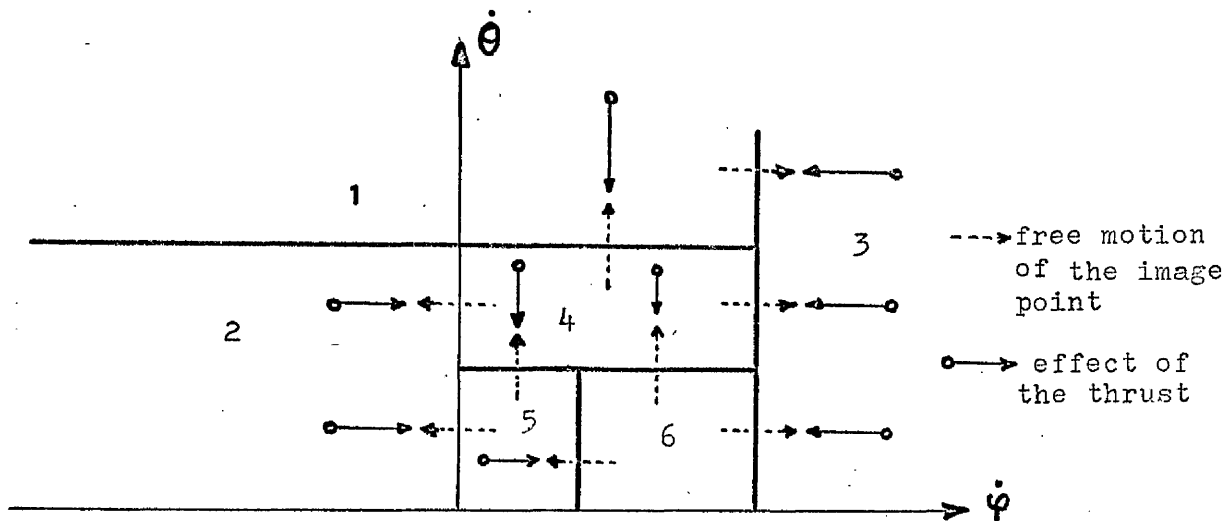


Fig.I.13. Boundaries susceptible to oscillations

However, those oscillations which take place in the half plane will either end up as rendezvous, because the operator would be always approaching to the vehicle, or will cease.

Having that in mind it remains only to study possible oscillations 2-4 and 2-5. The latter one will not arise if the radial thrust F_2 is continued (in the region 5) until a recognizable positive approach velocity ($\dot{\varphi}$) is achieved. (see flow-chart), but oscillation 2-4 may still occur, which is why region 5 is allowed to override region 4.

Note that any model trying to simulate intelligent behaviour should avoid situations like the oscillation which could happen around the border 2-4. If it happened, since $\dot{\varphi}$ is very small the man would continuously be applying transverse and radial thrust in a successive sequence, but would always remain at nearly the same distance from the vehicle. Although he might at first do this, he would ultimately try some other strategy.

A decision diagram without this inconvenience is the one of fig.I.9. in which area 5 overrides area 4. This diagram has been the one used in the present study. In area 6 no action is called for.

It remains a particularly hard problem to determine plausible boundaries of each one of the decision diagram areas for every value of φ , (i.e. for all the distances from the parent vehicle).

I.4. DECISION BOUNDARIES

Let us call (see fig. I.14.)

$B_{\dot{\theta}}$ to the upper boundary for $\dot{\theta}$

$b_{\dot{\theta}}$ to the lower " " $\dot{\theta}$

$B_{\dot{\varphi}}$ to the upper boundary for $\dot{\varphi}$

$b_{\dot{\varphi}}$ to the lower " " $\dot{\varphi}$

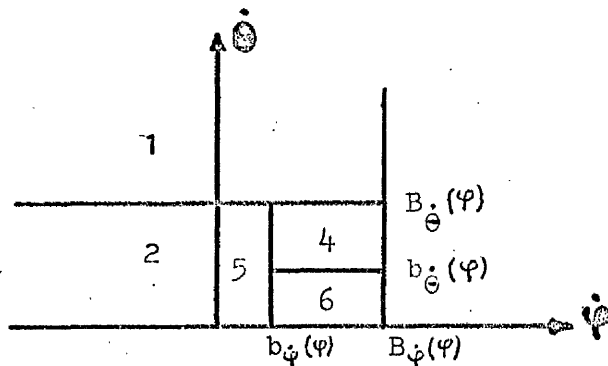


Fig. I.14. Boundaries

We note that at $\varphi \rightarrow 0$,
i.e. $r \rightarrow \infty$, all the boundary
limits must tend to zero,
since they must correspond
to finite velocities.

The easiest model would
be then based on boundary
limits which increase

with φ , reaching the greatest values at the rendezvous
distance. This seems logical, and agrees well enough with what
has been observed in the analog experiments. Accordingly it seems
natural, as a first suggestion, to devise a model with boundaries
linearly increasing with φ (fig. I.15.).

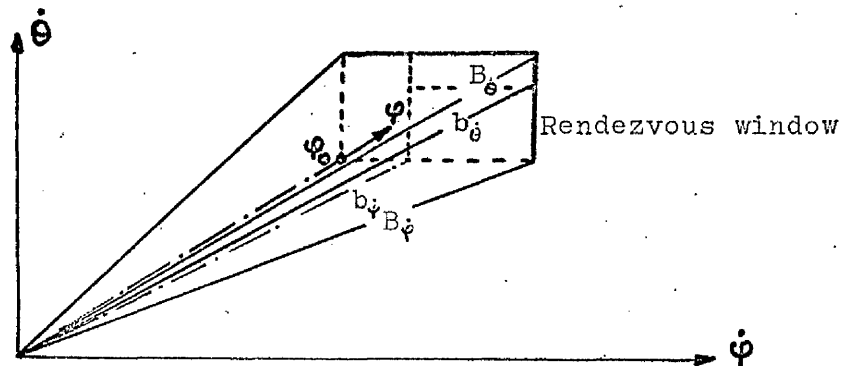


Fig. I.15. Linearly increasing boundaries

I.4.1. Boundaries for $\dot{\varphi}$

An obvious choice might be a boundary function of φ^n

$$B_{\dot{\varphi}} = K \cdot \varphi^n \quad (16)$$

Unfortunately the simple relation $n = 1$, (i.e. the linear boundary), with

$$B_{\dot{\varphi}} = \frac{v_0 \cdot \varphi}{r_0} \quad (17)$$

does not seem to suffice.

To try to explain why, let us consider a trivial condition of a purely radial approach with continuous deceleration to zero velocity at zero radial distance. Then

$$\dot{r}^2 = 2ar \quad (18)$$

$$\dot{\varphi}^2 = 2a\varphi^3/\alpha_0 \quad (19)$$

If $\dot{r} = v_0$ at $r = r_0$, which is the limiting rendezvous condition, then $a = v_0^2/2r_0 = v_0^2 \cdot \varphi_0/2\alpha_0$, and

$$\dot{\varphi} = \frac{v_0^2 \cdot \varphi_0}{\alpha_0^2} \cdot \varphi^{3/2} \quad (20)$$

The limit variation linear with φ (eq.(17)) is seen to imply a larger $\dot{\varphi}$ without the existence of a decision to apply a thrust. Consequently, the variation in proportion to $\varphi^{3/2}$ would seem to be preferable, as there would be little dispute, in the example cited, that the constant deceleration would be a "natural", if idealized, human strategy. Further, it seems reasonable to relate the values of v_0 to r_0 , so as to imply (on the above basis) a realistic and acceptable value of deceleration: that is, we assume a relation

$$v_0^2 = 2ar_0 \quad (21)$$

According to these considerations it seems convenient and realistic to define our boundary B_φ as

$$B_\varphi^2 = f_1 \cdot \frac{v_0^2 \cdot \varphi_0}{\alpha_0^2} \cdot \varphi^3 \quad (22) \quad (f_1 \text{ is a factor, } 0 < f_1 < 1)$$

Notice that the fact that B_φ depends on the values of a and v_0 is significant, as it can be interpreted in the sense that the man knows "a priori" these values (a and v_0), and he will act with more or less caution depending on that knowledge.

The boundary b_φ defining area 5 may be stated as having the same form that the preceding B_φ , but with a different value of the factor f_1 , which can be a data parameter of the program. In fact our calculations have been made with $f_1 = 1/2$ for B_φ and with the value $f_1 = 1/3$ for the function b_φ .

1.4.2. Boundaries for $\dot{\theta}$

As we have said before, the easiest and quickest way to control the transverse motion is to reduce $\dot{\theta}$ substantially, right from the beginning of the rendezvous manoeuvre. However the nearer the man comes to the vehicle, the greater will be his tolerance for $\dot{\theta}$.

In our model the boundary B_θ has been chosen linearly increasing with φ , and with a maximum value:

$$f_2 \cdot v_0 / r_0$$

(which corresponds to a transverse velocity of $f_2 \cdot v_0$ at the rendezvous distance). f_2 is a factor $0 < f_2 < 1$, but studies have shown that the choice of f_2 close to unity lead to unrealistic situations, and the results quoted here have been taken with $f_2 = 0.1$.

The limit for immediate correction of $\dot{\theta}$ (i.e. $B_{\dot{\theta}}$) has to coincide with the preceding one in both limiting conditions $\varphi = 0$ and $\varphi = \alpha_0 / r_0$, and it must be greater than $b_{\dot{\theta}}$ in all other conditions. There are many functions accomplishing this. After many trials, a function of the form $K \cdot \sqrt{\varphi}$ has been accepted as answering well enough for the case. Then

$$B_{\dot{\theta}} = f_2 \frac{v_0}{\sqrt{\alpha_0 r_0}} \sqrt{\varphi} \quad (23)$$

Remembering that

$$b_{\dot{\theta}} = f_2 \frac{v_0}{\alpha_0} \cdot \varphi \quad (24)$$

we notice that the difference between $B_{\dot{\theta}}$ and $b_{\dot{\theta}}$ (the width of the area 4) is maximum at $r = 4 r_0$. In other words, at that distance the indecision margin for controlling the transverse component of the velocity is maximum at four times the rendezvous distance: it is difficult to associate any special significance to this precise number, but it represents qualitatively an undoubted effect, as has been observed in the analog simulation.

I.4.3. Effect of Observational Uncertainties on Decision Boundaries

The differential threshold in the frontal plane refers to the minimum change of the component of angular velocity of an object, at right angles to the line of sight, which can be detected by a human being. This threshold depends upon the magnitude of the angular speed. When this is zero, the minimum speed which is perceived as motion is called rate threshold in the frontal plane. This depends on the contrast level and on the fixed visual reference.

The definition of rate threshold in depth refers in a similar manner to the minimum change in the radial speed which can be detected.

Although it has been given values of these rate thresholds (ref.1) such as 1 or 2 minutes of arc per second, it must be noticed that these values are perhaps very different in a rendezvous process. On one hand it will depend largely on the particular circumstances of illumination of the vehicle and the star field which surrounds it, and on the other, it has to be observed that in general both types of motion are present (i.e. radial and transverse) making it more difficult to discriminate either component of motion.

The rate thresholds appear in our model as lower uncertainty

level for each one of the boundaries specified in the decision diagram. Then the lowest value for the functions $B_{\dot{\varphi}}$ and $b_{\dot{\varphi}}$ would be Θ_{or} , the radial rate threshold, and for the functions $B_{\dot{\theta}}$ and $b_{\dot{\theta}}$ would be Θ_{ot} , the transverse rate threshold.

Both rate thresholds are considered as data parameters in the program, so that their individual effect could be studied.

I.5. REACTION TIME

By the term reaction time we include the period from the instant the man first observes a particular situation to the instant he takes the corresponding action (whether it is to apply a thrust, or to wait).

As can be anticipated, the problem of determining the reaction time corresponding to any situation is highly difficult, since it depends largely of what has happened immediately before, and on peculiar characteristics of any human response, such as training, momentary distractions, etc. With the idea of formulating it in some way, it has been assumed that the time involved in taking a decision leading to a thrust is of the form:

$$t = t_0 e^{-K_a \delta} \quad (25)$$

where

t_0 is the maximum decision time,

δ is a parameter associated with the angular velocity concerned with the decision ($\dot{\theta}$ or $\dot{\psi}$)

and K_a is a constant related to the ability of the operator.

Obviously the reaction time is positive, and equally obviously, it will decrease with training, or decrease due to the certainty attached to the observation; the formula suggested appears to be a convenient way of including these effects.

To avoid the inconvenience represented by the different

range of $\dot{\psi}$ and $\dot{\theta}$, the variable δ has been normalized, so that its value is 1 for the maximum permitted values of $\dot{\psi}$ and $\dot{\theta}$ at the rendezvous distance. As these values are v_0/r_0 for $\dot{\theta}$ and $v_0 \cdot \alpha_0/r_0^2$ for $\dot{\psi}$, δ is either

$$\frac{r_0}{v_0} \dot{\theta} \quad \text{or} \quad \frac{r_0^2}{v_0 \cdot \alpha_0} \dot{\psi}$$

The time involved in a waiting decision is called t_{wd} and a fixed value is generally assumed. Since the decision to wait does not involve any physical preparation, and is usually made in a sequence of such decisions, there is good reason to presume that this time t_{wd} is less than t_0 .

The parameters t_0, K_a and t_{wd} form part of the data parameters of the program.

I.6. APPLICATION OF THRUST

As we have mentioned earlier it is assumed that the acceleration is applied during a number of discrete intervals of time, whose length is t_f , so that the impulse applied will be always integer multiple of $(a \cdot t_f)$, which is the "quantum" impulse.

The effect of applying a force is simulated by calculating the position of the image point then apply a "quantum" of impulse repeating this procedure until the decision program indicates that other action should be taken.

The aiming error committed by the operator is simulated by randomizing the components of a unit vector in the direction the thrust is intended to be applied. This gives another direction in which the real thrust will act, (i.e. if the thrust is desired to be applied in the direction of the unit vector \underline{u} , it will be in fact applied in the direction of $(\underline{u} + \underline{p})$, where \underline{p} is a random vector. The standard deviation used to randomize the components of the unit vector is a data parameter to the simulation taking account of the errors of implementation.

I.6.1. Limitation of the product $a \cdot t_f$

The minimum amount of impulse applied to the man is proportional to $a \cdot t_f$ (a is acceleration and t_f is minimum thrust time). Associated with the "quantum" impulse is the increment of velocity $\Delta v = a \cdot t_f$. Therefore v_0 has to be determined so that its value is higher than this minimum difference between discrete levels of speed.

I.7. THE PROGRAM

Flow-chart (See Fig.I.16.)

If the man is not in rendezvous condition the subroutine Image (b) calculates the variables φ , $\dot{\varphi}$ and $\dot{\theta}$ and randomizes them to take account of the errors of observation.

Following this is calculated (c) the time spent to take the next decision, which of course will depend on the new values of φ , $\dot{\varphi}$ and $\dot{\theta}$.

In the next step (d) the position and attitude of the man is updated to the instant he is going to take an action: This action is determined by the subroutine (f) with aid of the data provided by (e).

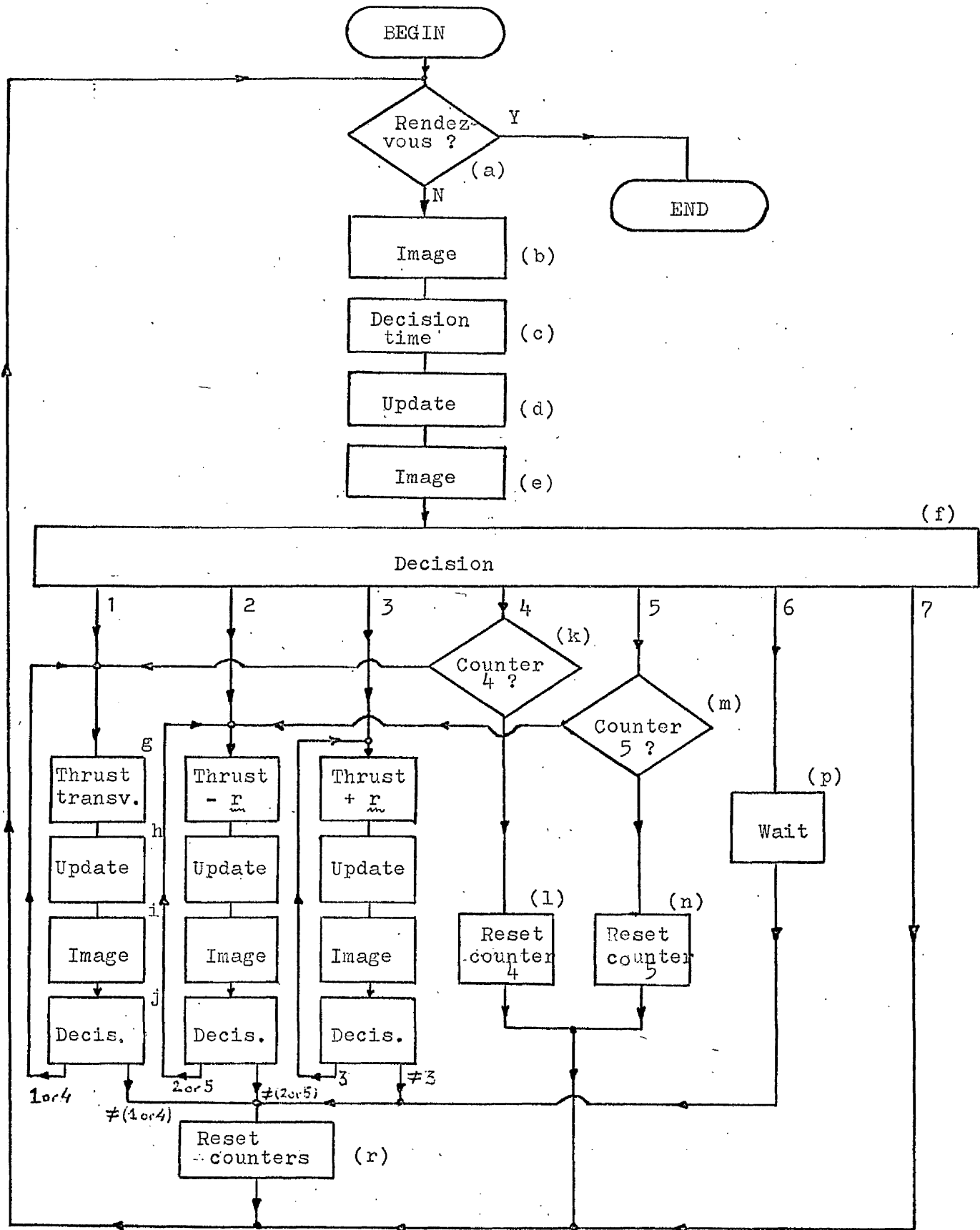
There are seven different exits of this subroutine decision:

Exit 1. It has been decided to apply a thrust in the transverse direction, so as to cancel the transverse component of velocity, that is to decrease $|\dot{\theta}|$:

The thrust is applied for a discrete time t_f (minimum duration of the thrust), and position and velocity of the man are updated (h), new values of φ , $\dot{\varphi}$ and $\dot{\theta}$ are calculated (i) and it is tested (j) whether or not more thrust has to be applied. This branch simulates the fact that the operator applies thrust until he judges it is no longer necessary.

Exit 2. This branch is similar to 1 except that the thrust being applied is that required to approach the vehicle (i.e. towards $-r$).

Fig.I.16. FLOW-CHART OF THE PROGRAM



Exit 3. Here the thrust is applied to recede, that is towards + r.

Exit 4. Sometimes an action is not taken as soon as possible, as it would be in the three preceding cases. After a close observation, an action which is not absolutely necessary but merely convenient would be taken to improve the process. This decision 4 means really that there is a small component of transverse velocity. If nothing more important to do arises it will be followed by a jump to the branch 1, but only after passing several times consecutively through this branch 4, as is indicated by a counter 4 (k).

Exit 5. Similar considerations apply as for branch 4 with the difference that it is associated with a jump to branch 2 instead of to branch 1. Decision 5 means that although the man is approaching the vehicle, the motion is too slow.

Notice that both counters 4 and 5 are cleared in every branch except in those in which they are updated.

Exit 6. The process seems to be controlled. The man decides to wait.

Exit 7. This means that virtually the rendezvous condition has been reached. This decision has been inserted only to provide an exit of the preceding branches in case of eventual rendezvous.

The conditions to take each of these decisions are
(see fig.I.14.) :

<u>Decision</u>	<u>Conditions</u>
1	$(\dot{\varphi} < B_{\dot{\varphi}}) .AND. (\dot{\theta} > B_{\dot{\theta}})$
2	$(\dot{\varphi} < 0) .AND. (\dot{\theta} > B_{\dot{\theta}})$
3	$(\dot{\varphi} > B_{\dot{\varphi}})$
4	$(\dot{\varphi} < B_{\dot{\varphi}}) .AND. (\dot{\varphi} > b_{\dot{\varphi}}) .AND. (\dot{\theta} > b_{\dot{\theta}}) .AND. (\dot{\theta} < B_{\dot{\theta}})$
5	$(\dot{\varphi} > 0) .AND. (\dot{\varphi} < b_{\dot{\varphi}}) .AND. (\dot{\theta} < B_{\dot{\theta}})$
6	$(\dot{\varphi} < B_{\dot{\varphi}}) .AND. (\dot{\varphi} > b_{\dot{\varphi}}) .AND. (\dot{\theta} < b_{\dot{\theta}})$
7	$(\varphi > \alpha_0 / r_0)$

and the corresponding flow-chart is squetched in fig.I.17..

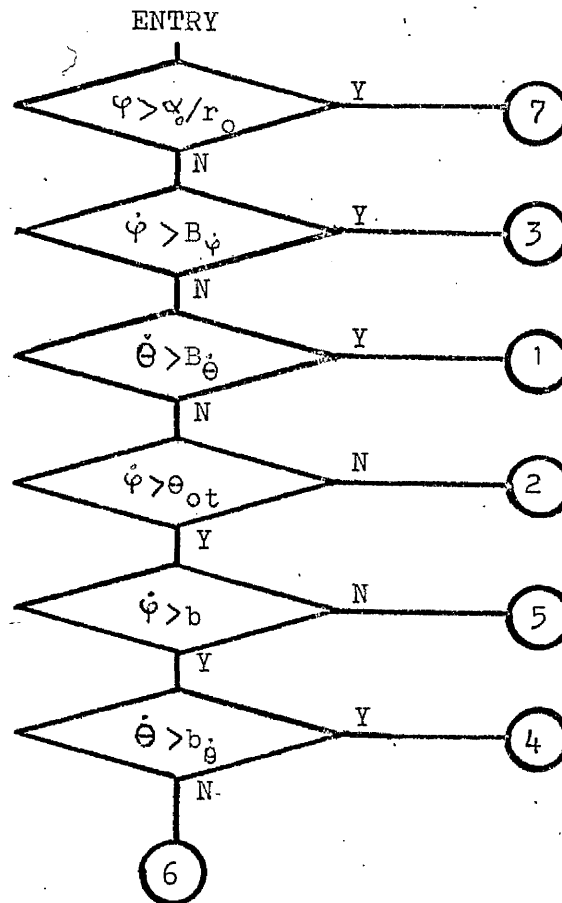


Fig.I.17. Decision Flow-Chart

Part II. ANALOGUE SIMULATION

II.1. Introduction

II.2. Target Trace

II.3. Star Field

II.4. Equations of Motion

II.5. Control Voltages

II.6. Oscilloscope Display

II.7. Presentation of Non-Visual Data

II.1. INTRODUCTION

It is the intention of the experiment described here to assess the performance of a human operator in controlling a system which has certain similarities with the rendezvous manoeuvre in deep space.

The operator is presented with a display on an oscilloscope representing:

- 1) a target, the size of its image on the scope being adjusted to represent the true angular size of the spacecraft, as it would appear during rendezvous, and its centre being at the centre of the scope, and
- 2) a star "background" adequately represented by three moving spots of light on the scope, having the same relative angular motion at the operator's position with respect to the (fixed) target centre, as the target would have relative to the star background in rendezvous.

The simulation is of course carried out in a true time scale. The unit of length corresponding to 1 volt is, by definition, the rendezvous distance r_0 .

No derived physical quantities involved in the simulation

need to introduce a mass unit.

Since the target is fixed in the scope and the star field moves, the frame of reference is as if the astronaut keeps his body orientation fixed relative to the line of sight.

As an initial objective, it is suggested that we imagine he also keeps his body orientation fixed with respect to the apparent plane of motion of the target so that the direction of motion of the star field is fixed, (for instance, horizontally on the scope). In order to provide a continuous moving reference, any star reaching the edge of the scope would need to be re-injected into the field of view at the opposite edge.

Consistent with this limited objective, the operator is given a control mechanism which, by means of the simulation, appears to consist of reaction thrusts either

- in radial direction, towards or away from the target vehicle, or
- in transverse direction, i.e. at right angles of the line of sight, causing the apparent motion of target relative to star background.

We shall now describe the components of the simulation in detail. Of these components only the generation of the visual presentation calls for a certain amount of ingenuity (i.e. the Target Trace Generation, the Star Field Presentation and the Scope Display).

II.2. TARGET TRACE

To represent the target we choose a figure-of-eight rather than a circle, as the former provides meaningful information even when the scale of angular magnification is such that only part of the figure-of-eight can be contained on the scope display: thus at closest approach the figure of eight would consist of two diagonal lines across the screen, intersecting at the centre.

This could be generated by a signal voltage

$$x_o = R_o(t) \sin \omega t$$

$$y_o = R_o(t) \sin \omega t \cdot \cos \omega t$$

where ω is a frequency high enough that, to the eye, the figure appears continuous, and where $R_o(t)$ is generated to provide the appropriate angular size of image, to the operator.

An electronic resolver could be used in the polar-to-rectangular resolution mode, with continuous rotation circuitry, and with a fixed voltage input to provide the appropriate ω , and a variable voltage $R_o(t)$ as input. This would provide output values of $-R_o \sin \omega t$, $R_o \cos \omega t$ and $U \sin \omega t$ volts ($U =$ voltage corresponding to 1 M.U.). The two latter could be passed to a multiplier to produce $-R_o \sin \omega t \cdot \cos \omega t$ and consequently the values of $-x_o$ and $-y_o$ obtained for the scope display, from the single variable voltage $R_o(t)$. A proper adjustment of the

time constant of the resolver's integrator can give a value of ω near 50 cps. which is adequate for the purpose.

Although this arrangement has proved to work perfectly well, it has some disadvantages: in the particular installation the resolvers have a lower reliability than the rest of the equipment, and there are "teeth" accompanying the output wave, in continuous mode, at this frequency.

For these reasons it was judged better to build an oscillator without using resolvers:

The basic idea is to get a sinusoidal function of frequency ω from a solution of the second order differential equation

$$y'' + \omega^2 y = 0$$

but as in any practical case the amplitude would decrease with time, due to damping resulting from capacitor leakage and the integrator's input-resistor. This damping can however be compensated by designing into the circuit a negative damping so that the differential equation to be solved is apparently

$$y'' - 2\sigma y + \omega^2 y = 0$$

This has been found to be a perfectly satisfactory expedient to overcome the difficulty, and the selection of the appropriate value of σ to eliminate the inherent damping is not difficult.

The circuit to generate the sinusoidal wave is shown in fig.II.1, and it has been used to generate frequencies near 100 cps.

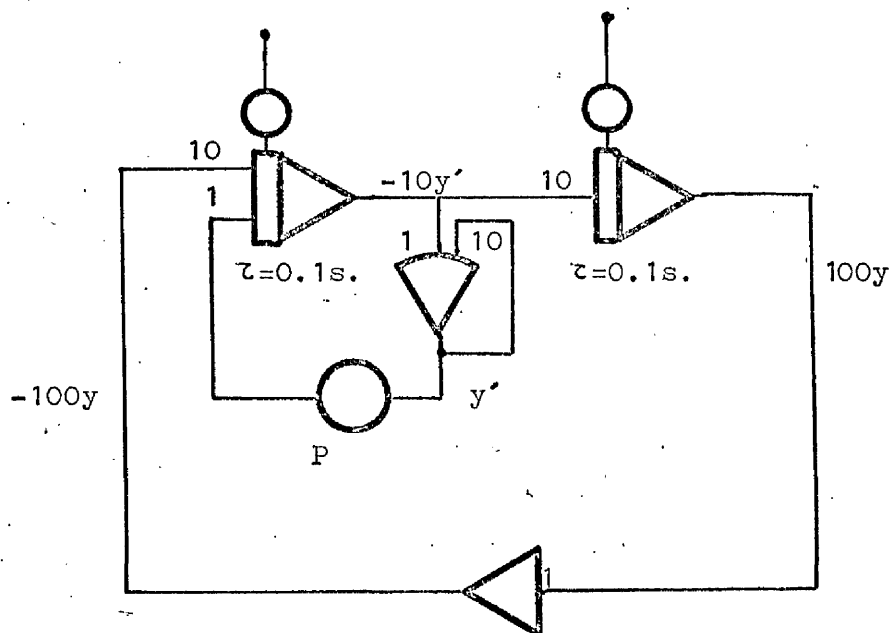


Fig.II.1. Amplitude constant sinusoidal oscillator

(Observe that the time constant of the two integrators has to be 0.1 secs.). The circuit provides both $\sin \omega t$ and $\cos \omega t$ and with the aid of multipliers we generate the functions $R_0 \sin \omega t$ and $R_0 \sin \omega t \cdot \cos \omega t$ to provide the required target trace.

The potentiometer P in fig.II.1. is continuously adjustable by hand setting, and a suitable setting is obtained by observing the effect of applying a voltage from the main loop to the Y-plates of an oscilloscope. In practise, values of P corresponding to 0.01ω are found necessary.

II.3. STAR FIELD

This is represented by three moving spots of light. This limitation on the number of spots is only dependent on the availability of equipment.

The problem of providing such a display can conveniently be divided into three parts:

- a) Generate the stars apparent speed. The position of the star image (as distinct from its motion) is of little importance.
- b) When any star reaches either the right or the left edge of the oscilloscope screen that star and only that one must be re-injected onto the screen at the opposite edge.
- c) The stars and the target trace must be displayed on the single beam oscilloscope.

We shall explain steps a) and b) in this paragraph, leaving c) to be discussed in paragraph II.6.

a) The apparent speed of the stars \dot{x}_1 will be proportional to $\dot{\theta}$, angular velocity of the rendezvous subject relative to the target, which is generated when solving the equations of motion (see paragraph II.4.). An integration of $-\dot{x}_1$ will give the position of the stars, and the coefficient of proportionality between \dot{x}_1 and $\dot{\theta}$ can be selected by use of a potentiometer.

b) Calling $\pm V_e$ the voltages corresponding to the edges of the

scope's screen, re-injection implies that if $|x_i| > |V_e|$, then $-2|V_e| \text{sgn}(x_i)$ must be added "instantaneously" to x_i .

As this is not a periodic function in the normal sense (since the variation of x_i is not expressible in formal terms), there is no transfer function description of it.

The effect is achieved with sufficient accuracy by testing the conditions $x_i > V_e$, or $x_i < -V_e$, by two comparators; they are used to drive a relay so as to add a large voltage to x_i of the sign needed to decrease the absolute value of x_i , and at the same time to change the comparison level effected by the comparator, as we shall now explain: actuating

The circuit used is shown in fig.II.2. The value of the

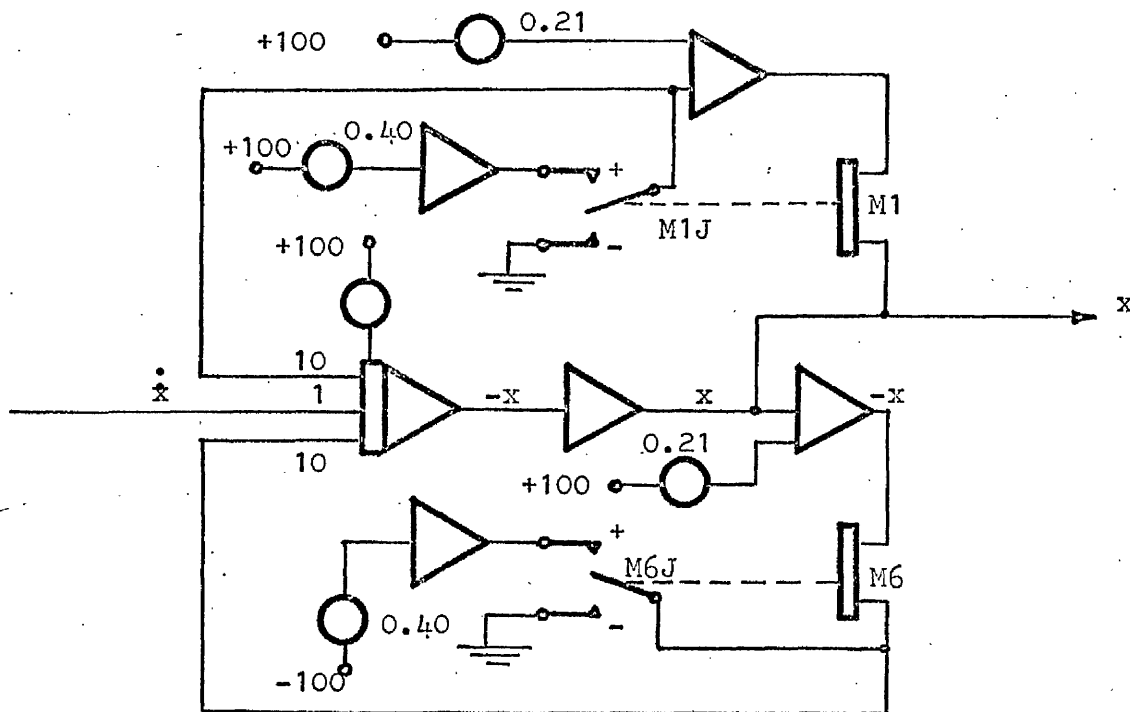


Fig.II.2. Star re-injection circuit

voltage needed to reach the edge, V_e , is here 21 volts. If $|x| < 21$ volts, neither of the two comparators (M1 and M6) will be actuated, and the arms of both relays will be connected to ground voltage. Further \dot{x} is the only input voltage to the integrator (providing $-x$).

If x increases and reaches +21 volts, comparator M1 will switch and actuate the arm of relay M1J to the + position, connecting - 40 volts to the input of the integrator (which consequently will rapidly increase the value of $-x$), and at the same time the voltage to be compared with x by the comparator M1 is changed to $-40 + 21 = -19$ volts, consequently this will stay in the + position only until x drops below - 19 volts, when it will revert once more to the normal position (outputting ground zero voltage). Therefore the variation of x reverts to the integration of \dot{x} .

If x decreases and reaches - 21 volts, a similar situation (with opposite polarity) will happen with comparator M6 and relay M6J interacting in a similar manner with the integrator for x .

The time needed for the voltage x to change sign is of the same order as the relay switching time (1.5 msec.).

As the motion of the star background is constrained to represent apparent motion in a plane, the ordinate of each star is a constant. This constant voltage is easily obtained by means of a potentiometer.

II.4. EQUATIONS OF MOTION

If r is the radial distance of the target, and d_0 its diameter, its apparent size (represented by R_0) would be proportional to $\arctan(d_0/2r)$. This function could be generated (from r) by use of an electronic resolver. However for $r \gg d_0$, evidently $\arctan(d_0/2r) \simeq d_0/2r$, and for smaller values of r the field of view of the target is in any case restricted in our simulation, so that it is adequate to regard R_0 as inversely proportional to r (the constant of proportionality being chosen according to the values of d_0 and the distance between the oscilloscope screen and the observer).

The problem of representing the motion consists essentially therefore of the generation of values for r and $\dot{\theta}$ from the voltages a_r and a_θ representing the radial and tangential accelerations. This can be done by solving the pair of differential equations

$$\ddot{r} = a_r + v_\theta \dot{\theta}$$

$$\frac{d}{dt} (rv_\theta) = ra_\theta$$

for r and $v_\theta = r\dot{\theta}$, subject to the initial conditions that $r = r_i$, $\dot{r} = \dot{r}_i$, and $v_\theta = v_{\theta i}$ at time $t = 0$.

The method of solution employing quarter square diode multipliers, in our simulation is represented in the circuit of fig. II.3.

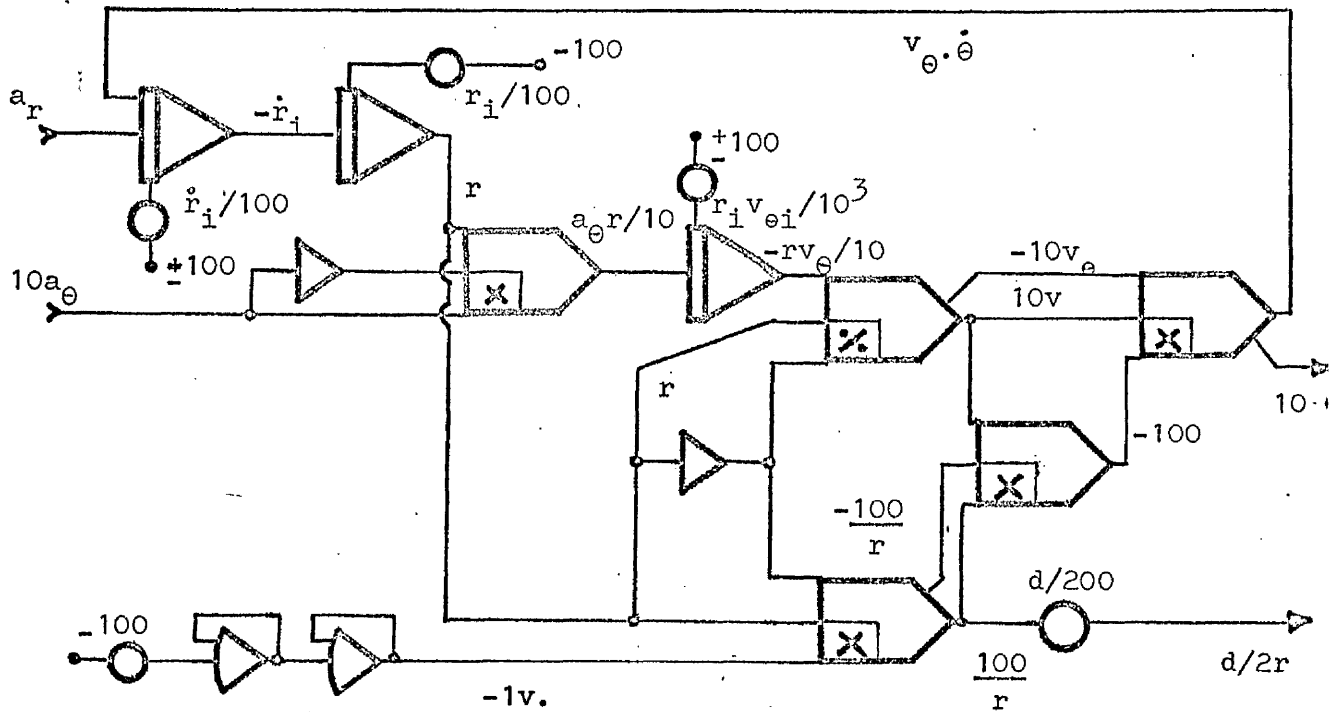


Fig. II.3. Equations of Motion

Two considerations are paramount: The voltages must be kept as high as possible to the inputs of the multipliers and to the denominators of those multipliers used as dividers; but the voltages must nowhere exceed 100 volts which would overload the amplifiers. In designing the circuit shown, it is supposed that the values of r will be in the range from 1 to 100 volts and that the velocity component v_θ does not exceed 10 volts.

II.5. CONTROL VOLTAGES

Ideally the control voltages (for a_r and a_θ) would best be supplied from a hand-held control unit provided for the operator. However in the simulation we have conducted, two hand operated 3-pole switches (on the PACE console) have been used to provide a "bang-bang" control voltage, separately representing a_r or a_θ , without attempting to introduce the element of human error in directing the acceleration vector. With the time scaling used in the integration, values of a_r and a_θ of about 1 volt are suitable. Fig.II.4 shows the connections of the 3-pole switches.

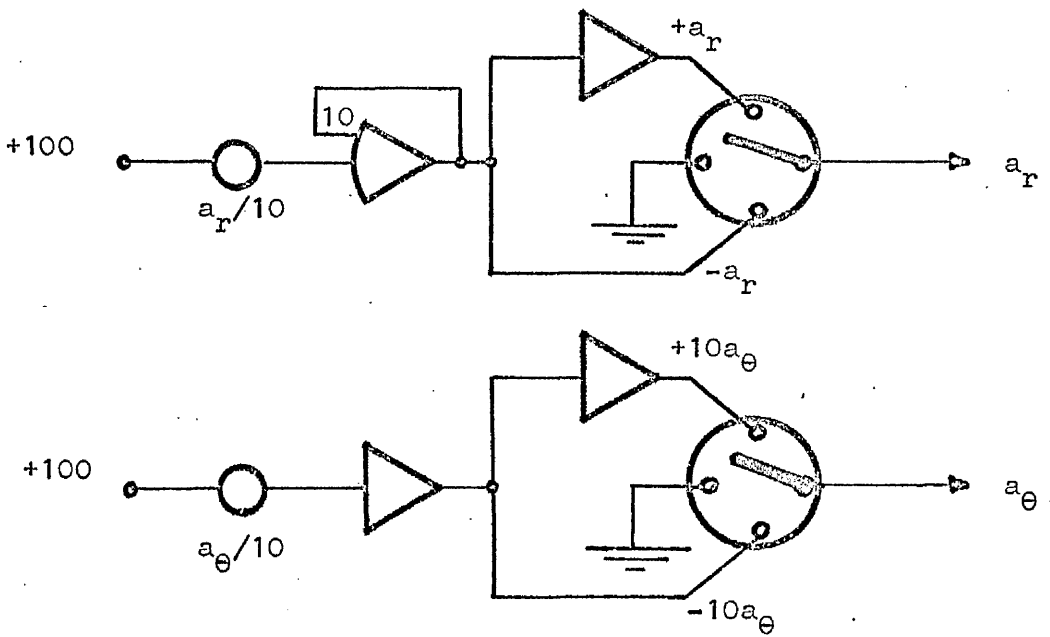


Fig.II.4. Control Voltages

II.6. OSCILLOSCOPE DISPLAY

To represent adequately on the single beam scope the target and the three stars forming the background, it was decided to use a chopped signal alternating rapidly between the voltages representing the target trace (x_0, y_0), and the spot position of the i -th star (represented by x_i, y_i).

The values of y_i are constants and x_i is independent of i (see paragraph II.3.). The variation of x_0, y_0 has been discussed in para.II.2.

By suitable choice of the chopping signal we can provide the appearance of four separate signals and four separate beams.

The PACE equipment has repetitive cycling operation facilities which allow this chopping to be done. This equipment produces a rectangular wave output in which the duration at the high and low levels can be adjusted digitally to values between 99.9 msec. and 0.1 msec., in steps of 0.1 msec. There are two independent rectangular wave generators of this kind providing the voltages that we are calling A and B (fig.II.5). The complements \bar{A} and \bar{B} are also available.

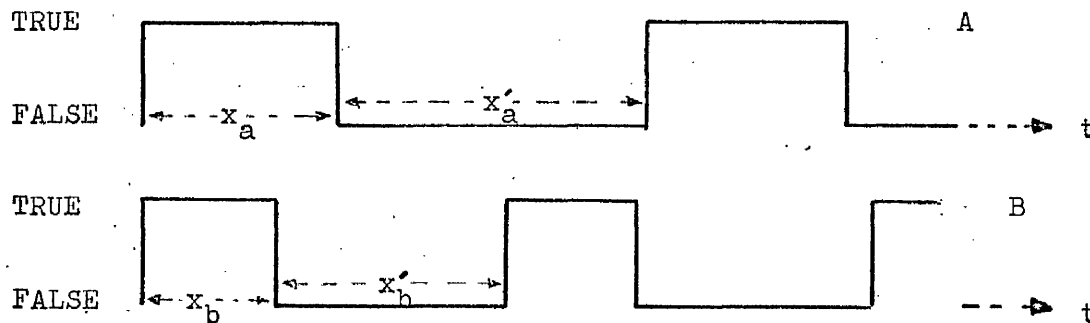


Fig.II.5. Rectangular waves A and B

By means of these voltages A and B and four AND gates we can have the four logic signals AB , $A\bar{B}$, $\bar{A}B$, and $\bar{A}\bar{B}$, which can drive D/A switches, so as to provide the required signal, as in fig.II.6. S are D/A switches, closed when the indicated logic signal is TRUE, and opened if it is in FALSE condition.

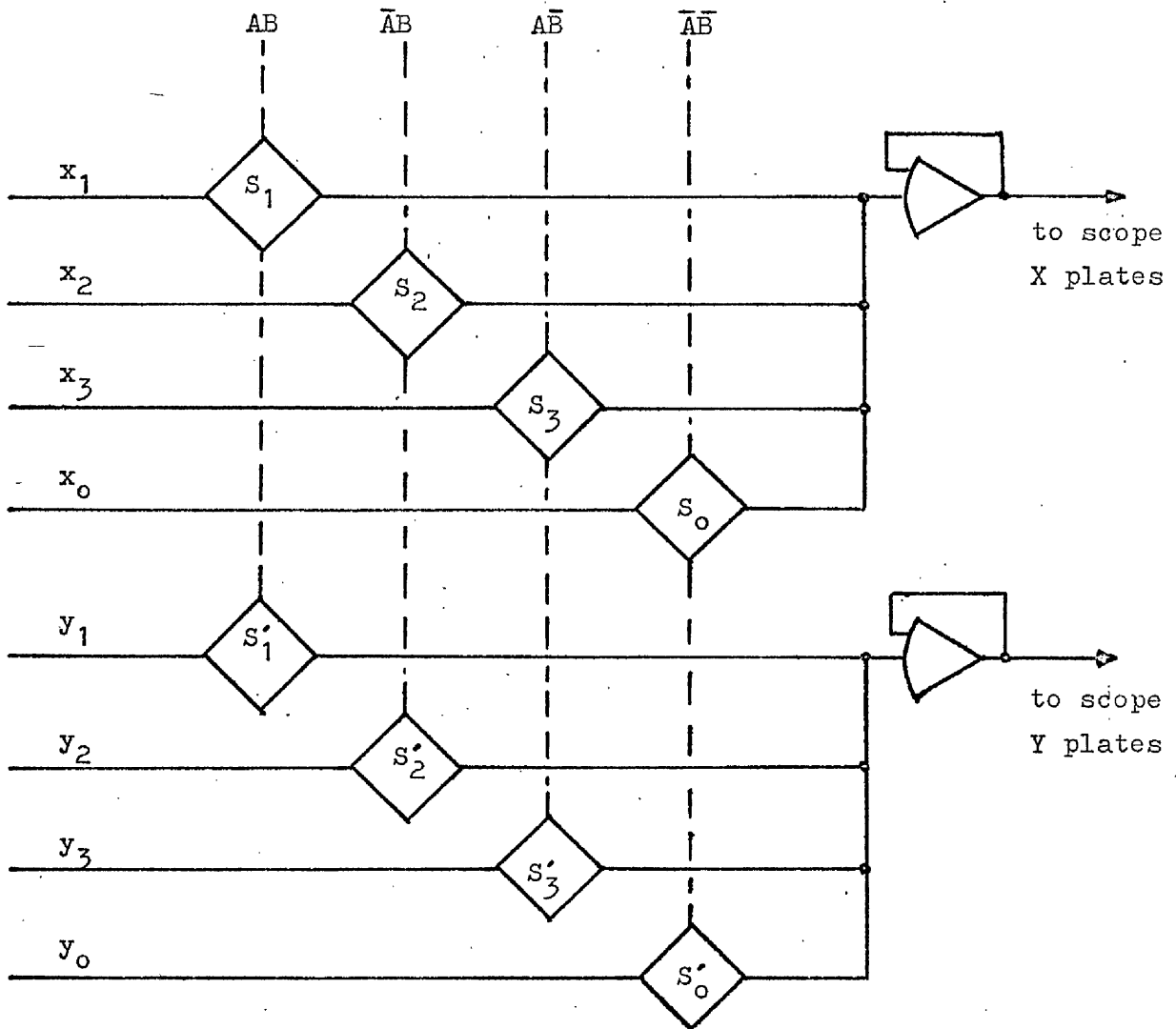


Fig.II.6. Chopping Process

A proper setting of the time the voltages A and B are in TRUE and in FALSE condition (that is, the values of x_a, x'_a, x_b and x'_b in fig.II.5) enables both apparent image continuity and brightness to be adjusted.

The mean time that A is TRUE during one unit of time, (or the probability of A being TRUE), is

$$p(A) = \frac{x_a}{x_a + x'_a}$$

and reasoning similarly

$$p(B) = \frac{x_b}{x_b + x'_b}, \quad p(\bar{A}) = \frac{x'_a}{x_a + x'_a} \quad \text{and} \quad p(\bar{B}) = \frac{x'_b}{x_b + x'_b}$$

In the same way, the chopping signal AB is TRUE the following fraction of time

$$p(AB) = \frac{x_a}{x_a + x'_a} \cdot \frac{x_b}{x_b + x'_b}$$

with similar relations for the other three signals $\bar{A}\bar{B}$, $A\bar{B}$, $\bar{A}B$.

These probabilities are related to the brightness of the image associated with each logic signal. However since

$$\frac{p(AB)}{p(\bar{A}\bar{B})} = \frac{p(A\bar{B})}{p(\bar{A}B)}$$

it is not possible to arrange for the three star images to have the same brightness, unless the target brightness is also the same as that of the stars. Similarly if the target is to be much

brighter than the stars, one of the stars has to be brighter than the two others. Choosing for instance the following values, which by observation have been found appropriate:

$$\begin{array}{ll} x_a = 11.0 \text{ msec.} & x'_a = 29.9 \text{ msec.} \\ x_b = 1.1 \text{ msec.} & x'_b = 10.1 \text{ msec.}, \end{array}$$

the relative luminance of the star images are in the ratio 1:2.54:9.35, and 25.3 that of the target.

The continuity of the images is obviously related to the absolute time scale of the chopping process.

II.7. PRESENTATION OF NON-VISUAL DATA

The simulation has been provided with means of recording parameters such as the elapsed time and the fuel consumption (in terms of the impulse). It has also been found useful to provide a visual signal to the operator showing when the rendezvous is achieved, and whether or not it was successful.

II.7.1. Fuel Consumption

The output voltage of an integrator is used to represent the fuel consumed (in arbitrary units) or, what is the same thing, the total impulse applied. The input to the integrator is the absolute value of any acceleration (either radial or transverse) applied during the process. This can be checked by observing the outputs of the summing amplifiers used to determine the moduli, and remedied by adjustment of the potentiometers P and P' (see fig.II.7).

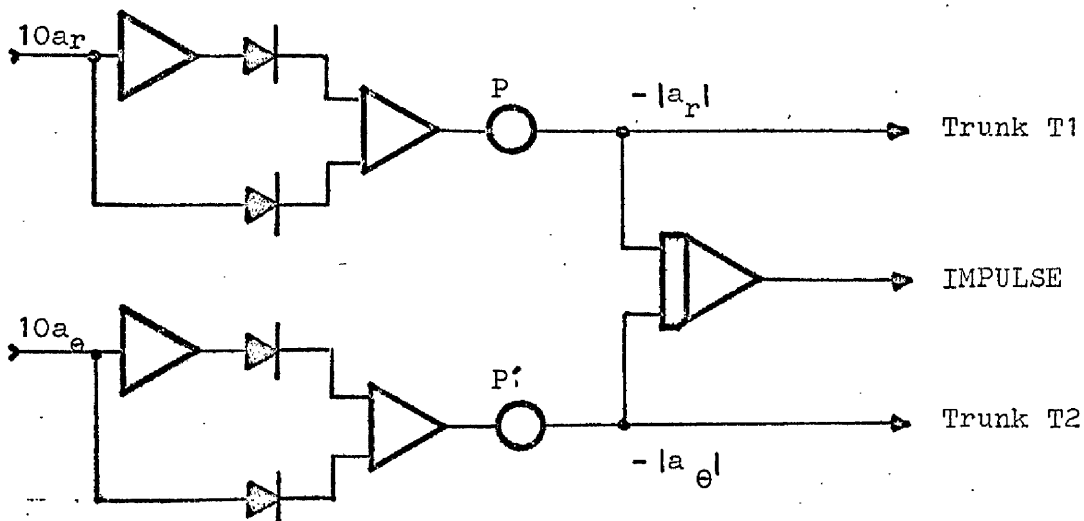


Fig.II.7. Fuel Indicator

II.7.2. Clock

This is an integrator whose constant input is switched off when rendezvous is achieved, thus recording the duration of the manoeuvre.

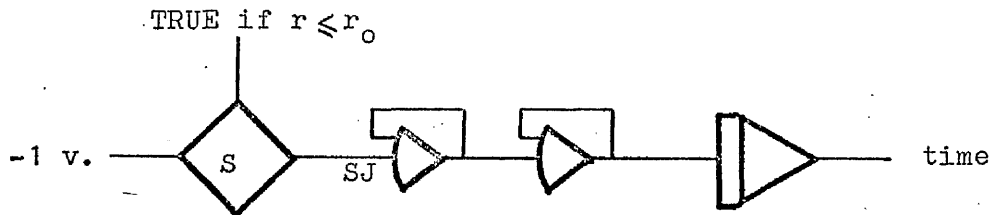


Fig.II.8. Clock.

II.7.3. Rendezvous Indicator

When the variable r is less than r_0 (rendezvous distance), the figure-of-eight appearance of the target is changed. Provided the manoeuvre is successful, (i.e. the arrival speed is lower than v_0), the target appearance becomes an ellipse. However, should this not be the condition (i.e. the arrival can be interpreted as a "crash"), the target figure will turn into an inclined line (fig.II.9.)

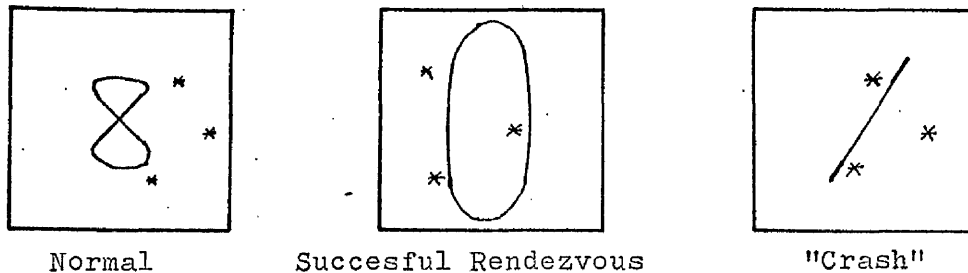


Fig.II.9. Screen Display

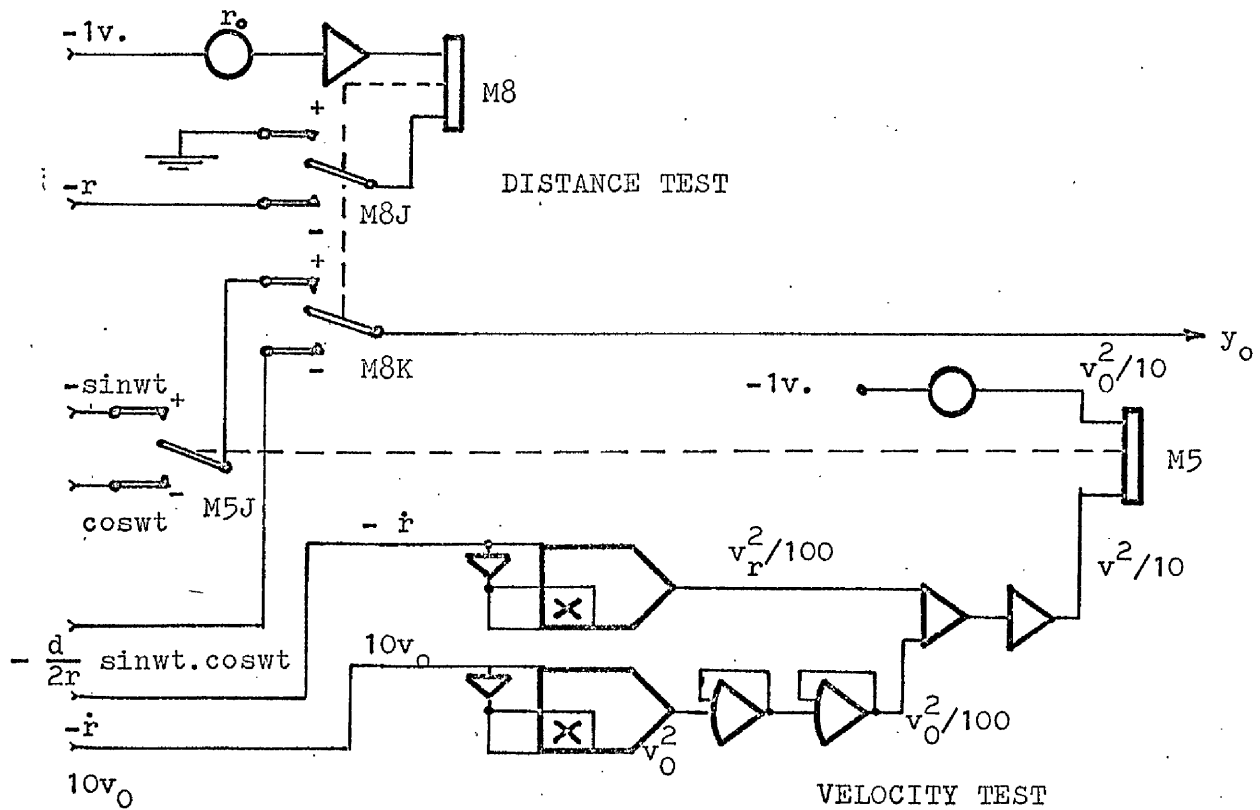


Fig.II.10. Distance and Velocity Tests

If $r < r_0$ (fig.II.10.), comparator M8 drive relays M8J and M8K to the + condition and it will remain clamped (notice + of M8J connected to ground voltage). Then if comparator M5 (which is testing the condition $v > v_0$) is in the TRUE state, y_0 will be proportional to $\sin\omega t$, and both x_0 and y_0 will have the same phase (thus generating a straight line on the screen). On the other hand if $v < v_0$, the relay M5J is connected to the negative terminal, and y_0 is proportional to $\cos\omega t$, causing the figure on the screen to become an ellipse symmetrical with respect to the x, y axes.

Part III. RESULTS

- III.1. Introduction
- III.2. Initial Angle
- III.3. Size of the Target
- III.4. Acceleration
- III.5. Initial Distance
- III.6. Rate Thresholds
- III.7. Minimum Impulse Duration
- III.8. Errors of Observacion and Implementation
- III.9. Maximum Reaction Time
- III.10. Analog Experiments.
- III.11. Conclusions
- III.12. Suggestion: for Further Work

III.1. INTRODUCTION

In the next paragraphs we shall attempt to determine the effect (on the process) of both specific variables of the manoeuvre and specific variables of the human operator:

- Initial angle of operators' velocity with the line of sight
- Size of the target
- Initial velocity of the operator relative to the target.
- Acceleration.
- Initial distance of the operator from the target.
- Rate thresholds (see parr. I.4.3.)
- Human errors (i.e. errors of visual observation and error committed in aiming the thrust, each represented by its corresponding standard deviation, for we assume they are normally distributed).
- Maximum reaction time of the operator (by convention this includes observation, decision, alignment of thruster and thrust initiation).
- Minimum duration of the impulse (level of uncertainty of the on-off thrust time).

The most important characteristics of the manoeuvre can be reduced to: a) Impulse consumption (product acceleration by time

of application) , . . . which is directly proportional to the amount of fuel used, b) Time employed in the whole process, and c) The ratio ρ of the Total time to the time the impulse has been applied, i.e. total time /action time. We can regard this as a measure of the facility of the manoeuvre, since if the ratio is large, then for most of the time there is no need for action by the man. Clearly (a) is a measure of how costly, (b) how quick, and (c) how easy; the process appears.

The standard deviation of these parameters with respect to their mean are likewise of importance: they measure the variability of these qualities in respect to a single manoeuvre. However it should be noted that these deviations are caused solely by the simulated human errors of observation and implementation, because without those the strategy of each manoeuvre with prescribed initial conditions would be identical.

III.2. INITIAL ANGLE

As in any case the manoeuvre consists of reducing substantially the transverse component of the initial velocity (i.e. $v_i \sin \beta$) and similarly, but separately, the radial component (i.e. $v_i \cos \beta$), we may expect that the Impulse consumption is proportional to $|\sin \beta| + |\cos \beta|$, or in other words to $|\cos(\beta - \pi/4)|$. This reaches a maximum value for initial velocities having the same transverse and radial components.

Fig.III.3. shows a polar diagram of the Impulse consumption versus the initial angle (of the operator's velocity with the line of sight) for two different values of this initial velocity $v_i = 1$, and $v_i = 5$. We can see that the results fit reasonably with the expectation mentioned above.

The indentations at $\beta = 0$ and $\beta = \pi$ are easily explained, for the manoeuvre would be made easier under such a particular circumstance. The peaks in the curve corresponding to $v_i = 5$ for values of β around 50° are due to the fact that the transverse component of the velocity has not been eradicated before the operator has passed by the target for a first time,^(*) consequently he has to reverse a receding radial component. Note that the same effect is not shown at the lower velocity

(*) an effect that we shall call "fly-past".

III.3. SIZE OF THE TARGET

Table III.3. shows the value of the Total time and Impulse consumption for different target sizes (α_0), and for different initial velocities (v_i). As could be expected there is no apparent influence of the target size on the manoeuvre.

III.4. ACCELERATION

Fig.III.2. shows the Impulse consumption versus acceleration for different values of the initial velocity v_i . The figure suggests the existence of a locus of the minimum value of impulse for each initial velocity which has a quite realistic significance as we shall see later. Thus we presume the existence of an optimum acceleration for each value of v_i . We have shown in fig.III.3. the mean and confidence interval calculated for different values of v_i . Note the increasing amplitude of the confidence interval as the acceleration increases, due to the effects of mismanagement of a large acceleration.

III.5. INITIAL DISTANCE

If v_i is assumed zero, the time spent in the manoeuvre seems to increase in proportion to $r_i^{1/2}$. This of course would result if the motion involved only uniform radial acceleration. The Impulse consumption seems to be a linear function of r_i . This is shown by figs.III.4. and III.5.

An interesting fact is that with zero initial velocity, low accelerations seem to imply a smaller fuel consumption: This trend of reduction in optimal acceleration by reducing v_i is also apparent from fig.III.3.

In the figs.III.6., III.8. and III.9. the parameter of variation of the curves is the rendezvous distance r_0 instead of acceleration. Observe the minimum, both of time and impulse, originated from the occurrence of "fly-past" (see parr.III.2.). The Impulse consumption again varies linearly with r_i and depends less sensitively than the total time on the ratio (r_i/r_0).

III.6. RATE THRESHOLDS

Considering the results of fig.III.10, we infer that an increase of the rate threshold values, which define the decision process (parr.I.4.3), reduces the variation of impulse with

acceleration. Nevertheless there still remains a range of optimal acceleration.

The influence of Θ_0 (rate thresholds) is more noticeable at low accelerations. Fig. III.12, likewise, showing the effect of Θ_0 at low accelerations on the total manoeuvre time, again points to the desirability of a large "dead zone" in the decision strategy.

The operator, of course, who is "hyper-sensitive" to error (i.e. he has a small Θ_0) may well cause more error by over-reacting.

III.7. MINIMUM IMPULSE DURATION

The fig.III.13, shows the Impulse consumption versus acceleration, for different values of t_f (minimum impulse duration). Apparently there is no great influence of this parameter, although the Impulse consumption decreases slightly for low values of t_f .

III.8 ERRORS OF OBSERVATION AND IMPLEMENTATION

It appears that the time spent in the manoeuvre increases roughly with the visual observation error (see fig. III.14). Note that although the Impulse consumption (fig. III.16) does not change much with this unitary error, both standard deviation of impulse and total time (figs. III.15 and III.17) certainly increase with the observation error.

Fig.-III.19 suggests that the impulse consumption increases with the error committed at pointing the thrust (implementation error).

III.9. MAXIMUM REACTION TIME

The appearance of figs. III.18 to III.25 would suggest that the total manoeuvre time depends almost linearly of the maximum reaction time of the operator, t_0 , but from values of t_0 from 6 or 8 secs. upwards, both manoeuvre time and impulse consumption increase rapidly with t_0 .

III.10. ANALOG EXPERIMENTS

Experiments have been made varying the relation initial distance to rendezvous distance and the acceleration.

After a sufficient training of the operator so as to familiarize with the manoeuvre, we took 4 samples of each experiment and obtained the results indicated in tables III.1. and III.2., plotted in figs. III.26 and III.27.

The results were performed with equal initial values of r_i and $v_{\theta i}$, condition which seems to be the most unfavourable (see para.III.2). Although we have taken arbitrarily as value of the initial velocity $v_i = 5$, this value pretends in some way, represent an uneasy case. It is not out of logic, then, to consider the circumstance that v_i is 5 times per second the rendezvous distance r_0 . In any case the value of v_i must be the predicted maximum initial velocity in the manoeuvre.

Note in fig. III.27 the optimum value of acceleration corresponding to minimum fuel consumption. This value depends on the parameter r_i , but an acceleration of 0.6 times the value of r_0 per sec^2 , approximately, seems convenient.

Further, with this value of acceleration, the control of the manoeuvre appears to be easier.

III.11. CONCLUSIONS

- 1) The most unfavourable angle (for minimum impulse consumption) of the initial velocity with respect to the line of sight is about 45° or 50° .
- 2) Target size has no apparent influence on the rendezvous process, assuming that it is large enough to be visible.
- 3) An optimum acceleration seems to exist for every value of the initial speed. This optimum acceleration increases with the initial speed and the rendezvous distance. Up to velocities of 5 units per second, the optimum is about 0.5 units/sec^2 (a unit being the rendezvous distance, and meaning by this the distance from the parent craft at which rendezvous is deemed to be completed).
- 4) Statistical deviations in Impulse consumption (i.e. the integral with respect to time of the absolute applied acceleration) increase with acceleration.
- 5) The impulse consumption seems to be proportional to the initial distance, whereas the total time of the manoeuvre seems to be proportional to the square root of the initial distance.
- 6) The influence of the Rate Thresholds (which represent the uncertainty levels of human vision -see para.I.4.3-) is most noticeable at low accelerations, whereas it becomes smaller for values of acceleration above the optimum.

7) The minimum thrust time (which determines the least value of impulse associated with a discrete action) does not have much importance in the process, provided it is a small fraction of the human reaction time (measured from decision to action).

8) An increase in visual observation errors causes an increase in manoeuvre time, although the impulse consumption is not greatly affected. However, the deviations of both time and consumption parameters (about their respective means) increase noticeably with such errors. An increase in the error committed in aiming the thrust seems to imply, an increase in impulse consumption and its deviation.

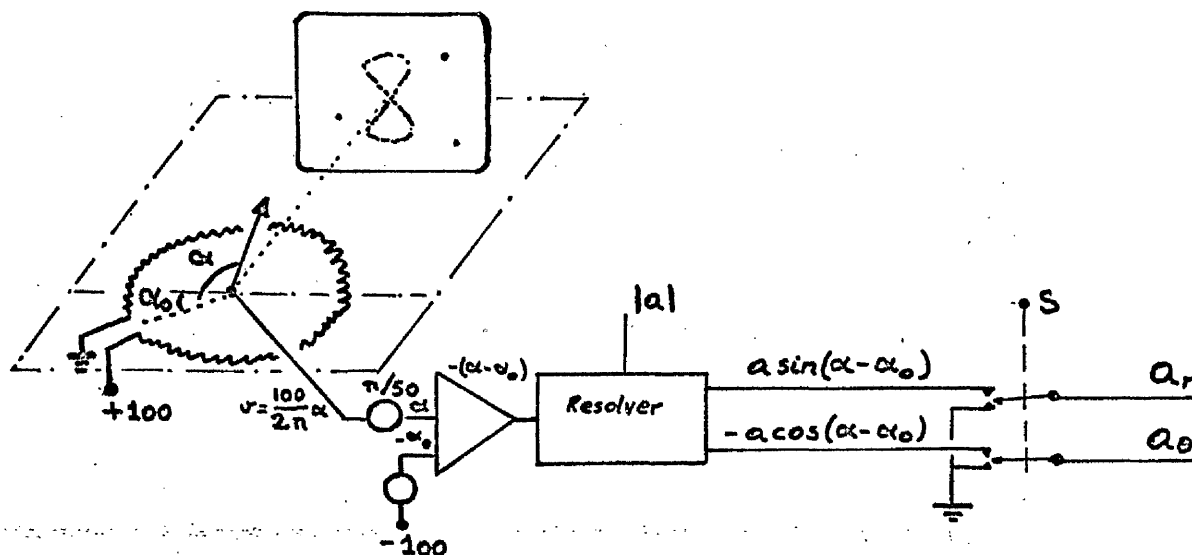
9) The Impulse consumption is least for values of the maximum reaction time (see para. I.5) in the range from 1 to 5 secs, increasing at smaller values than this, and increasing very rapidly for greater values of the maximum reaction time of the operator. (i.e. "Festina lente").

III.12. SUGGESTIONS FOR FURTHER WORK

Of course it would be highly desirable to provide a simulation of this manoeuvre with 6 degrees of freedom, but it would imply more sophisticated techniques. Perhaps the rotation about the roll axis could be omitted as it rarely would arise (ref.2).

The simulation work presented here could, however, be extended in some ways, as we feel it may be interesting:

- 1) To make a digital program so as to simulate (as close as possible) the analog device, coordinating in that way the two simulations.
- 2) To admit (in the Analog Simulation) the possibility of committing thrust-aiming errors. It might be done either by introducing a random voltage added to both transverse and radial accelerations, or by means of a linear potentiometer (see adjoint fig.) whose arm would be aimed as if it was a thruster (the thrust being then



A possible aiming-error circuit

applied by means of the four-pole switch S), or by means of another similar device.

3) To devise a mathematical model (perhaps a factorial model) able to describe the interaction between different parameters of the manoeuvre. It would be useful both in making tests of hypothesis about the interactions, main parameters, and in analyzing the variance.

4) To study the effect of the second derivative of the solid angle subtended by the target ($\ddot{\varphi}$) with relation to the decision-making process in the digital program.

5) To try to achieve rendezvous employing the minimum fuel amount (perhaps waiting until auto-cancellation of the transverse velocity v_{θ}), and compare the results with the values obtained if we try to achieve rendezvous in the minimum time.

6) To study the trajectory

7) To devise some sort of "manoeuvre-sequencing" so that we can consider the process in such a way that a complete study of a component of this sequence would permit us to infer what will happen in a completed sequence. For instance:

If we assume that the initial distance is always the unit of length, any successful rendezvous would consist of a displacement of the operator from the spherical surface of radius $r=1$, to the surface of radius r_0 (r_0 is the rendezvous distance, here being $r_0 < 1$). The units of velocity and acceleration would be then related to the initial conditions of the problem. Any manoeuvre could be considered as a succession of several such component manoeuvres (each reducing the distance by a factor r_0). However, in this sequence we could lose the physical significance of the process, as the arrival velocity in the n -th step would need to be the initial velocity in the $(n+1)$ -th step. But as that velocity is unpredictable both in modulus (it can vary from 0 to v_0 , the rendezvous velocity), and direction, we are not able to know the modulus and direction of initial velocity in the $(n+1)$ -th step, other than as a probability.

Nevertheless it may be interesting to carry on this study, by considering that both the initial and the final velocity are zero, or near zero.

Another way to sequence the process is by assuming that the initial velocity is unity, and modifying the timescale so that 1 sec. of simulation = F secs in the reality, with the factor $F = \text{initial distance}/\text{initial velocity}$. However if we do that, any time dependant variable (e.g. reaction time, acceleration,...etc.), will be related to the initial velocity.

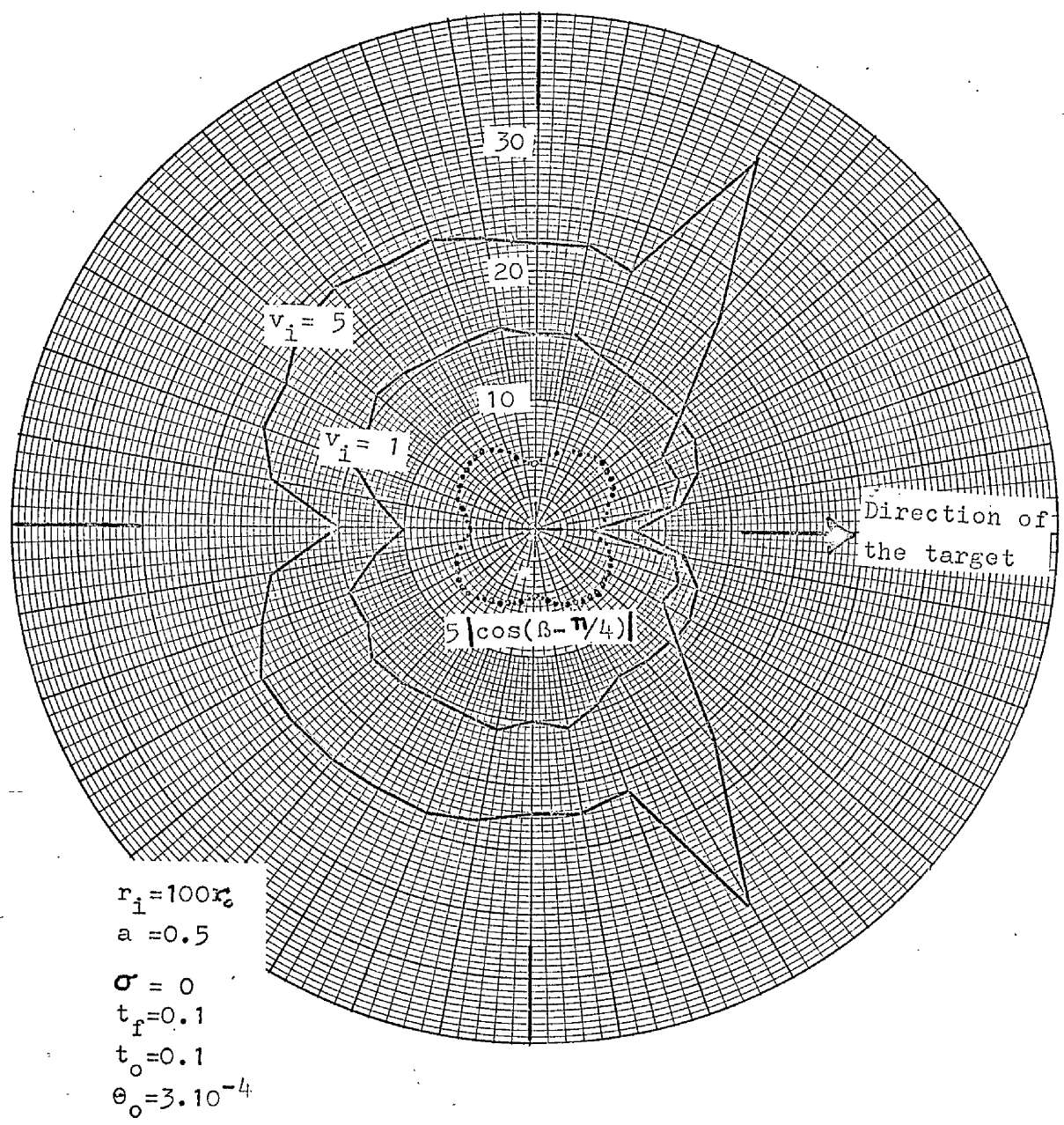
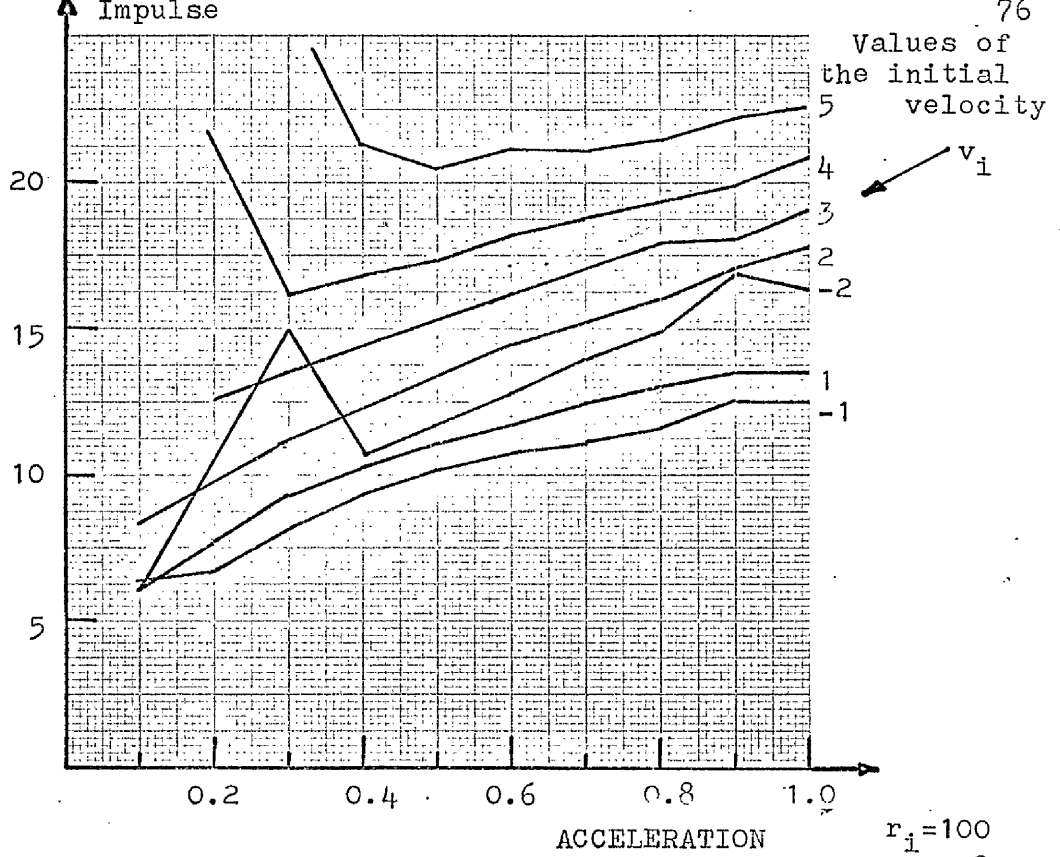
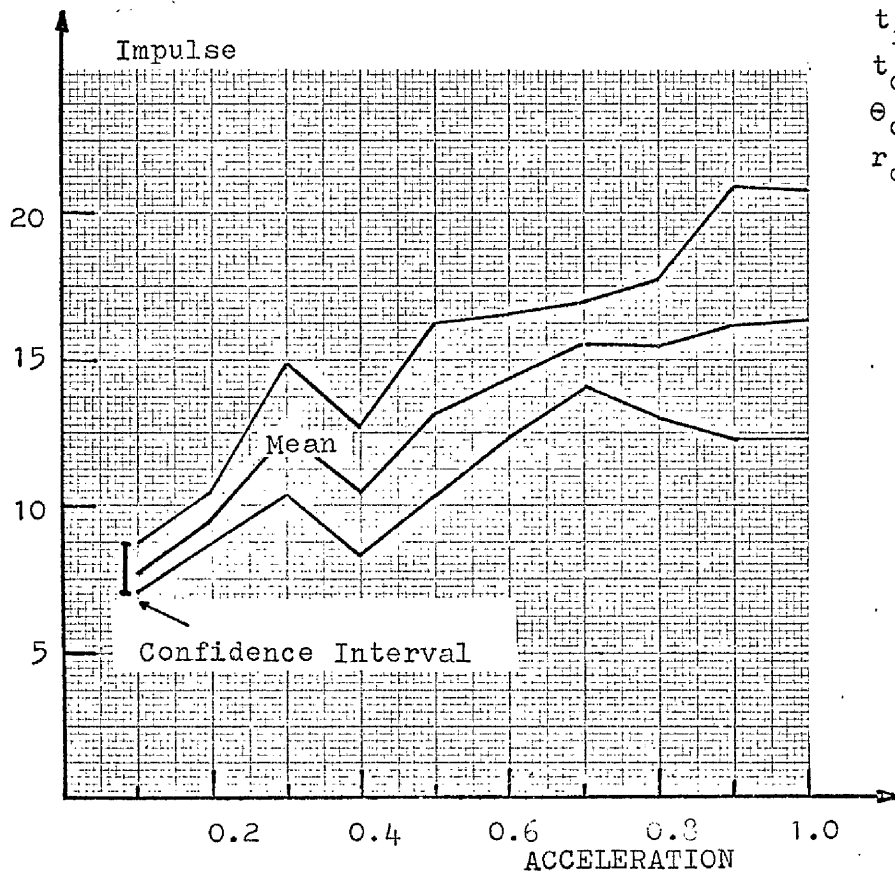


Fig.III.1 Impulse Consumption versus angle of the Initial Velocity v_i



$r_i = 100$
 $B = 50^\circ$
 $\sigma = 0.02$
 $t_f = 0.1$
 $t_o = 1$
 $\theta_o = 3 \cdot 10^{-4}$
 $r_o = 1$



Figs. III.2 and III.3

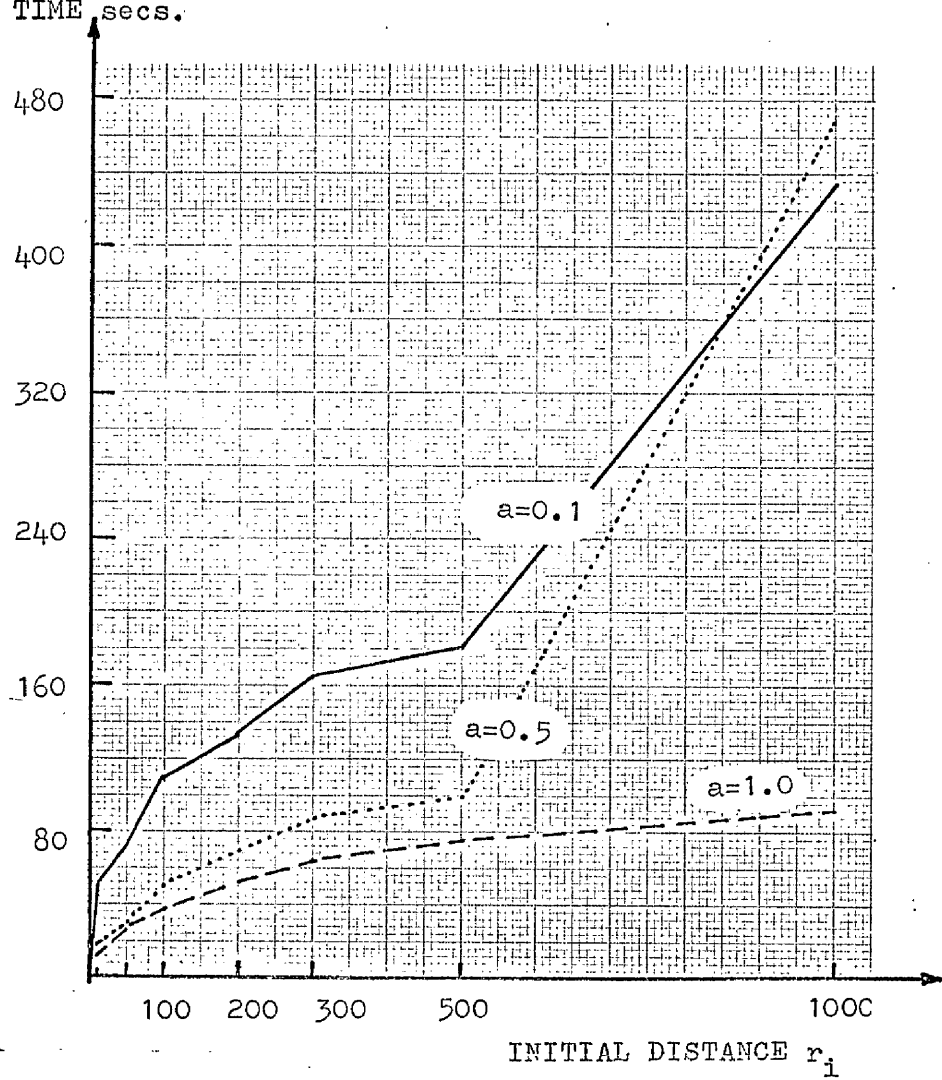


Fig III.4

$\beta = 50^\circ$
 $v_i = 0$
 $\sigma = 0.05$
 $t_f = 0.1$
 $t_o = 1$
 $\theta_o = 3 \cdot 10^{-4}$
 $r_o = 1$

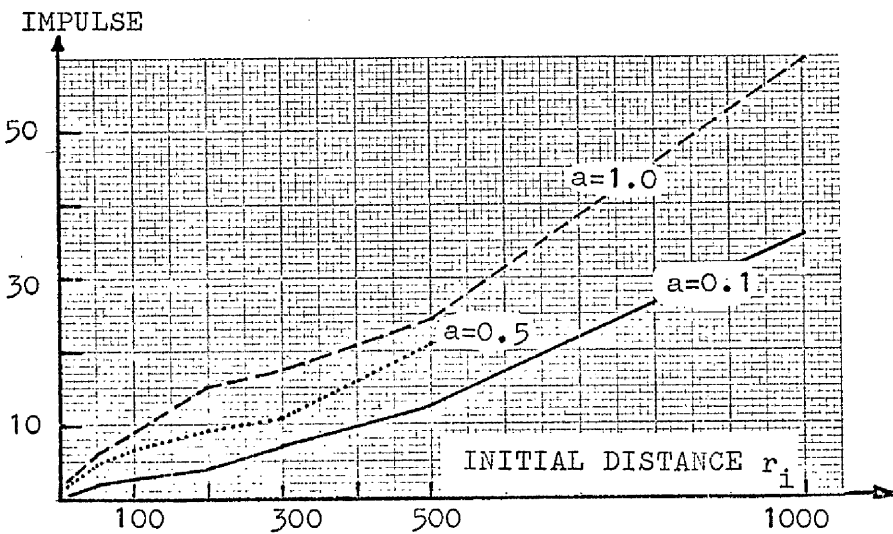
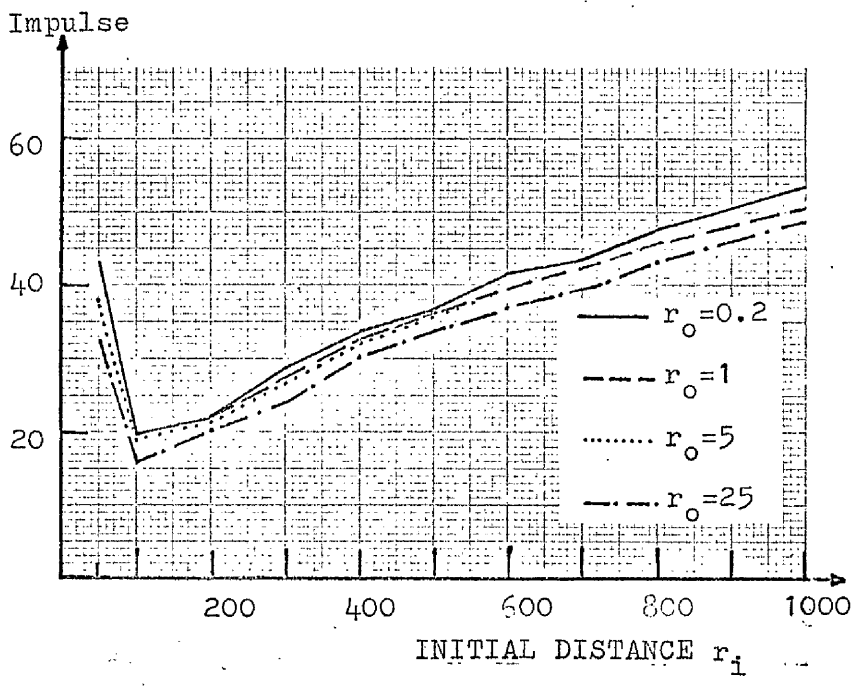
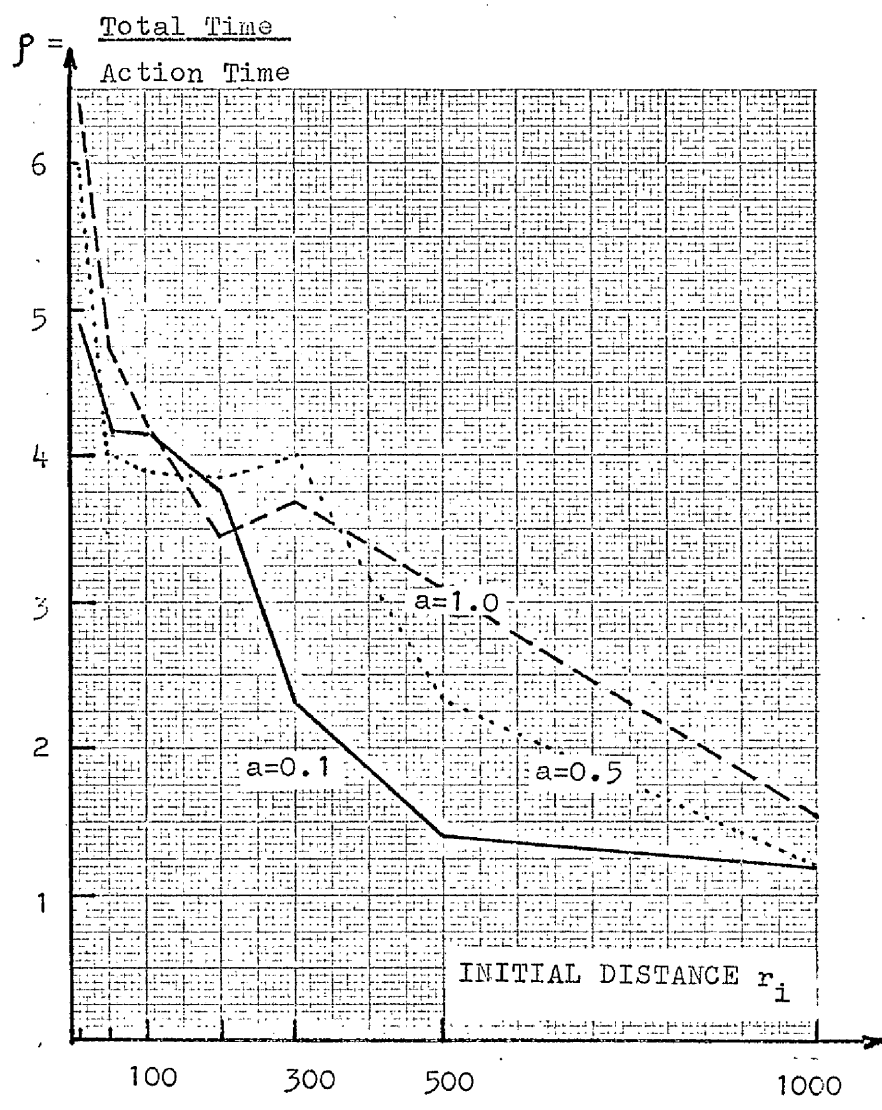


Fig. III.5



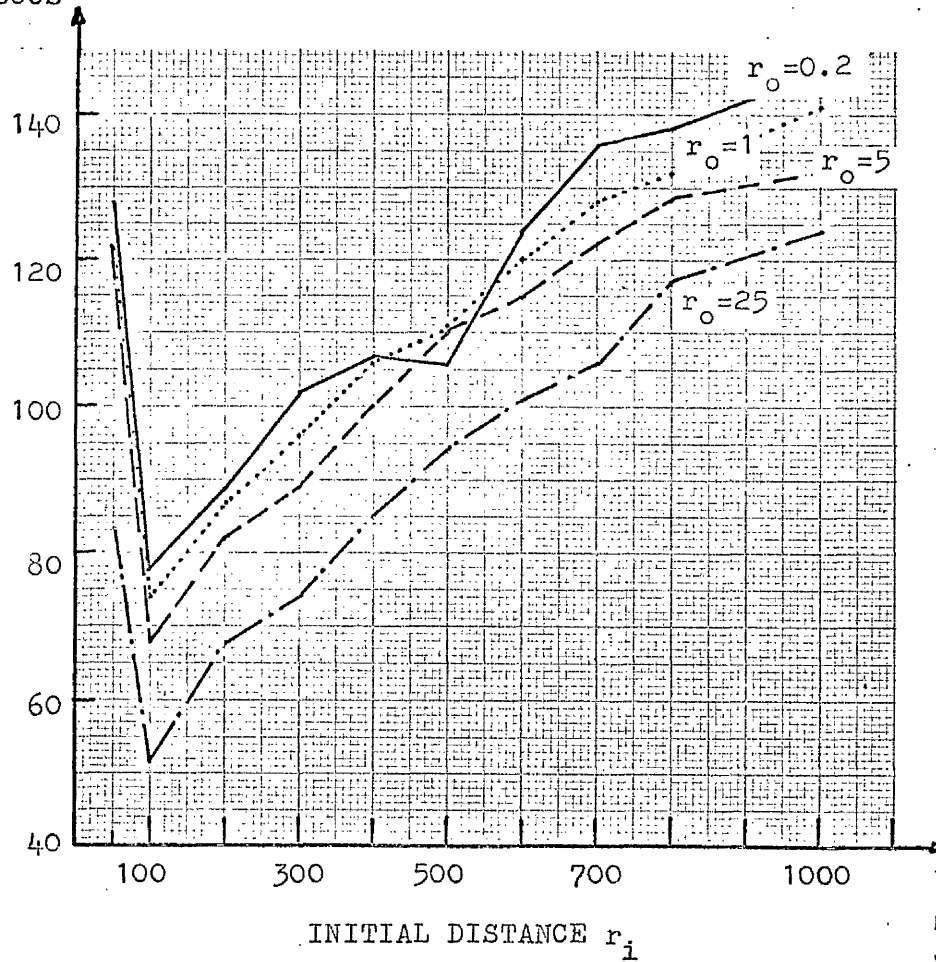
$v_i = 5$
 $\beta = 50^\circ$
 $a = 0.5$
 $\sigma = 0.02$
 $t_f = 0.1$
 $t_o = 1$
 $\theta_o = 3 \cdot 10^{-4}$
 $r_o = 1$

Fig.III.6



$r_i = 100$
 $v_i = 0$
 $\sigma = 0.05$
 $t_f = 0.1$
 $t_o = 1$
 $\theta_o = 3 \cdot 10^{-4}$
 $r_o = 1$

Fig.III.7



INITIAL DISTANCE r_i

$v_i = 5$
 $\beta = 50^\circ$
 $a = 0.5$
 $\sigma = 0.02$
 $t_f = 0.1$
 $t_o = 1$
 $\theta_o = 3.10$

Fig. III.8

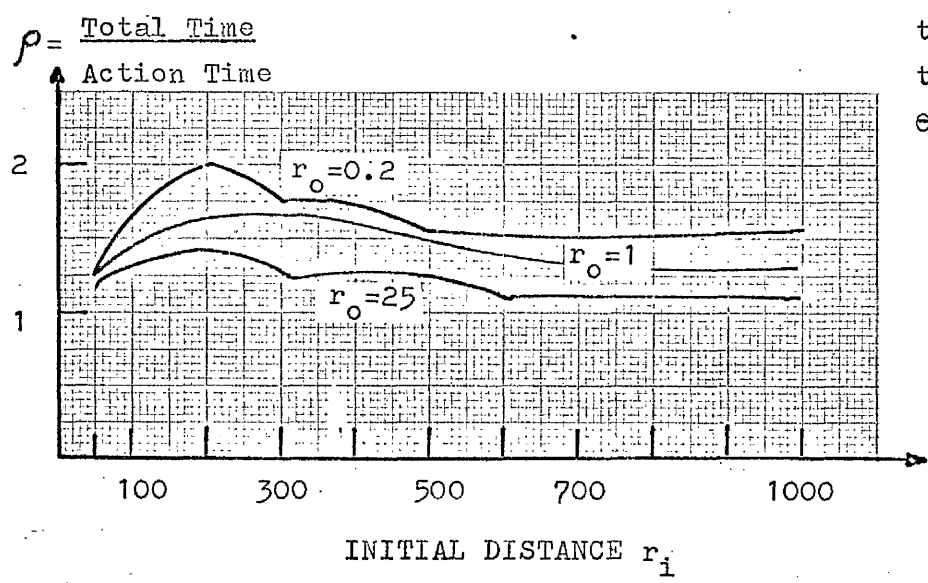


Fig. III.9

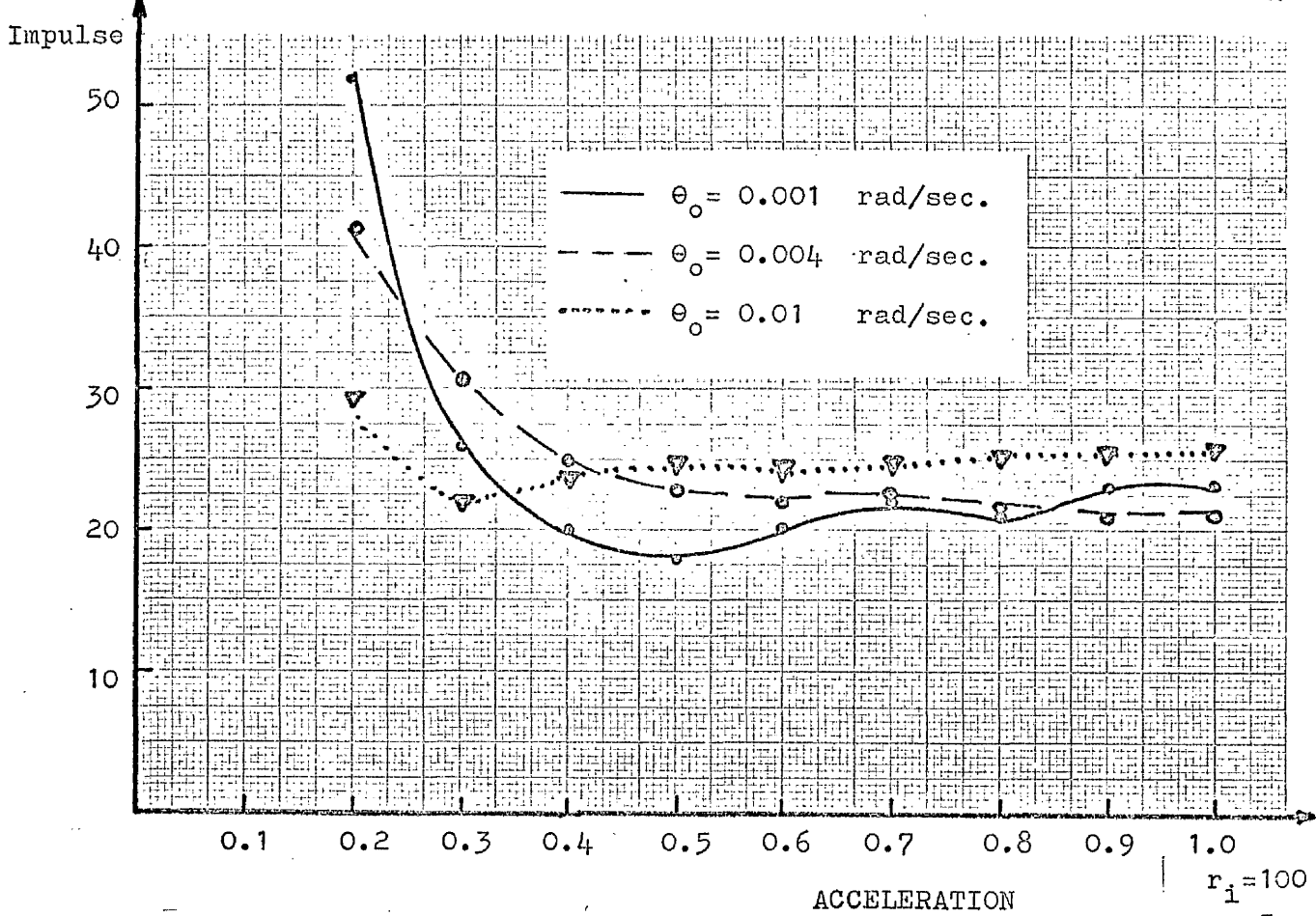


Fig.III.10

$r_i = 100$
 $v_i = 5$
 $\beta = 50^\circ$
 $\sigma = 0.05$
 $t_f = 0.1$
 $t_0 = 1$
 $r_0 = 1$

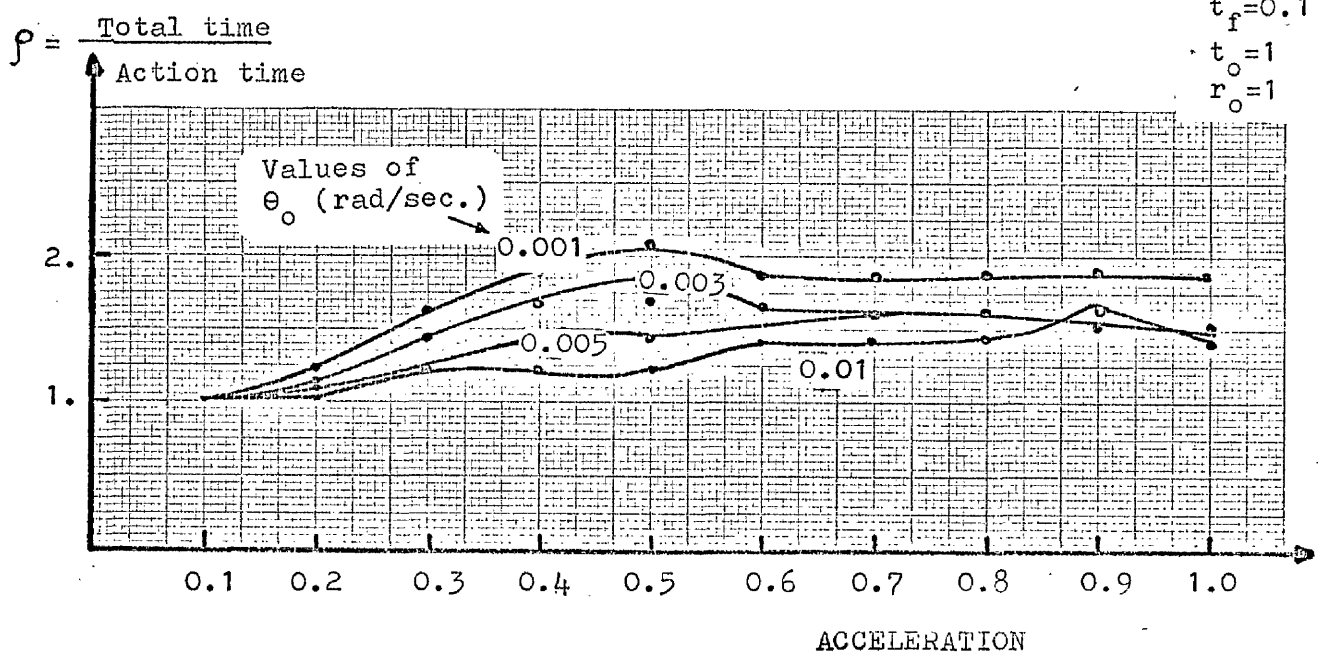


Fig.III.11

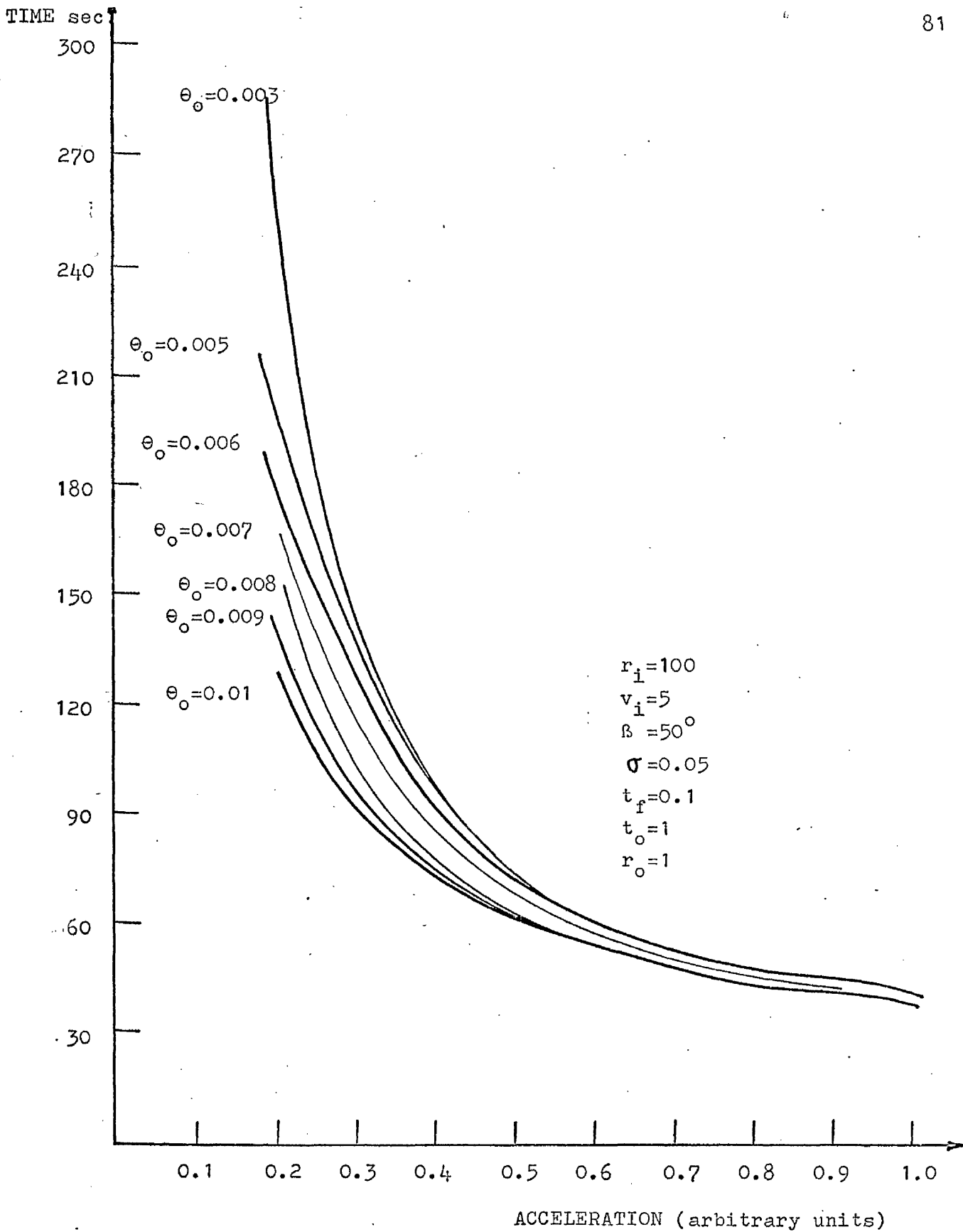
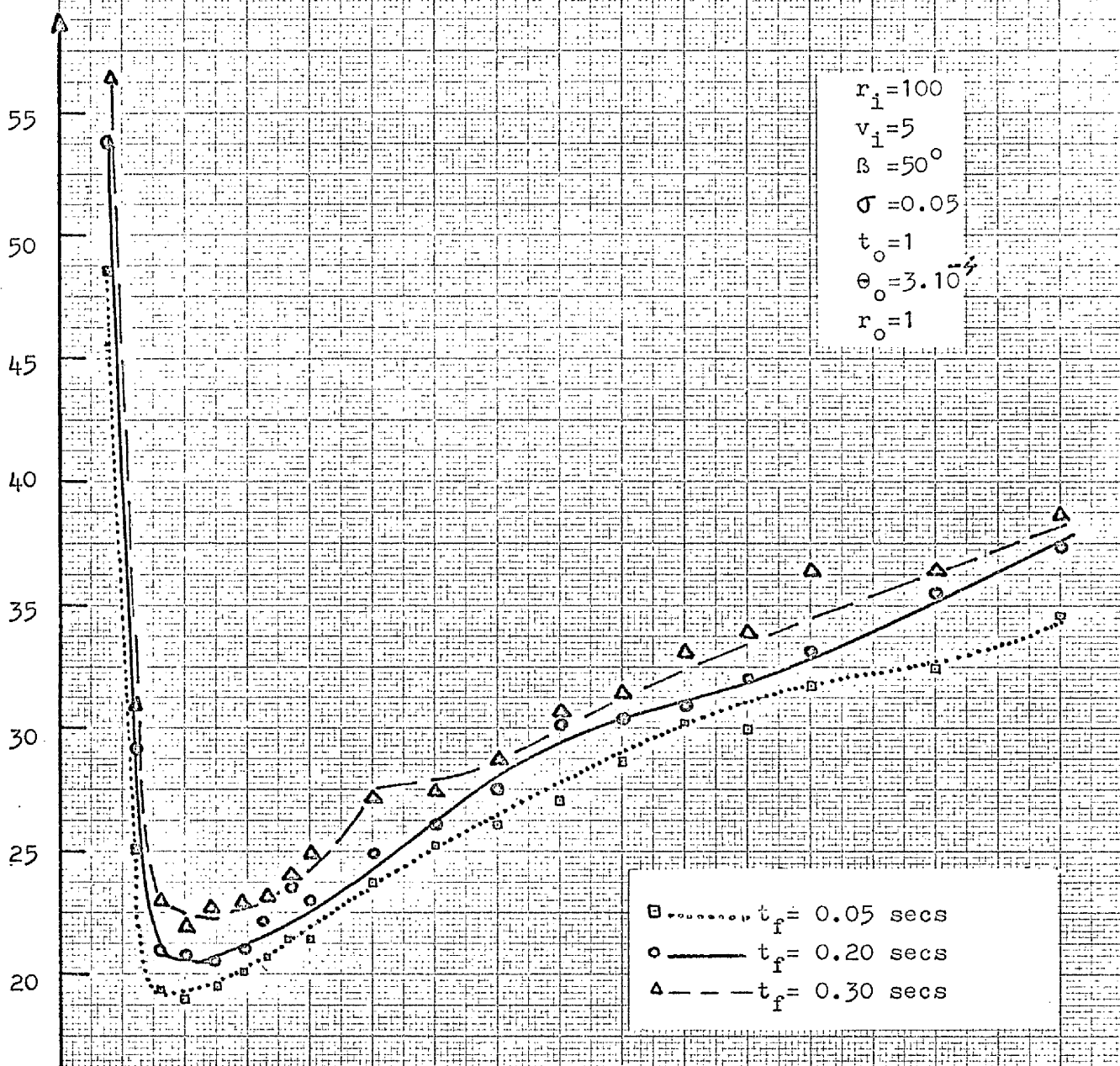


Fig.III.12

Impulse



$$\rho = \frac{\text{Total time}}{\text{Action time}}$$

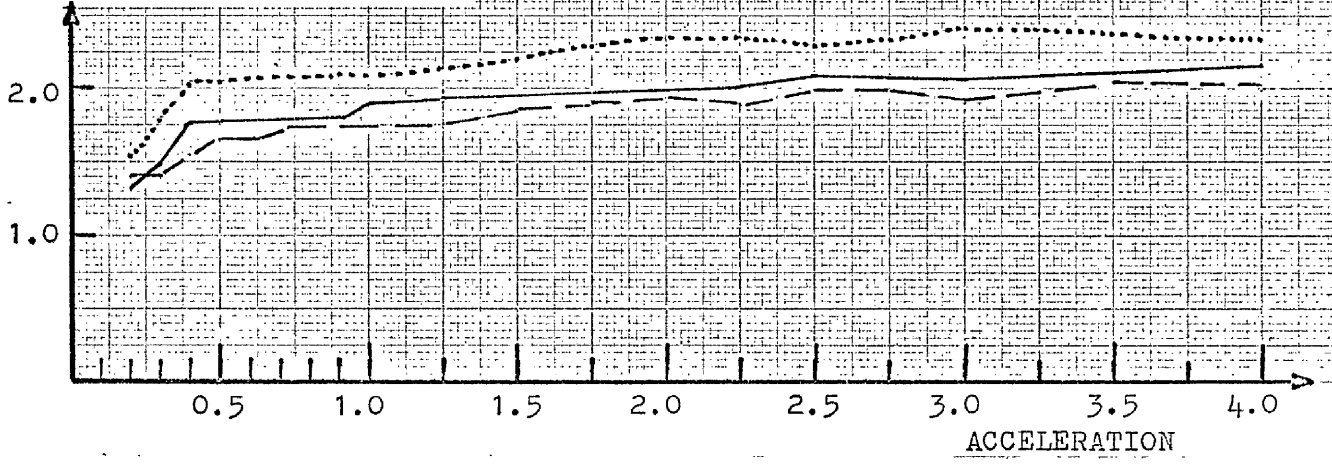


Fig.III.13

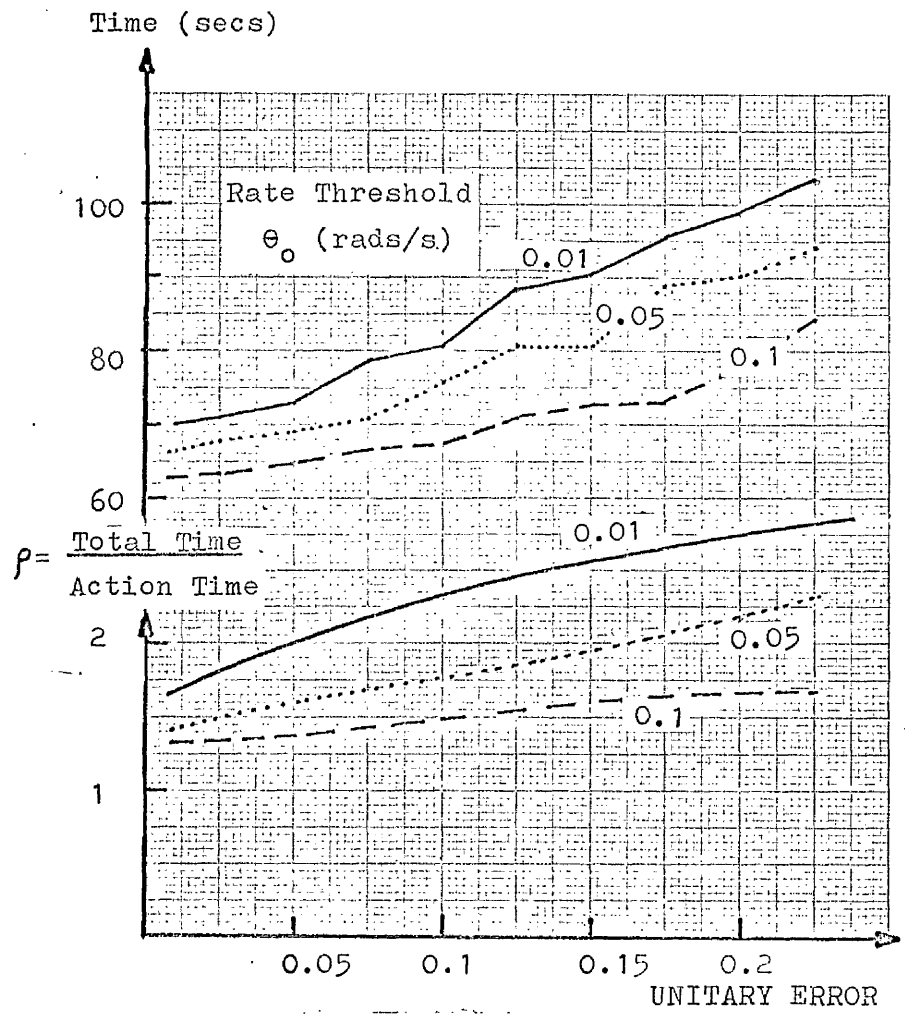


Fig.III.14

$r_i = 100$
 $v_i = 5$
 $\beta = 50^\circ$
 $a = 0.5$
 $t_f = 0.1$
 $t_0 = 1$
 $r_0 = 1$

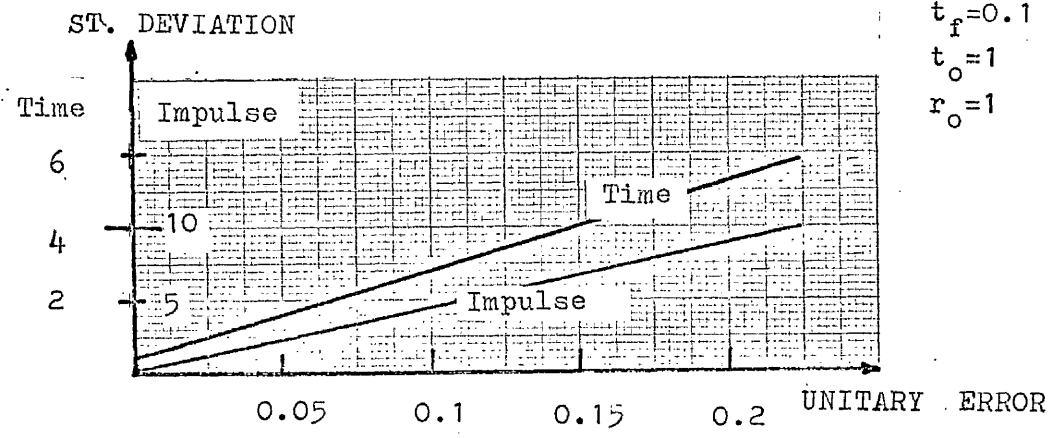


Fig.III.15

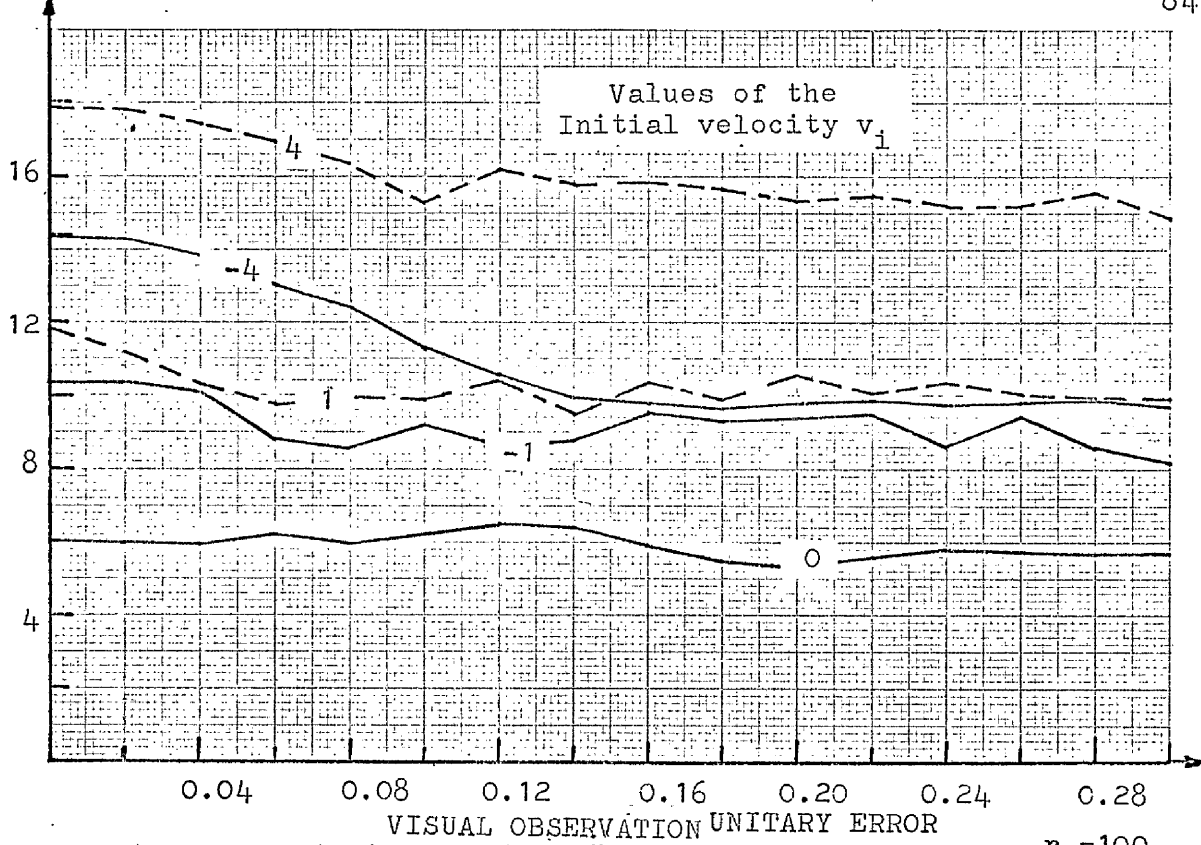


Fig.III.16

$r_i = 100$
 $B = 50^\circ$
 $a = 0.5$
 $t_f = 0.1$
 $t_o = 1$
 $e_o = 3 \cdot 10^{-4}$
 $r_o = 1$

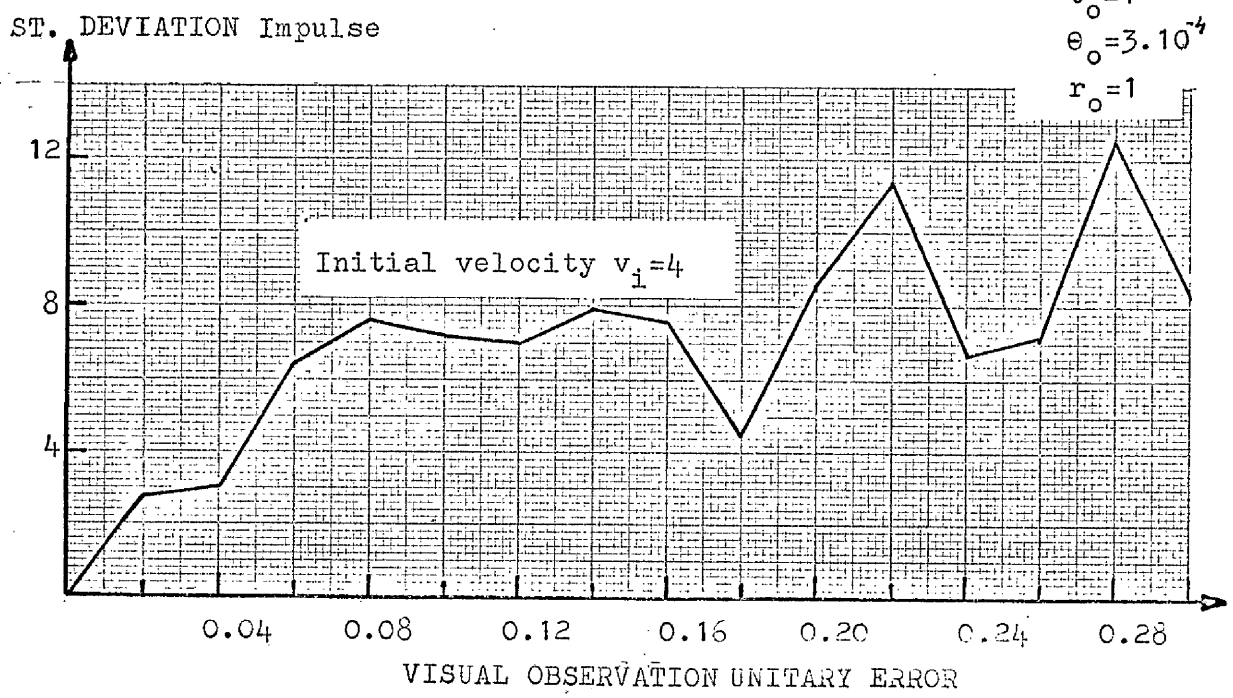


Fig.III.17

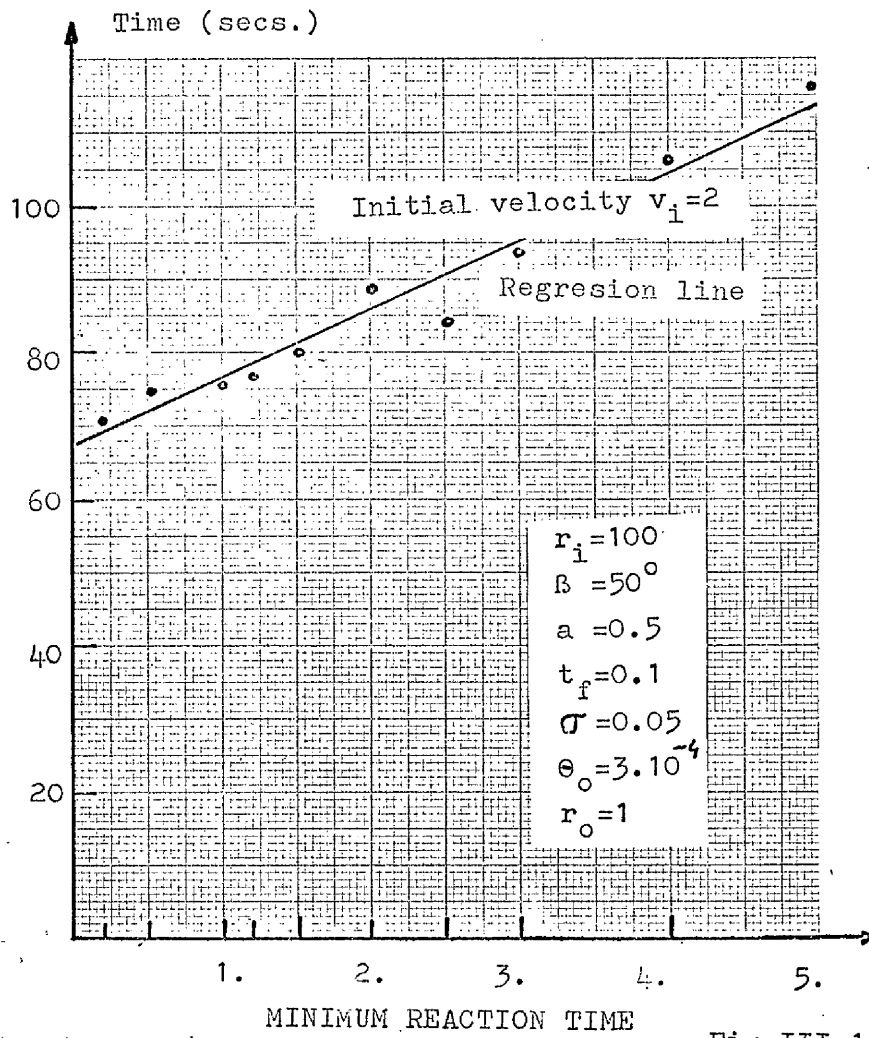


Fig.III.18

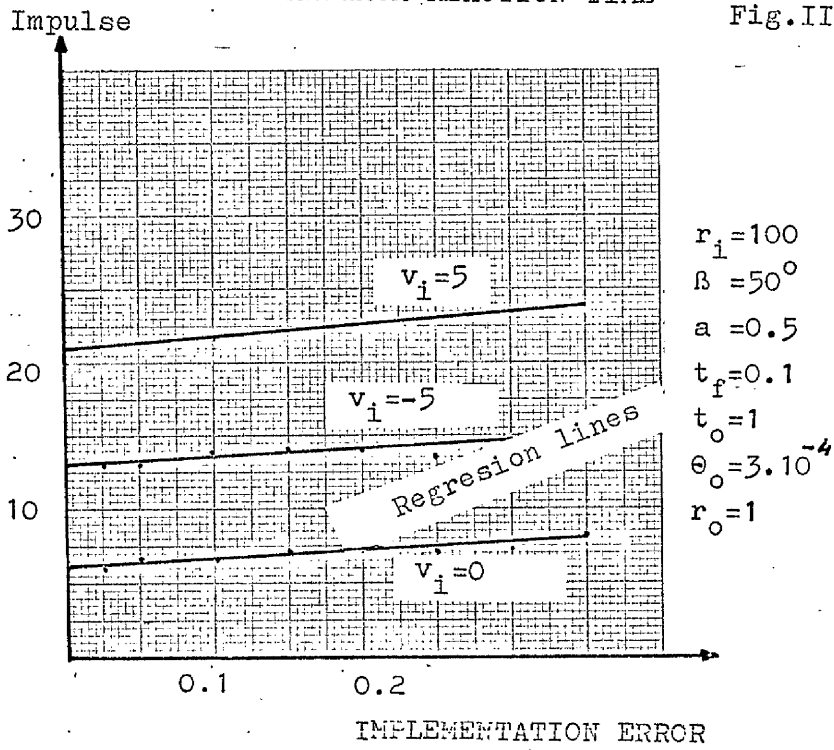


Fig.III.19

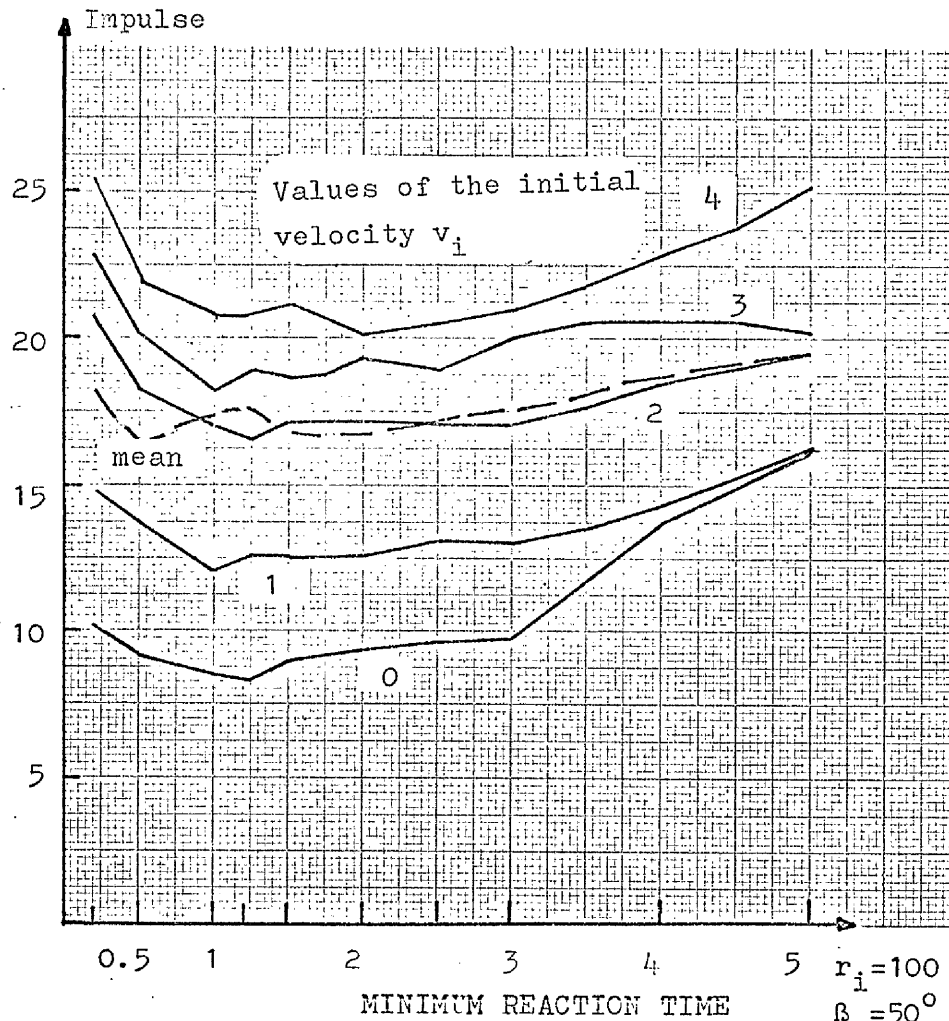


Fig. III.20

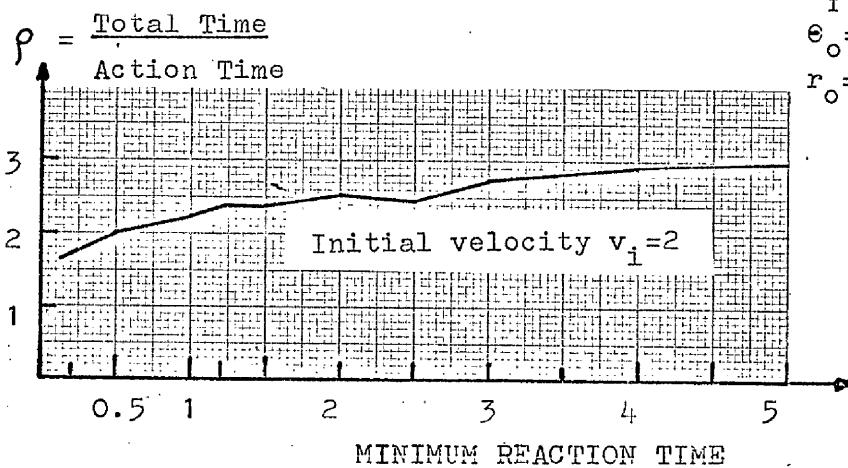


Fig. III.21

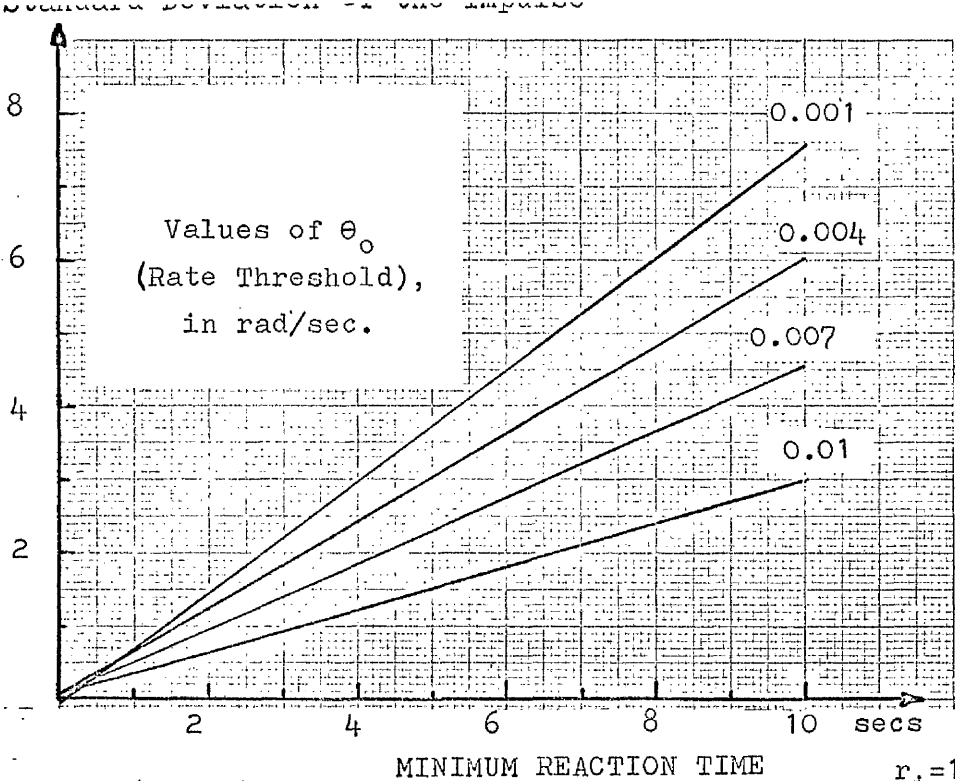


Fig.III.22

$$\rho = \frac{\text{Total Time}}{\text{Action Time}}$$

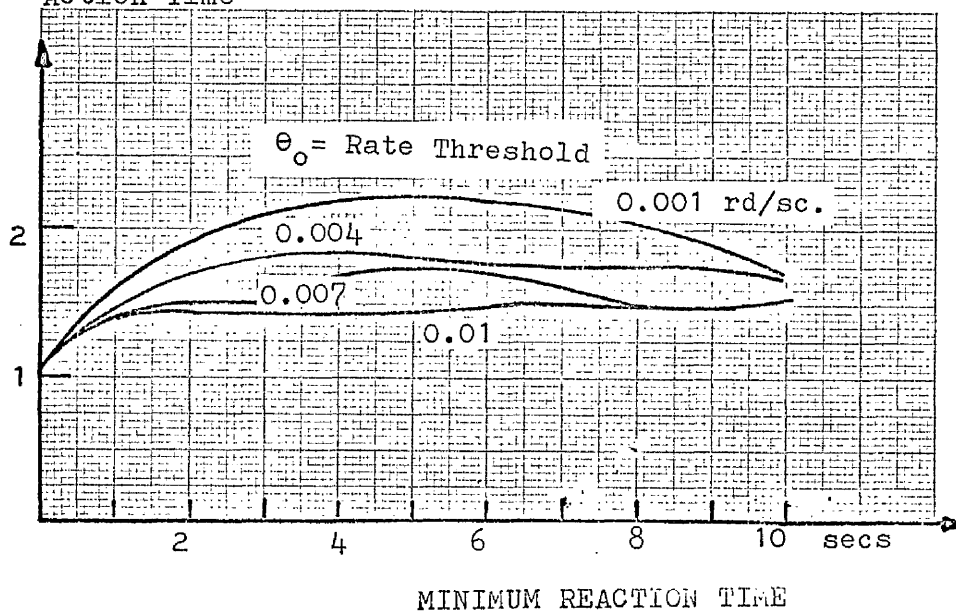


Fig.III.23

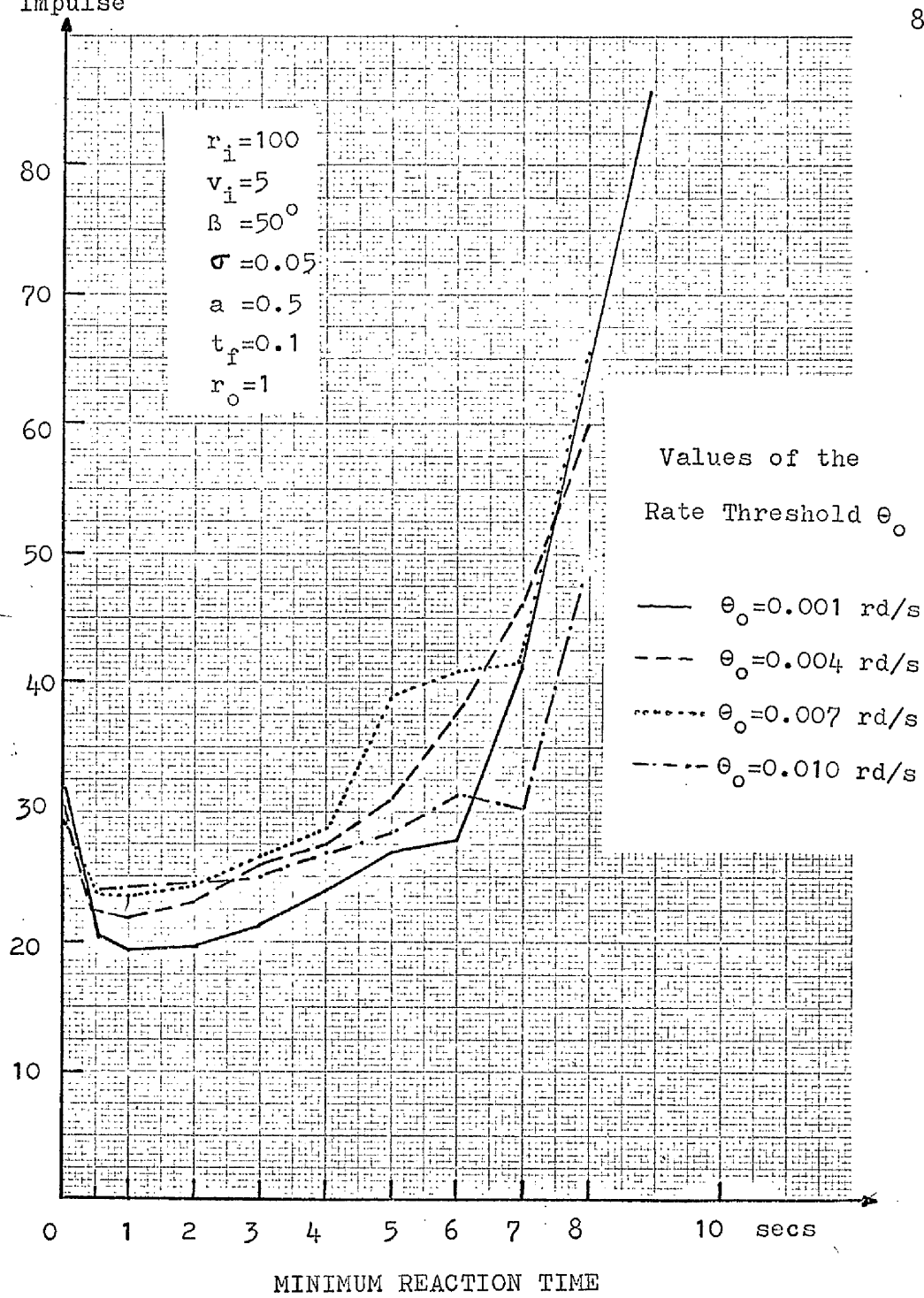


Fig III.24

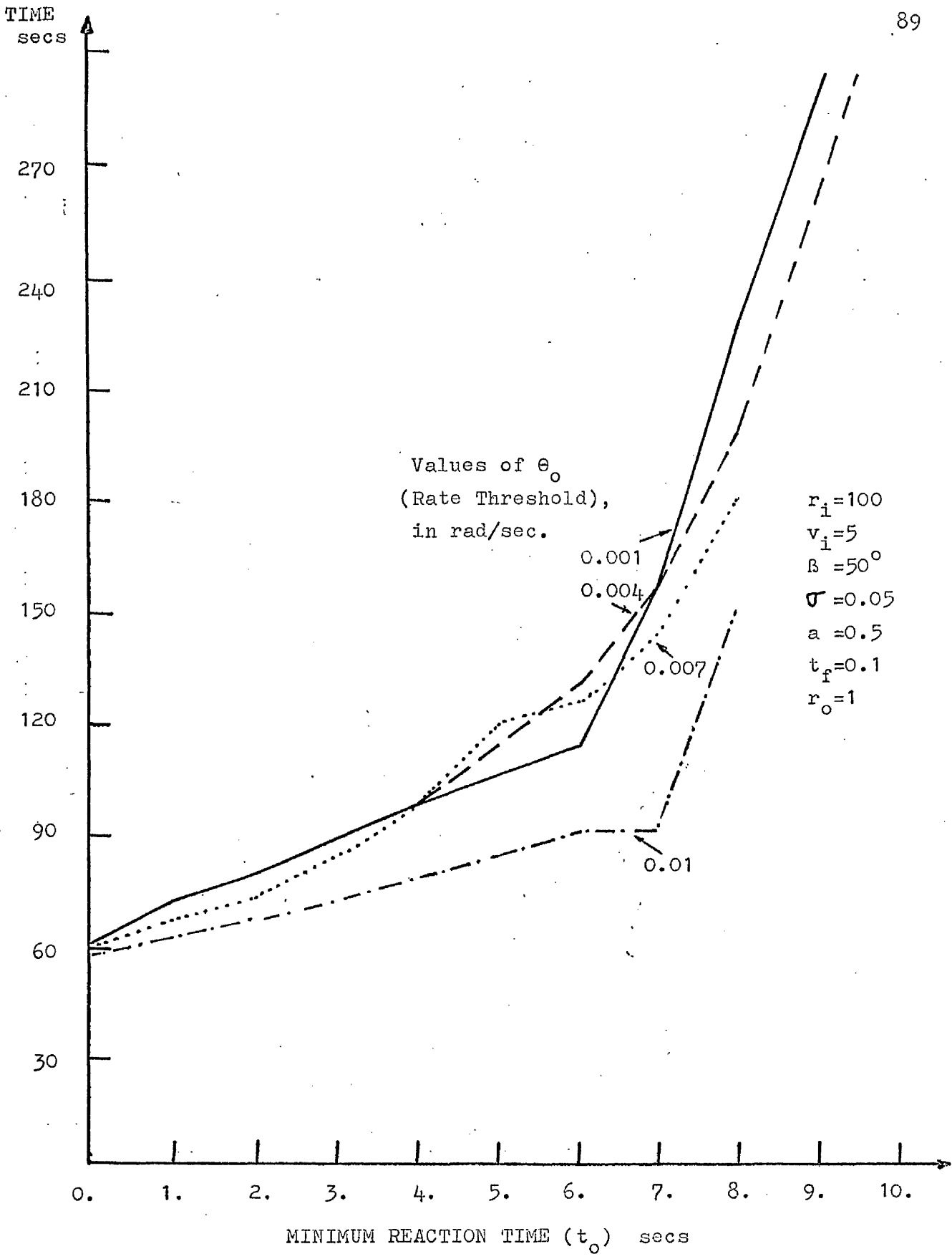


Fig.III.25

$v_i = 5$
 $\beta = 45^\circ$
 $\sigma = 0$
 $r_0 = 1$
 $v_0 = 1$

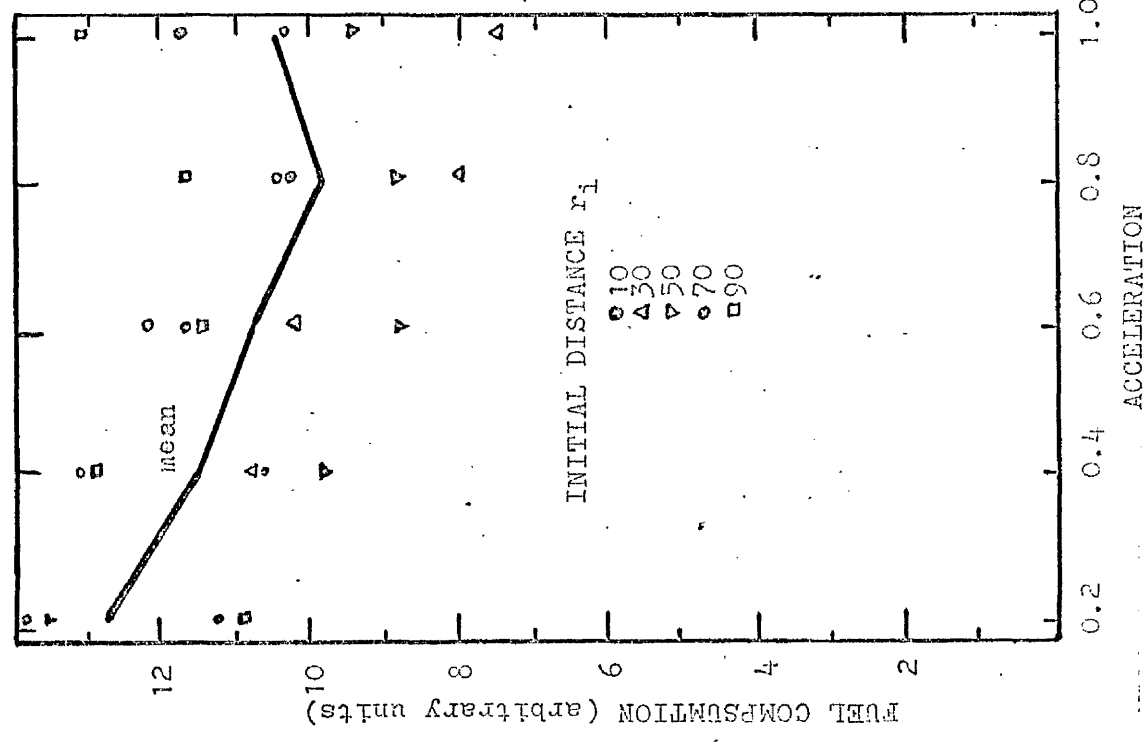


Fig. III.27

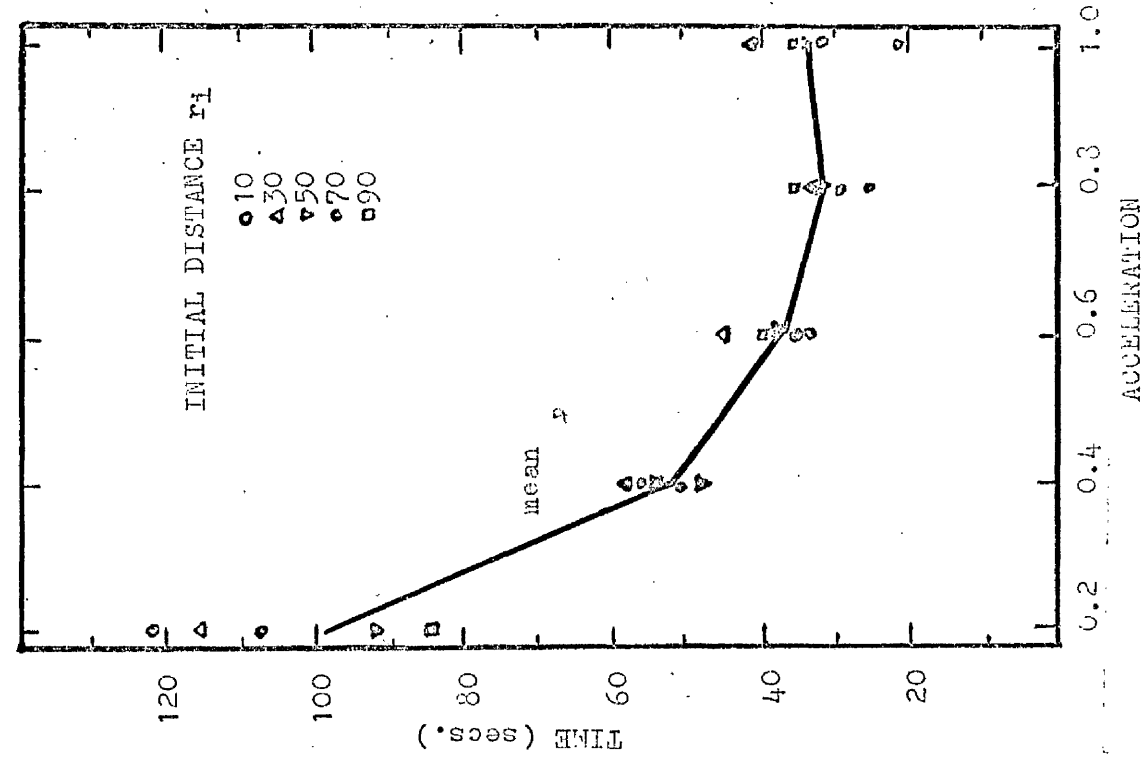


Fig. III.26

TABLE III.1 Results of 100 analog experiments (Time)

initial distance →							
acceleration ↓		10	30	50	70	90	mean
0.2		92.9	145.6	135.9	90.2	102.1	
		115.2	108.2	107.4	89.9	80.1	
		87.6	100.1	119.2	84.3	71.1	
		137.8	134.1	99.8	102.9	88.1	
	mean...	108.37	122.0	115.57	91.8	85.35	104.62
0.4		56.1	48.4	51.0	47.2	50.2	
		50.8	43.1	49.6	47.8	55.3	
		60.5	44.6	51.9	46.0	58.4	
		64.2	53.3	56.7	49.6	60.0	
	mean...	57.9	47.4	52.3	47.6	56.0	52.23
0.6		50.4	36.8	32.9	36.3	34.7	
		52.6	34.8	37.1	35.4	37.7	
		38.5	27.4	37.7	35.6	53.4	
		40.7	39.4	28.9	35.1	38.2	
	mean...	45.5	34.6	34.1	35.6	41.0	38.18
0.8		37.3	25.6	25.6	35.4	47.4	
		40.3	30.4	27.2	29.6	33.1	
		28.2	28.4	26.5	34.3	32.8	
		29.8	34.0	26.3	34.8	31.7	
	mean...	33.9	29.6	26.4	33.5	36.2	31.93
1.0		46.4	21.6	41.7	31.1	35.8	
		52.9	21.8	27.6	28.7	26.7	
		34.0	19.9	34.9	37.2	31.8	
		34.3	25.6	26.1	38.7	45.6	
	mean...	41.9	22.2	32.6	33.9	34.9	33.12
mean		57.5	51.1	52.2	48.5	50.7	52.01

TABLE III.2. Results of 100 analog experiments (Impulse)

initial distance acceleration ↓	10	30	50	70	90	mean
0.2	14.10	11.98	12.94	10.85	10.74	
	17.52	16.66	13.42	11.45	11.42	
	14.80	15.65	11.50	11.59	9.14	
	9.72	15.00	11.89	11.47	12.62	
	mean...	14.03	14.82	12.44	11.34	10.92
0.4	13.58	10.13	10.17	11.08	13.62	
	13.94	10.43	7.66	11.40	11.24	
	11.40	11.48	10.44	10.75	14.40	
	13.32	11.62	11.25	9.76	13.09	
	mean...	13.06	10.91	9.88	10.75	13.09
0.6	10.78	8.44	8.38	8.06	11.27	
	11.64	10.29	8.99	14.07	13.12	
	12.32	9.44	9.70	13.71	11.23	
	14.28	9.06	8.22	11.23	10.79	
	mean...	12.25	9.31	8.82	11.77	11.60
0.8	9.77	7.48	11.20	10.75	12.50	
	10.80	7.52	8.34	8.55	11.58	
	10.82	9.81	8.20	9.89	11.65	
	10.53	7.36	7.73	12.43	11.58	
	mean...	10.48	8.04	8.87	10.40	11.83
1.0	10.69	6.74	11.18	9.97	12.38	
	9.80	8.15	9.50	15.52	12.75	
	10.35	6.01	9.70	11.47	15.97	
	11.12	9.22	7.58	10.23	11.75	
	mean...	10.49	7.53	9.49	11.80	13.21
mean	12.06	10.12	9.90	11.21	12.13	11.08

TABLE III.3 Effect of Target Size

v_i	α_0	Time	Action Time	Impulse	
3.	5	51.3	18.5	9.25	
3.	15	51.9	17.6	8.80	$r_i=100$
3.	25	51.6	19.2	9.60	$B=50^\circ$
3.	35	52.1	19.6	9.80	$\sigma=0.05$
3.	40	51.9	18.2	9.10	$a=0.5$
3.5	10	53.5	19.1	9.50	$t_f=0.1$
3.5	15	53.4	19.8	9.90	$t_0=1$
3.5	25	53.9	19.6	9.80	$\theta_0=3.10^{-4}$
3.5	30	52.6	20.2	10.00	$r_0=1$
3.5	50	54.9	20.5	10.00	
4.	1	55.0	20.4	10.20	
4.	10	56.2	21.6	10.70	
4.	20	55.3	21.3	10.70	
4.	25	54.7	20.6	10.00	
4.	35	56.2	20.0	10.00	
4.	40	54.8	20.7	10.40	
4.	50	55.0	20.6	10.00	
5.	1	45.0	26.3	13.10	
5.	5	44.5	24.8	12.40	
5.	10	45.1	27.1	13.50	
5.	15	44.5	25.6	12.80	
5.	20	44.3	28.3	14.10	
5.	25	43.7	26.9	13.40	
5.	30	45.0	26.6	13.30	
5.	35	44.4	24.9	12.40	

REFERENCES

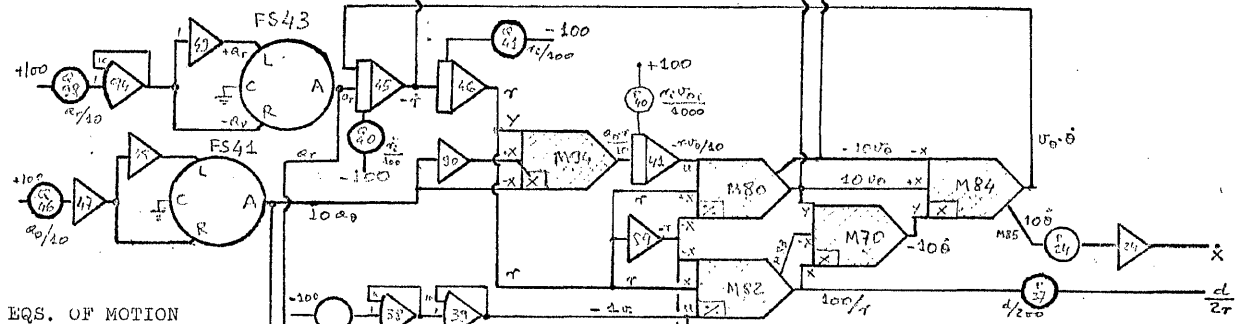
- (1) Bioastronautics Data Book
NASA SP-3006 1964
- (2) Gemini Summary Conference
NASA SP-138 Feb.1967
- (3) Summary of Gemini Extravehicular Activity
NASA SP-149 1967
- (4) Wortz, Browne, Schreck, Macek, Robertson and Gafvert
"Study of Astronaut Capabilities to Perform Extravehicular
Maintenance and Assembly Functions' in Weightless
Conditions"
NASA CR-859 Sept. 1967
- (5) Loats, Mattingly and Hay
"Correlation Study of the Simulation of Gemini
Extravehicular Activity with Flight Results"
NASA CR-1146 Feb. 1969
- (6) Wortz, Schreck, Robertson, Lamb and Brownie
"A Study of Astronauts' Extravehicular Work
Capabilities in Weightless Conditions"
NASA CR-1334 May 1969
- (7) Leonov and Lebedev
"Perception of Space and Time in Outer Space"
Nauka Press. Moscow.1968
NASA TTF-545 May 1969
- (8) Trout and Bearley
"Simulation of Gemini Extravehicular Tasks by
Neutral-Buoyancy Techniques"
NASA TND-5235 June 1969

Appendix A: ANALOG PATCH PANEL and SIMULATION RECORDS

Table A.1 POTENTIOMETER ADJUSTMENT

Pot.	Variable	Setting
Q13		0.21
Q23		"
P29		"
Q29		"
Q33		"
Q34		"
Q14		0.40
Q27		"
Q12		"
Q79		"
P11		"
Q44		"
Q19		0.15
P56		0.7 (adjust for stable sinusoid amplitude)
P21	x_{1i}	0.1
P26	x_{2i}	0.0
P31	x_{3i}	0.1
Q87	y_{1i}	0.1
Q88	y_{2i}	0.1
Q89	y_{3i}	0.2
Q10	Sinusoid Ampl.	0.90
P37	$\alpha/200$	0.99
P22		0.99
Q97	r_o	0.99
Q09	$v_o^2/10$	0.10
Q98	$a_r/10$	
Q40	$\dot{r}_i/100$	
Q41	$r_i/100$	
P40	$r_i v_{ei}/1000$	
Q46	$a_e/10$	
P64	In IC mode, adjust for T16 = $-a_e$	
P61	" " " " T17 = $-a_r$	

VELOCITY TEST



EQS. OF MOTION

RENDEZVOUS

IMPULSE CONSUMPTION

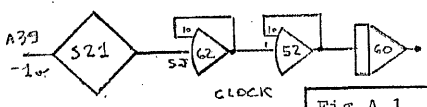
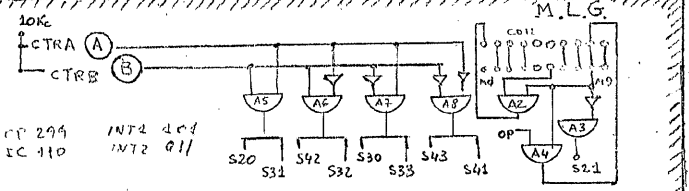
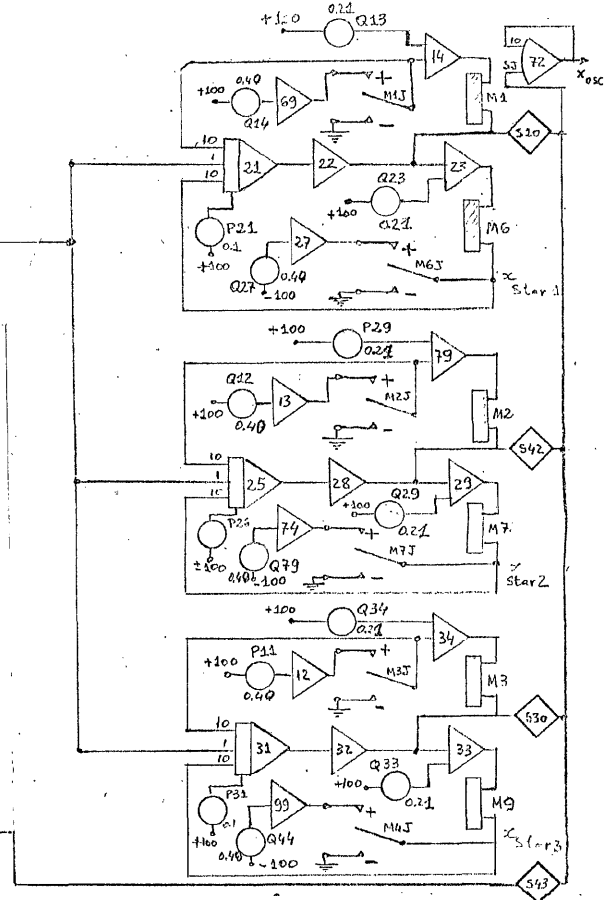
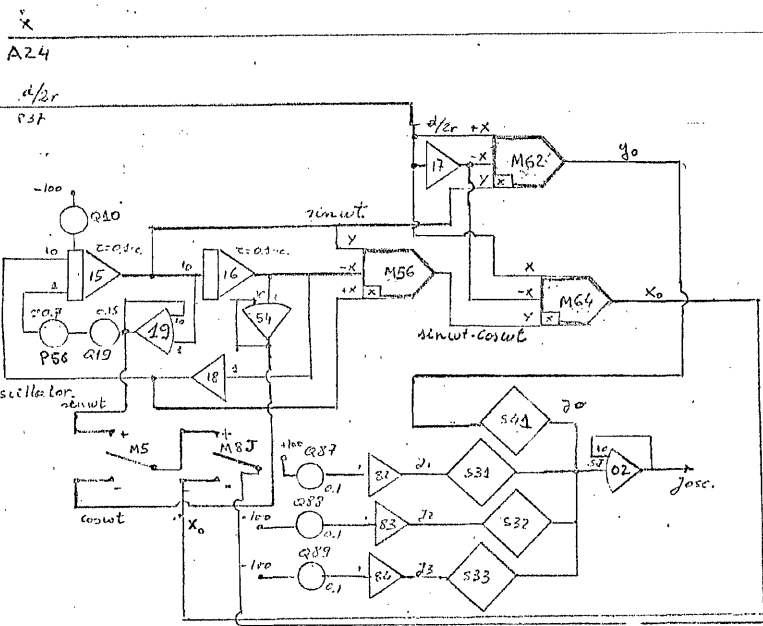
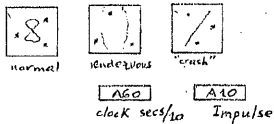
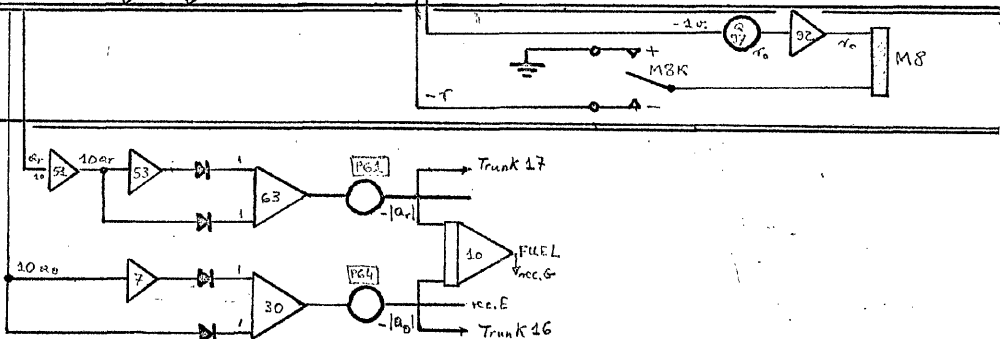


Fig. A.1. ANALOG PATCH PANEL

r

v^2

v_θ

v_r

a_θ

a_r

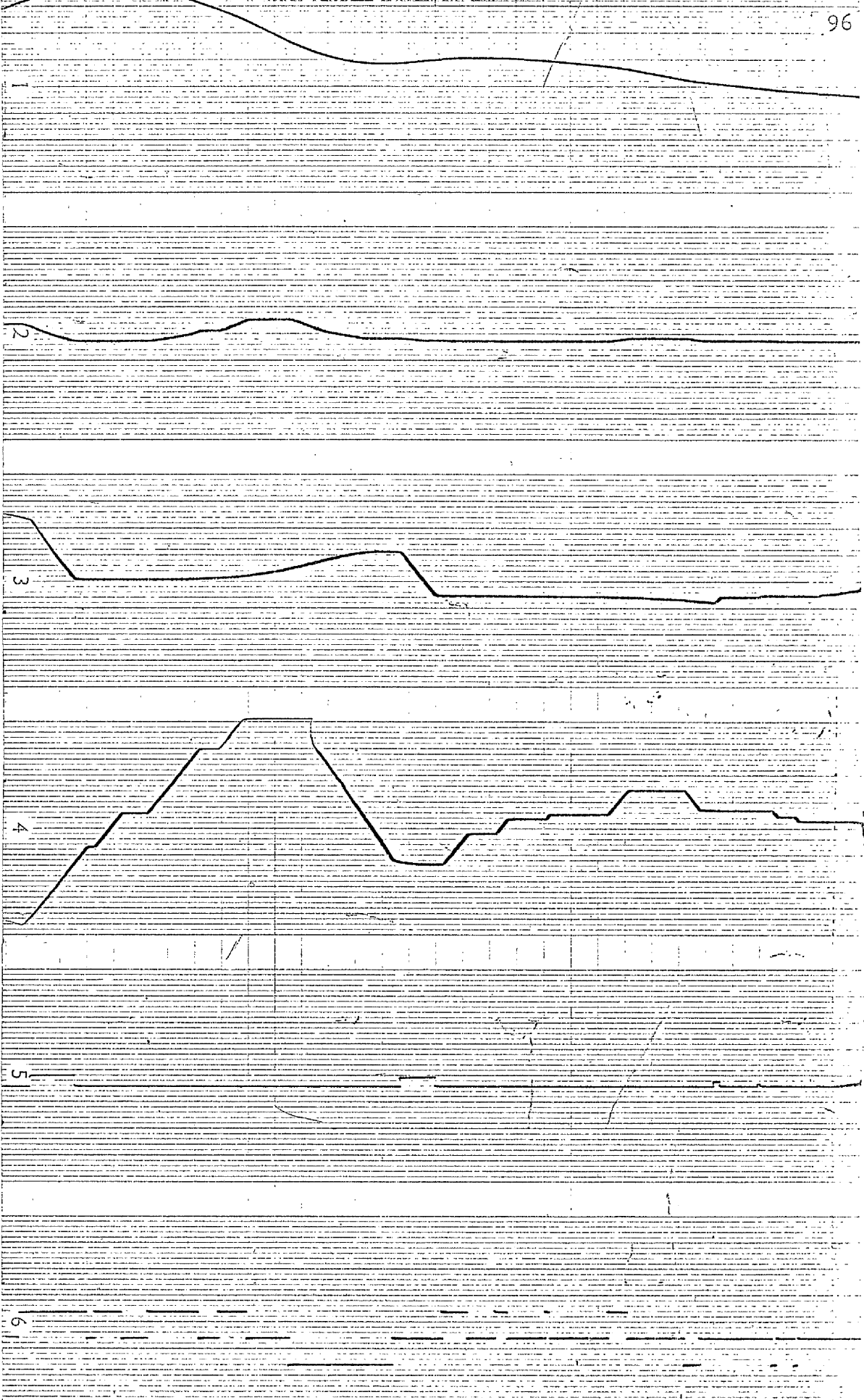


Fig A.2. Typical record of Analog Simulation

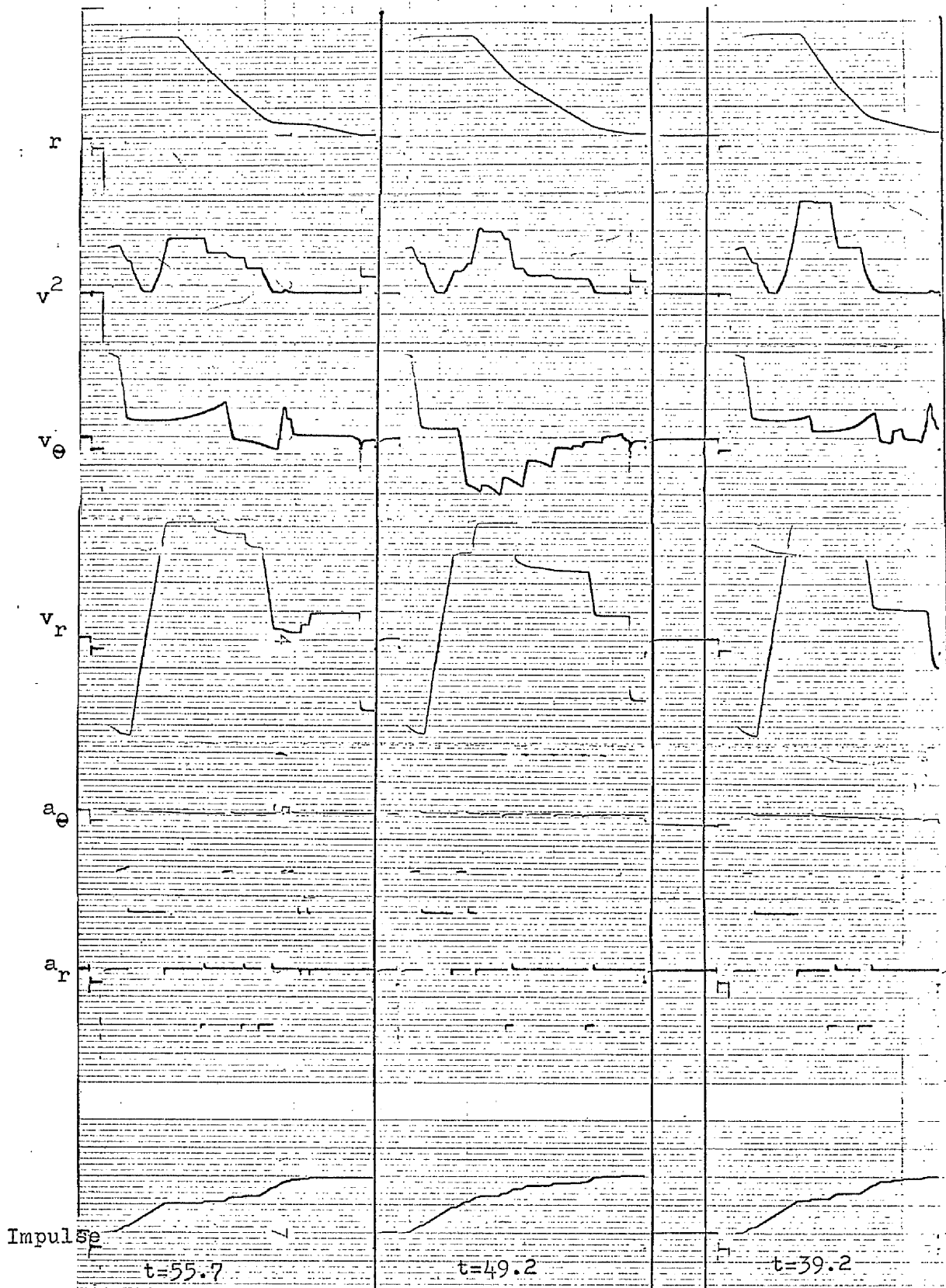


Fig. A.3. Typical records of Analog Simulation

Appendix B

GENERAL IMAGE POINT MOTION

The motion of the image point in $(\dot{\theta}, \dot{\varphi}, \varphi)$ space is given for the free motion in para. I.2.1. If the motion is forced we cannot in general determine the motion uniquely, since we do not necessarily know the time history of the applied acceleration. However we may determine the instantaneous direction of motion of the image point at any given coordinate $(\dot{\theta}, \dot{\varphi}, \varphi)$. This is relevant to the problem of finding whether the decision boundaries involve the possibility of looping (as in para. I.3.). Since the image point motion has a component in the φ -direction, one cannot determine the component of motion perpendicular to the boundaries without a knowledge of their variation in shape with φ .

For the particular decision boundaries that we choose (para. I.4.). We may determine that, on these boundaries, $\dot{\theta}/\varphi^{1/2}$ and $\dot{\varphi}/\varphi^{3/2}$ are constants, and consequently if we determine the direction of image point motion in terms of these "normalized" values of $\dot{\theta}$ and $\dot{\varphi}$, then in effect we are resolving the motion of the image point into components perpendicular and parallel to the boundary.

Now

$$\frac{d(\dot{\theta}/\varphi^{1/2})}{dt} = \frac{\ddot{\theta}}{\varphi^{1/2}} - \frac{\dot{\theta}\dot{\varphi}}{2\varphi^{3/2}} = \frac{dy}{dt}, \text{ say}$$

and

$$\frac{d(\dot{\varphi}/\varphi^{3/2})}{dt} = \frac{\ddot{\varphi}}{\varphi^{3/2}} - \frac{3\dot{\varphi}^2}{2\varphi^{5/2}} = \frac{dx}{dt}, \text{ say}$$

and from the equations of motion:

$$\Delta \dot{\theta} \approx \ddot{\theta} = \frac{2\dot{\theta}\dot{\varphi}}{\varphi} + \frac{a_{\theta}}{\alpha_0} \varphi$$

$$\Delta \dot{\varphi} \approx \ddot{\varphi} = \frac{2\dot{\varphi}^2}{\varphi} - \varphi\dot{\theta}^2 - \frac{a_r}{\alpha} \varphi^3$$

Hence

$$\frac{dy}{dx} = \frac{\frac{3}{2} \frac{\dot{\theta}\dot{\varphi}}{\varphi^{3/2}} + \frac{a_{\theta}}{\alpha_0} \varphi^{1/2}}{\frac{\dot{\varphi}^2}{2\varphi^{5/2}} - \frac{\dot{\theta}^2}{\varphi^{1/2}} - \frac{a_r}{\alpha_0} \varphi^{1/2}}$$

and with $a_r = a_{\theta} = 0$ we obtain

$$\frac{dy}{dx} = \frac{3xy}{x^2 - 2y^2}$$

On integrating this differential equation we obtain

$$x^2 = (C - \ln y)y^2$$

loci of directions sketched in fig. B.1

If the thrusts are impulsive then the directions of motion are as shown in the text fig. I.10. Clearly in conditions where the thrust is finite, the loci of directions will be intermediate between these two extremes as sketched in fig. B.2.

It is interesting to note that with $f_1=1$ and $f_2=0.5$, the diagonal line representing an image point free motion in the direction of the $\dot{\theta}$ - axis passes through the corner of the decision diagram.

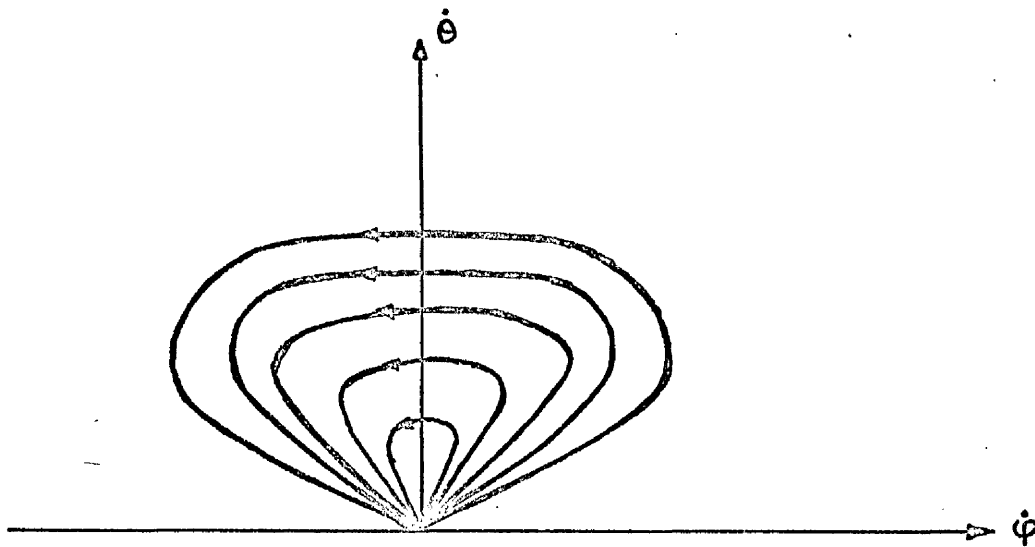


Fig.B.1. Loci of Image Point Directions. No Thrust

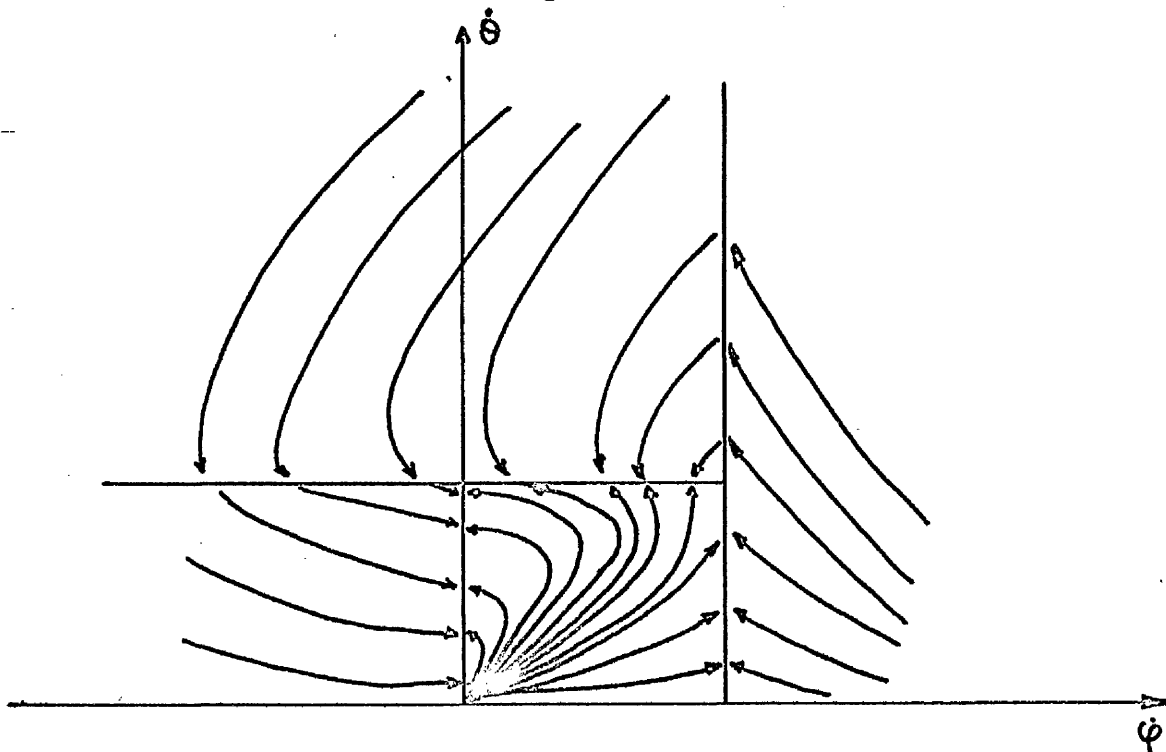


Fig.B.2. Loci of Image Point Directions. Finite Thrust

APPENDIX CDIGITAL SAMPLE SIZE

With the purpose of determining the number of samples able to give a reliable statistics we chose a random set of variables which produced the following values of rendezvous time for the different sized samples:

<u>Sample Size N</u>	<u>Mean Time μ</u>	<u>Standard Deviation</u>
10	168.1	7.62
20	168.5	8.95
30	168.5	9.99
40	171.3	10.67
50	170.8	11.33
60	171.9	10.72
70	168.3	7.80
80	170.5	9.78
90	170.8	9.78
100	168.2	8.20

Comparing the two samples of size $N_1 = 10$ and each one of the remaining and testing the hypothesis

$$H_0 : \mu_1 - \mu_2 = 0 \quad (\text{The difference of means is due merely to chance})$$

$$H_1 : \mu_1 - \mu_2 \neq 0 \quad (\text{There is a significant difference})$$

we can tabulate for the remaining samples the difference of sample means, the standard deviation of the difference of means

$$\sigma_{\bar{\mu}_1 - \bar{\mu}_2} = \sqrt{\frac{\sigma_1^2}{N_1} + \frac{\sigma_2^2}{N_2}}$$

(using the sample standard deviations as estimates of σ_1 and σ_2), and the standardized variable $z = (\bar{\mu}_1 - \bar{\mu}_2) / (\sigma_{\bar{\mu}_1 - \bar{\mu}_2})$, obtaining that for a two-tailed test, the results are significant at a 0.5 level. Hence we conclude that it is enough to take samples of 10 digital simulations.

APPENDIX D: DIGITAL PROGRAM

Table D.1.

DIGITAL DATA CARDS TABLE

<u>Card</u>	<u>Parameter</u>	<u>Format</u>
1	XM1,XO1 (Axis scale for graphs)	2E10.3
2	XM2,XO2 id.	2E10.3
3	YMT,YOT id. Y-axis (Time)	2E10.3
4	YMTD,YOTD id. Y-axis (st.dev. time)	2E10.3
5	YMR,YOR id. Y-axis (ρ)	2E10.3
6	YMI,YOI id. Y-axis (impulse)	2E10.3
7	YMID,YOID id. Y-axis (st.dev. impulse)	2E10.3
8	NRRAN (first random number)	I11
9	JNSIM (Number of simulations)	I11
10	TIMMAX (max time allowed for each simul.)	E11.3
11	NDDATA1 (Variable to change)	I11
12	NDDATA2 id.	I11
13 to 27	All the variables (but two), in order: r_i, v_i, β , unitary st.dev. errors observ., st.dev.errors implem., t_f, t_o , Waiting time, final rendezvous time, $\theta_{Dr}, \theta_{ot}, \alpha_o, r_o, a,$ $K_a, f_1/f_2$	E11.3
28	JNREPT (Number of repetitions each simul.)	I11
29	NE1 (Number of values for var. NDDATA1)	I11
30 to (29+NE1)	Values acquired by var.NDDATA1	E11.3
(30+NE1)	NE2 (Number of values for var. NDDATA2)	I11
(31+NE1) to (30+NE1+NE2)	Values acquired by var.NDDATA2	E11.3

Total number of cards: (30+NE1+NE2)

MAIN PROGRAM

```

1*      CALL SINGRA
2*      CALL SINFIT
3*      CALL EXIT
4*      END

```

END OF COMPILATION: NO DIAGNOSTICS.

```

1*      SUBROUTINE RENDEZ
2*      COMMON/BL1/X,Y,Z,VX,VY,VZ,ALPHA,PHI,DPHI,DTNET,ST1
3*      COMMON/BL2/PHI0,V0,THRTR,THRRD,CTE,ALPH
4*      COMMON/BL3/NRAN
5*      COMMON/BL4/KNRAN,PAR1,PAR2,ART,AST,ARF,ASF,ARI,ASI,KWRO
6*      COMMON/BL5/NE1,NE2,ARR
7*      DIMENSION DAT(30),ARR(10,2),COMB(100,2)
8*      DIMENSION SFUEL(100),SFAT(100)
9*      DIMENSION KNRAN(100),PAR1(100),PAR2(100),ART(100),AST(100)
10*     DIMENSION ARF(100),ASF(100),ARI(100),ASI(100),KWRO(100)
11*     AMODUL(X,Y,Z)=SQRT(XX**2+YY**2+ZZ**2)
12*     NSIM=1
13*     READ 63,NRAN
14*     READ 63,NJSIM
15*     READ 61,TIMMAX
16*     61  FORMAT(E11.3)
17*     READ 63,NDATA1
18*     READ 63,NDATA2
19*     63  FORMAT(I11)
20*     DO 2003 I=1,17
21*     IF((1.NE.NDATA1).AND.(1.NE.NDATA2)) READ 61,DAT(I)
22*     2003 CONTINUE
23*     READ 63,NREPT
24*     READ 63,NE1
25*     DO 2004 I=1,NE1
26*     READ 61,ARR(I,1)
27*     2004 CONTINUE
28*     READ 63,NE2
29*     DO 2005 I=1,NE2
30*     READ 61,ARR(I,2)
31*     2005 CONTINUE
32*     NE12=NE1*NE2
33*     DO 2921 I=1,NE12
34*     IC1=1+INT((I-1)/NE2)
35*     IC2=MOD(I,NE2)
36*     IF(IC2.EQ.0) IC2=NE2
37*     COMB(I,1)=ARR(IC1,1)
38*     COMB(I,2)=ARR(IC2,2)
39*     2921 CONTINUE
40*     PRINT 2807
41*     2807 FORMAT(///19H INITIAL PARAMETERS///)
42*     PRINT 2802,DAT(1),DAT(4),DAT(6),DAT(11),DAT(13),DAT(16)
43*     2802 FORMAT(6H DIST=,E14.3,4HST1=,E16.3,3HTF=,E17.3,6HTHRRD=,
44*     1E14.3,6HALPHA=,E14.3,3HCT=,E17.3)
45*     PRINT 2803,DAT(2),DAT(5),DAT(7),DAT(12),DAT(14),DAT(17)
46*     2803 FORMAT(3H V=,E17.3,4HST2=,E16.3,3HTO=,E17.3,6HTHRTR=,E14.3,
47*     13HRO=,E17.3,4HCTE=,E16.3)
48*     PRINT 2804,DAT(3),DAT(8)
49*     2804 FORMAT(6H BETA=,E8.3,26X,6HTWAIT=,E8.3)

```

```

50*      PRINT 2805,DAT(15),DAT(9)
51*      2805 FORMAT(3H A=,E17.3,20X,4HTWD=,E16.3)
52*      PRINT 2806,DAT(10)
53*      2806 FORMAT(40X,4HTRD=,E16.3)
54*      PRINT 2808,NDATA1,NDATA2
55*      2808 FORMAT(///2I4)
56*      PRINT 65,TIMMAX,JNREPT
57*      65  FORMAT(//10X,7HTIMMAX=,F10.3,4X,6HNREPT=,I7)
58*      C
59*      C
60*      PRINT 2701
61*      2701 FORMAT(5H1NSIM,4X,4HNRRAN,27X,4HTIME,5X,7HST.DEV.,2X,
62*      11HACTION TIME,2X,7HST.DEV.,4X,7HIMPULSE,4X,7HST.DEV.,
63*      24X,7HUNSUCC./)
64*      2922 CONTINUE
65*      KNRRAN(NSIM)=NRRAN
66*      NREPT=1
67*      NSWR=0
68*      DAT(NDATA1)=COMB(NSIM,1)
69*      DAT(NDATA2)=COMB(NSIM,2)
70*      2012 CONTINUE
71*      X=DAT(1)
72*      V=DAT(2)
73*      BETA=DAT(3)
74*      ST1=DAT(4)
75*      ST2=DAT(5)
76*      TF=DAT(6)
77*      T0=DAT(7)
78*      TWAIT=DAT(8)
79*      TWD=DAT(9)
80*      TRD=DAT(10)
81*      THRRD=DAT(11)
82*      THRTR=DAT(12)
83*      ALPHA=DAT(13)
84*      R0=DAT(14)
85*      A=DAT(15)
86*      CT=DAT(16)
87*      CTE=DAT(17)
88*      C
89*      C
90*      C
91*      Y=0.0
92*      Z=0.0
93*      VZ=0.0
94*      AX=0.0
95*      AY=0.0
96*      AZ=0.0
97*      T=0.0
98*      TIME=0.0
99*      TFUEL=0.0
100*     VX=V*COS(BETA*0.01745329252)
101*     VY=SQRT(V**2-VX**2)
102*     ALPH=ALPHA
103*     PHIO=1.0/R0
104*     V0=SQRT(2.0*A*R0)
105*     ID=0
106*     C

```

```

107* C
108* C
109* C
110* 2100 CONTINUE
111* IF(((X**2+Y**2+Z**2).LT.R0**2).AND.((VX**2+VY**2+VZ**2).LT.
112* 1V0**2)) GOTO 2820
113* 506 FORMAT(3E20.3,E20.8,15)
114* IF(ID.EQ.7) GOTO 2801
115* IF(TIME.GT.TIMMAX) GOTO 2801
116* CALL YIMAGE
117* CALL DECIS(PHI0,R0,ID)
118* CALL DECTIM(ID,PHI,DPHI,DTHET,T0,CT,TWD,TRD,T)
119* X=X+VX*T
120* Y=Y+VY*T
121* Z=Z+VZ*T
122* TIME=TIME+T
123* CALL YIMAGE
124* CALL DECIS(PHI0,R0,ID)
125* GOTO(2310,2320,2330,2340,2350,2360,2100),ID
126* C
127* C DECISION APPLY TRANSVERSAL FORCE
128* 2310 CONTINUE
129* ROOT1=AMODUL(X,Y,Z)
130* ROOT2=SQRT(VX**2*(Y**2+Z**2)+VY**2*(X**2+Z**2)+VZ**2*(X**2+
131* 1Y**2))*ROOT1
132* C COSINES DIRECTORS
133* A01=(VX*(Y**2+Z**2)-X*Y*VY-X*Z*VZ)/ROOT2
134* A02=(VY*(X**2+Z**2)-Y*X*VX-Y*Z*VZ)/ROOT2
135* A03=(VZ*(X**2+Y**2)-Z*X*VX-Z*Y*VY)/ROOT2
136* C ACCELERATION
137* AX=-A*RANORM(ST2,A01)
138* AY=-A*RANORM(ST2,A02)
139* AZ=-A*RANORM(ST2,A03)
140* C UPDATE
141* X=X+VX*TF+0.5*AX*TF**2
142* Y=Y+VY*TF+0.5*AY*TF**2
143* Z=Z+VZ*TF+0.5*AZ*TF**2
144* VX=VX+AX*TF
145* VY=VY+AY*TF
146* VZ=VZ+AZ*TF
147* TIME=TIME+TF
148* TFUEL=TFUEL+TF
149* IF(TIME.GT.TIMMAX) GOTO 2801
150* CALL YIMAGE
151* CALL DECIS(PHI0,R0,ID)
152* IF((ID.EQ.1).OR.(ID.EQ.4))GOTO 2310
153* GO TO 2390
154* C APPLY RADIAL FORCE TO APPROACH
155* 2320 CONTINUE
156* ROOT1=AMODUL(X,Y,Z)
157* C ACCELERATION
158* AX=-A*RANORM(ST2,X/ROOT1)
159* AY=-A*RANORM(ST2,Y/ROOT1)
160* AZ=-A*RANORM(ST2,Z/ROOT1)
161* C UPDATE
162* X=X+VX*TF+0.5*AX*TF**2
163* Y=Y+VY*TF+0.5*AY*TF**2

```

```

164*      Z=Z+VZ*TF+0.5*AZ*TF**2
165*      VX=VX+AX*TF
166*      VY=VY+AY*TF
167*      VZ=VZ+AZ*TF
168*      TIME=TIME+TF
169*      TFUEL=TFUEL+TF
170*      IF(TIME.GT.TIMMAX) GOTO 2801
171*      CALL YNAGE
172*      CALL DECIS(PHI0,R0,ID)
173*      507  FORMAT(10X,3E20.3,E20.8,I5)
174*      IF((ID.EQ.2).OR.(ID.EQ.5)) GOTO 2320
175*      GOTO 2390
176*      C   APPLY RADIAL FORCE TO RECEDE
177*      2330 CONTINUE
178*      ROOT1=AMODUL(X,Y,Z)
179*      C   ACCELERATION
180*      AX= A*RANORM(ST2,X/ROOT1)
181*      AY= A*RANORM(ST2,Y/ROOT1)
182*      AZ= A*RANORM(ST2,Z/ROOT1)
183*      C   UPDATE
184*      X=X+VX*TF+0.5*AX*TF**2
185*      Y=Y+VY*TF+0.5*AY*TF**2
186*      Z=Z+VZ*TF+0.5*AZ*TF**2
187*      VX=VX+AX*TF
188*      VY=VY+AY*TF
189*      VZ=VZ+AZ*TF
190*      TIME=TIME+TF
191*      TFUEL=TFUEL+TF
192*      IF(TIME.GT.TIMMAX) GOTO 2801
193*      CALL YNAGE
194*      CALL DECIS(PHI0,R0,ID)
195*      IF(ID.EQ.3) GOTO 2330
196*      GO TO 2390
197*      C   DECISION 4
198*      2340 CONTINUE
199*      IF(KTR4.GE.5) GOTO 2310
200*      KTR4=KTR4+1
201*      KTR5=0
202*      GOTO 2100
203*      C   DECISION 5
204*      2350 CONTINUE
205*      IF(KTR5.GE.5) GOTO 2320
206*      KTR5=KTR5+1
207*      KTR4=0
208*      GOTO 2100
209*      C   DECISION 6 WAIT TWAIT SECONDS
210*      2360 CONTINUE
211*      X=X+VX*TWAIT
212*      Y=Y+VY*TWAIT
213*      Z=Z+VZ*TWAIT
214*      TIME=TIME+TWAIT
215*      GOTO 2390
216*      C   RESET COUNTERS
217*      2390 KTR4=0
218*      KTR5=0
219*      GOTO 2100
220*      C   UNSUCCESSFUL RENDEZVOUS

```

```

221*      2801 NSWR=NSWR+1
222*          TIME=0.0
223*          TFUEL=0.0
224*          GOTO 2820
225*      C      RENDEZVOUS ACHIEVED
226*      2820 CONTINUE
227*          STIM(NREPT)=TIME
228*          SFUEL(NREPT)=TFUEL
229*          SFAT(NREPT)=TFUEL*A
230*          NREPT=NREPT+1
231*          IF(NREPT.LE.JNREPT) GOTO 2012
232*      C      ENDS A SIMULATION
233*          REPT=1.0/(JNREPT-NSWK)
234*          DO 2900 I=1,JNREPT
235*              SST=SST+3*STIM(I)
236*              SSF=SSF+SFUEL(I)
237*              SSA=SSA+SFAT(I)
238*      2900 CONTINUE
239*      C
240*      C
241*          SSTM=SST*REPT
242*          SSFM=SSF*REPT
243*          SSAM=SSA*REPT
244*      C
245*          DO 2901 I=1,JNREPT
246*              IF(STIM(I).LT.0.0001) GO TO 2902
247*              STQ=(STIM(I)-SSTM)**2+STQ
248*              SFQ=(SFUEL(I)-SSFM)**2+SFQ
249*              SAQ=(SFAT(I)-SSAM)**2+SAQ
250*      2902 CONTINUE
251*      2901 CONTINUE
252*      C
253*          STDT=SQRT(STQ*REPT)
254*          STDF=SQRT(SFQ*REPT)
255*          STDA=SQRT(SAQ*REPT)
256*          PAR1(NSIM)=DAT(NDATA1)
257*          PAR2(NSIM)=DAT(NDATA2)
258*          ART(NSIM)=SSTM
259*          AST(NSIM)=STDT
260*          ARF(NSIM)=SSFM
261*          ASF(NSIM)=STDF
262*          ARI(NSIM)=SSAM
263*          ASI(NSIM)=STDA
264*          KWRO(NSIM)=NSWR
265*          DO 2915 I=1,JNREPT
266*              STIM(I)=0.0
267*              SFUEL(I)=0.0
268*              SFAT(I)=0.0
269*      2915 CONTINUE
270*          SST=0.0
271*          SSF=0.0
272*          SSA=0.0
273*          STQ=0.0
274*          SFQ=0.0
275*          SAQ=0.0
276*          PRINT 2702,NSIM,KNRAN(NSIM),PAR1(NSIM),PAR2(NSIM),ART(NSIM),
277*          LAST(NSIM),ARF(NSIM),ASF(NSIM),ARI(NSIM),ASI(NSIM),KWRO(NSIM)

```



```

278*      2702 FORMAT(I4,I9,8F11.4,I8)
279*      NSIM=NSIM+1
280*      IF(NSIM.LE.JNSIM) GOTO 2922
281*      RETURN
282*      END

```

END OF COMPILATION: NO DIAGNOSTICS.

```

1*      SUBROUTINE YIMAGE
2*      COMMON/BL1/X,Y,Z,VX,VY,VZ,ALPHA,PHI,DPHI,DTHET,ST1
3*      DEN=1.0/(X**2+Y**2+Z**2)
4*      AUX1=ALPHA*SQRT(DEN)
5*      AUX2=-ALPHA*DEN*SQRT(DEN)*(X*VX+Y*VY+Z*VZ)
6*      AUX3=DEN*SQRT(VX**2*(Y**2+Z**2)+VY**2*(X**2+
7*      1Z**2)+VZ**2*(X**2+Y**2))
8*      PHI=RANORM(ST1*AUX1,AUX1)
9*      DPHI=RANORM(ST1*AUX2,AUX2)
10*     DTHET=RANORM(ST1*AUX3,AUX3)
11*     RETURN
12*     END

```

END OF COMPILATION: NO DIAGNOSTICS.

```

1*      SUBROUTINE DECTIM(ID,PHI,DPHI,DTHET,T0,CT,TWD,TRD,T
2*      COMMON/BL2/PHI0,V0,THRTR,THRRD,CTE,ALPH
3*      GOTO (1,2,3,1,3,6,7), ID
4*      1 T=T0*EXP(-CT*DTHET/(V0*PHI0))
5*      RETURN
6*      2 T=T0*EXP( CT*DPHI*ALPH/(PHI0*PHI0*V0))
7*      RETURN
8*      3 T=T0*EXP(-CT*DPHI*ALPH/(PHI0*PHI0*V0))
9*      RETURN
10*     6 T=TWD
11*     RETURN
12*     7 T=TRD
13*     RETURN
14*     END

```

END OF COMPILATION: NO DIAGNOSTICS.

```

1*      SUBROUTINE DECIS(PHI0,R0,ID)
2*      COMMON/BL1/ X,Y,Z,VX,VY,VZ,ALPHA,PHI,DPHI,DTHET,ST1
3*      ID=7
4*      IF((X**2+Y**2+Z**2).LT.(R0**2)) RETURN
5*      ID=3
6*      IF(DPHI.GT.ALIM1(PHI)) RETURN
7*      ID=1
8*      IF(DTHET.GT.ALIM4(PHI)) RETURN
9*      ID=2
10*     IF(DPHI.LT.0.0) RETURN
11*     ID=5
12*     IF(DPHI.LT.ALIM3(PHI)) RETURN
13*     ID=4
14*     IF(DTHET.GT.ALIM2(PHI)) RETURN
15*     ID=6
16*     RETURN
17*     END

```

END OF COMPILATION: NO DIAGNOSTICS.

```

1*      FUNCTION ALIM1(PHI)
2*      COMMON/BL2/ PHI0,V0,THRTR,THRRD,CTE,ALPH
3*      W=0.5*V0*PHI*SQRT(PHI0*PHI/ALPH)
4*      IF(W.LT.2.0*THRRD) W=2.0*THRRD
5*      ALIM1=W
6*      RETURN
7*      END

```

END OF COMPILATION: NO DIAGNOSTICS.

```

1*      FUNCTION ALIM2(PHI)
2*      COMMON/BL2/ PHI0,V0,THRTR,THRRD,CTE,ALPH
3*      Q=0.1*V0*PHI/ALPH
4*      IF(Q-THRTR)1,1,2
5*      1  ALIM2=THRTR
6*      RETURN
7*      2  ALIM2=Q
8*      RETURN
9*      END

```

END OF COMPILATION: NO DIAGNOSTICS.

```

1*      FUNCTION ALIM3(PHI)
2*      COMMON/BL2/ PHI0,V0,THRTR,THRRD,CTE,ALPH
3*      Q=0.5*V0*PHI*SQRT(PHI0*PHI/ALPH)/CTE
4*      IF(Q-THRRD)1,1,2
5*      1  ALIM3=THRRD
6*      RETURN
7*      2  ALIM3=Q
8*      RETURN
9*      END

```

END OF COMPILATION: NO DIAGNOSTICS.

```

1*      FUNCTION ALIM4(PHI)
2*      COMMON/BL2/ PHI0,V0,THRTR,THRRD,CTE,ALPH
3*      Q=0.1*V0*SQRT(PHI0*PHI/ALPH)
4*      IF(Q-THRTR)1,1,2
5*      1  ALIM4=THRTR
6*      RETURN
7*      2  ALIM4=Q
8*      RETURN
9*      END

```

END OF COMPILATION: NO DIAGNOSTICS.

```

1*      FUNCTION RANSQR(A,B)
2*      COMMON/BL3/NRAN
3*      NRAN=MOD(125*NRAN,2796203)
4*      RANSQR=(NRAN+0.5)*(B-A)/2796203.0+A
5*      RETURN
6*      END

```

END OF COMPILATION: NO DIAGNOSTICS.

```

1*      FUNCTION RANORM(SDEV,VALM)
2*      DATA TWOPI/6.28318530718/
3*      COMPLEX D
4*      VAR=SDEV**2
5*      D=CEXP(CMPLX(0.0,RANSQR(0.0,TWOPI)))*SQRT(-ALOG(RANSQR(0.0,
6*      11.0))*(VAR+VAR))
7*      RANORM=REAL(D)+VALM
8*      RETURN
9*      END

```

END OF COMPILATION: NO DIAGNOSTICS.

```

1*      SUBROUTINE GRAPH(P,IDENT,ID,XMAX,XORG,YMAX,YORG)
2*      C      THIS SUBROUTINE GIVES A PLOT OF THE ID POINTS WHOSE COORDINAT
3*      C      PROVIDED IN THE ARRAY P.
4*      C      THE AXES ARE CENTERED IN (XORG,YORG) AND XMAX, YMAX ARE THE U
5*      C      OF THE GRAPHIC.
6*      C      EACH POINT WILL BE PRINTED AS *,Q,X,..,A,B,C,D,E, OR F GIVI
7*      C      IDENTIFIER 0,1,2,3,4,5,6,7,8, OR 9 IN THE ARRAY IDENT.
8*      DIMENSION P(ID,2),IDENT(ID)
9*      DIMENSION P1(500,2),JS(121),IDENT1(500),AUX(500)
10*     AINTY=(YMAX-YORG)/25.0
11*     AINTX=(XMAX-XORG)/60.0
12*     JPOINT=1H*
13*     JBLANK=1H
14*     JONE=1HI
15*     JPLUS=1H+
16*     JMINUS=1H-
17*     JQQ=1HQ
18*     JAX=1HX
19*     JBX=1H.
20*     JA=1HA
21*     JB=1HB
22*     JC=1HC
23*     JD=1HD
24*     JE=1HE
25*     JF=1HF
26*     XMIN=2.0*XORG-XMAX
27*     YMIN=2.0*YORG-YMAX
28*     X12=XMIN+12.0*AINTX
29*     X24=XMIN+24.0*AINTX
30*     X36=XMIN+36.0*AINTX
31*     X48=XMIN+48.0*AINTX
32*     X61=XMIN+61.0*AINTX
33*     X72=XMIN+72.0*AINTX
34*     X84=XMIN+84.0*AINTX
35*     X96=XMIN+96.0*AINTX
36*     X108=XMIN+108.0*AINTX
37*     DO 49 I=1,ID
38*     AUX(I)=P(I,2)
39*     49  CONTINUE
40*     DO 48 I=1,500
41*     P1(I,1)=XMIN
42*     48  P1(I,2)=YMIN
43*     DO 4900 IL=1,ID
44*     AY=YMIN
45*     NY=1
46*     DO 4901 I=1,ID
47*     IF(P(I,2)-AY)4901,4902,4902
48*     4902 AY=P(I,2)
49*     NY=I
50*     4901 CONTINUE
51*     P1(IL,2)=AY
52*     P1(IL,1)=P(NY,1)
53*     IDENT1(IL)=IDENT(NY)
54*     P(NY,2)=YMIN
55*     4900 CONTINUE
56*     J=1
57*     DO 4903 I=1,ID
58*     IF((P1(I,1).GT.XMAX).OR.(P1(I,1).LT.XMIN).OR.(P1(I,2).GT.YMAX)
59*     CGOTO 4903

```

```

60*      P1(J,1)=P1(I,1)
61*      P1(J,2)=P1(I,2)
62*      IDENT1(J)=IDENT1(I)
63*      J=J+1
64*      4903 CONTINUE
65*      J=J-1
66*      PRINT 1
67*      1  FORMAT(1H1)
68*      DO 4904 I=1,121
69*      JS(I)=JBLANK
70*      4904 CONTINUE
71*      JS(61)=JONE
72*      IQ=1
73*      ILIN=1
74*      4905 IF(P1(IQ,2).LT.(YMAX-(ILIN-1)*AINTY)) GOTO 4915
75*      IF(IQ.GT.J) GOTO 4915
76*      KX=IFIX(((P1(IQ,1)-XMIN)/AINTX)+0.5)+1
77*      IKX=IDENT1(IQ)+1
78*      GO TO (4951,4950,4952,4953,4954,4955,4956,4957,4958,4959), IK
79*      4950 JS(KX)=JQQ
80*      GOTO 4970
81*      4951 JS(KX)=JPOINT
82*      GOTO 4970
83*      4952 JS(KX)=JAX
84*      GOTO 4970
85*      4953 JS(KX)=JBX
86*      GOTO 4970
87*      4954 JS(KX)=JA
88*      GOTO 4970
89*      4955 JS(KX)=JB
90*      GOTO 4970
91*      4956 JS(KX)=JC
92*      GOTO 4970
93*      4957 JS(KX)=JJ
94*      GOTO 4970
95*      4958 JS(KX)=JE
96*      GOTO 4970
97*      4959 JS(KX)=JF
98*      4970 IQ=IQ+1
99*      IF(ILIN.GE.52) GO TO 4920
100*     GO TO 4905
101*     4920 DO 4921 I=1,121
102*     P(I,2)=AUX(I)
103*     P1(I,1)=0.0
104*     P1(I,2)=0.0
105*     IDENT1(I)=0
106*     4921 CONTINUE
107*     PRINT 4940,AINTX,AINTY
108*     4940 FORMAT(62X,7HUNIT X=,E9.4/62X,7HUNIT Y=,E9.4)

```

```

109*      PRINT 1
110*      RETURN
111*      4915 IF(ILIN.EQ.26) GOTO 4907
112*          IF(MOD(ILIN-1,5).EQ.0) GOTO 4908
113*          IF(ILIN.EQ.27) GOTO 4909
114*      4906 PRINT 4910,(JS(L),L=1,121)
115*      5005 FORMAT(I10,4E15.4,2I10)
116*      4910 FORMAT(121A1)
117*      4911 ILIN=ILIN+1
118*          DO 4930 I=1,121
119*              JS(I)=JBLANK
120*      4930 CONTINUE
121*          JS(61)=JONE
122*          IF(ILIN.GE.52) GO TO 4920
123*          GO TO 4905
124*      4907 DO 4912 I1=1,121
125*          IF((JS(I1).EQ.JBLANK).OR.(JS(I1).EQ.JONE)) JS(I1)=JMINUS
126*      4912 CONTINUE
127*          DO 4931 I2=13,121,12
128*          IF(JS(I2).EQ.JMINUS) JS(I2)=JPLUS
129*      4931 CONTINUE
130*          GO TO 4906
131*      4908 YAX=YMAX-(ILIN-1)*AINTY
132*          PRINT 4913,(JS(L),L=1,53),YAX,(JS(L),L=61,121)
133*      4913 FORMAT(55A1,E7.2,61A1)
134*          GO TO 4911
135*      4909 PRINT 4914,XMIN,JS(8),JS(9),JS(10),X12,(JS(L),L=18,22),X24,
136*          1(JS(L),L=30,34),X36,(JS(L),L=42,46),X48,(JS(L),L=54,58),XORG,
137*          2(JS(L),L=66,70),X72,(JS(L),L=78,82),X84,(JS(L),L=90,94),X96,
138*          3(JS(L),L=102,106),X108,(JS(L),L=114,118),XMAX
139*      4914 FORMAT(E7.2,3A1,E7.2,9(5A1,E7.2))
140*          GO TO 4911
141*          END

```

END OF COMPILATION: NO DIAGNOSTICS.

```

1*      SUBROUTINE SIMFIT
2*
3*      C          GROUP 1 - NE2 LINES   TIME          VERSUS VAR1
4*      C          GROUP 2 - NE2 LINES   STD TIME      VERSUS VAR1
5*      C          GROUP 3 - NE2 LINES   RHO           VERSUS VAR1
6*      C          GROUP 4 - NE2 LINES   IMPULSE      VERSUS VAR1
7*      C          GROUP 5 - NE2 LINES   STD. IMPULSE VERSUS VAR 1
8*
9*      C          GROUP 6 - NE1 LINES   TIME VERSUS VAR 2
10*     C          GROUP 7 - NE1 LINES   STD. TIME VERSUS VAR2
11*     C          GROUP 8 - NE1 LINES   RHO VERSUS VAR2
12*     C          GROUP 9 - NE1 LINES   IMPULSE VERSUS VAR 2
13*
14*
15*
16*     COMMON/BL4/KNRAN,PAR1,PAR2,ART,AST,ARF,ASF,ARI,ASI,KWRO
17*     COMMON/BLS/NE1,NE2,ARR
18*     DIMENSION KNRAN(100),PAR1(100),PAR2(100),ART(100),AST(100)
19*     DIMENSION ARF(100),ASF(100),ARI(100),ASI(100),KWRO(100)
20*     DIMENSION ARR(10,2),AUX(100)
21*     DIMENSION X(10),Y(10)
22*     C          GROUPS WITH VAR 1
23*     PRINT 33
24*     33  FORMAT(/ /10X,12HVERSUS VAR 1/)
25*     NP=NE1*NE2
26*     DO 1 K=1,NE1
27*     1   X(K)=ARR(K,1)
28*     IL=1
29*
30*
31*     50  CONTINUE
32*     DO 10 I=1,NP
33*     10  AUX(I)=ART(I)
34*     ASSIGN 20 TO JUMP
35*     GO TO (100,200),IL
36*     20  DO 11 I=1,NP
37*     11  AUX(I)=AST(I)
38*     ASSIGN 21 TO JUMP
39*     GO TO (100,200),IL
40*     21  DO 12 I=1,NP
41*     12  AUX(I)=ART(I)/ARF(I)
42*     ASSIGN 22 TO JUMP
43*     GO TO (100,200),IL
44*     22  DO 13 I=1,NP
45*     13  AUX(I)=ARI(I)
46*     ASSIGN 23 TO JUMP
47*     GO TO (100,200),IL
48*     23  DO 14 I=1,NP
49*     14  AUX(I)=ASI(I)
50*     ASSIGN 24 TO JUMP
51*     GO TO (100,200),IL
52*     C          GROUPS WITH VAR 2
53*
54*     24  CONTINUE
55*     PRINT 34
56*     34  FORMAT(/ /10X,12HVERSUS VAR 2/)
57*     IF(IL.EQ.2) RETURN
58*     IL=2
59*     DO 5 K=1,NE2
60*     5   X(K)=ARR(K,2)
61*     GO TO 50

```

```

62*
63*
64*
65*   100  CONTINUE
66*       DO 2 I2=1,NE2
67*       DO 3 I1=1,NE1
68*       IN=(I1-1)*NE2+I2
69*       3  Y(I1)=AUX(IN)
70*       2  CALL FITLIN(NE1,X,Y)
71*       GO TO JUMP,(20,21,22,23,24)
72*
73*
74*
75*   200  CONTINUE
76*       DO 6 J=1,NE1
77*       DO 7 IA=1,NE2
78*       IN=IA+(J-1)*NE2
79*       7  Y(IA)=AUX(IN)
80*       6  CALL FITLIN(NE2,X,Y)
81*       GO TO JUMP,(20,21,22,23,24)
82*       END

```

END OF COMPILATION: NO DIAGNOSTICS.

```

1*   SUBROUTINE FITLIN(N,X,Y)
2*   C   PRINT Y=A1*X+A0 WHICH FITS BETTER THE N POINTS X,Y.
3*       DIMENSION X(10),Y(10),XY(10),X2(10)
4*       SX=0.0
5*       SY=0.0
6*       SXY=0.0
7*       SX2=0.0
8*       DO 1 I=1,N
9*       XY(I)=X(I)*Y(I)
10*      1  X2(I)=X(I)*X(I)
11*       DO 2 I=1,N
12*       SX=SX+X(I)
13*       SY=SY+Y(I)
14*       SXY=SXY+XY(I)
15*      2  SX2=SX2+X2(I)
16*       D=1.0/(N*SX2-SX*SX)
17*       A0=D*(SY*SX2-SX*SXY)
18*       A1=D*(N*SXY-SX*SY)
19*       PRINT 5,A1,A0
20*      5  FORMAT(10X,2HY=,E12.5,5H *X +,E12.5)
21*       RETURN
22*       END

```

END OF COMPILATION: NO DIAGNOSTICS.


```

1*      SUBROUTINE SIMGRA
2*      C          IT GIVES 10 GRAPHICS WITH SUBR. GRAFO
3*
4*      C          1.TIME VERSUS VAR1
5*      C          2.STD. TIME VERSUS VAR 1
6*      C          3.RHO VERSUS VAR 1
7*      C          4.IMPULSE VERSUS VAR 1
8*      C          5.STD. IMPULSE VERSUS VAR 1
9*      C
10*     C          6.TIME VERSUS VAR 2
11*     C          7.STD. TIME VERSUS VAR 2
12*     C          8.RHO VERSUS VAR 2
13*     C          9.IMPULSE VERSUS VAR 2
14*     C          10.STD. IMPULSE VERSUS VAR 2
15*
16*     COMMON/BL1/X,Y,Z,VX,VY,VZ,ALPHA,PHI,DPHI,DTHET,ST1
17*     COMMON/BL2/ PHIO,V0,THRTR,THRRD,CTE,ALPH
18*     COMMON/BL3/NRAN
19*     COMMON/BL4/KNRAN,PAR1,PAR2,ART,AST,ARF,ASF,ARI,ASI,KWRO
20*     COMMON/BL5/NE1,NE2,AKR
21*     DIMENSION KNRAN(100),PAR1(100),PAR2(100),ART(100),AST(100)
22*     DIMENSION ARF(100),ASF(100),ARI(100),ASI(100),KWRO(100)
23*     DIMENSION P(100,2),IDENT(100)
24*     READ 30,XM1,XO1
25*     READ 30,XM2,XO2
26*     READ 30,YMT,YOT
27*     READ 30,YMTD,YOTD
28*     READ 30,YMR,YOR
29*     READ 30,YMI,YOI
30*     READ 30,YMID,YOID
31*     30  FORMAT(2E10.3)
32*     CALL RENDEZ
33*     NP=NE1*NE2
34*     DO 1 I=1,NP
35*     P(I,2)=ART(I)
36*     P(I,1)=PAR1(I)
37*     1  IDENT(I)=MOD((I-1),NE2)
38*     CALL GRAFO(P,IDENT,NP,XM1,XO1,YMT,YOT)
39*     DO 3 I=1,NP
40*     3  P(I,2)=AST(I)
41*     CALL GRAFO(P,IDENT,NP,XM1,XO1,YMTD,YOTD)
42*     DO 5 I=1,NP
43*     5  P(I,2)=ART(I)/ARF(I)
44*     CALL GRAFO(P,IDENT,NP,XM1,XO1,YMR,YOR)
45*     DO 7 I=1,NP
46*     7  P(I,2)=ARI(I)
47*     CALL GRAFO(P,IDENT,NP,XM1,XO1,YMI,YOI)
48*     DO 9 I=1,NP
49*     9  P(I,2)=ASI(I)
50*     CALL GRAFO(P,IDENT,NP,XM1,XO1,YMID,YOID)
51*     DO 2 I=1,NP
52*     P(I,2)=ART(I)
53*     P(I,1)=PAR2(I)

```

```

54*   2   IDENT(I)=(I-1)/NE2
55*   CALL GRAFO(P,IDENT,NP,XM2,XO2,YMT,YOT)
56*   DO 4 I=1,NP
57*   4   P(I,2)=AST(I)
58*   CALL GRAFO(P,IDENT,NP,XM2,XO2,YMTD,YOTD)
59*   DO 6 I=1,NP
60*   6   P(I,2)=ART(I)/ARF(I)
61*   CALL GRAFO(P,IDENT,NP,XM2,XO2,YMR,YOR)
62*   DO 8 I=1,NP
63*   8   P(I,2)=ARI(I)
64*   CALL GRAFO(P,IDENT,NP,XM2,XO2,YMI,YOI)
65*   DO 10 I=1,NP
66*  10   P(I,2)=ASI(I)
67*   CALL GRAFO(P,IDENT,NP,XM2,XO2,YMID,YOID)
68*   RETURN
69*   END

```

END OF COMPILATION: NO DIAGNOSTICS.

```

1*   SUBROUTINE MATIN(A,B,N,DEL)
2*   C   MATRIX INVERSION BY ELIMINATION WITH PARTIAL PIVOTING
3*
4*   C   ORIGINAL MATRIX = A, INVERSE MATRIX = B
5*   DIMENSION A(N,N),B(N,N)
6*   EPS=0.0000001
7*
8*   C   CONSTRUCT IDENTITY MATRIX B(I,J)=I
9*   DO 6 I=1,N
10*  DO 5 J=1,N
11*  IF(I-J) 4,3,4
12*  3   B(I,J)=1.0
13*  GOTO 5
14*  4   B(I,J)=0.0
15*  5   CONTINUE
16*  6   CONTINUE
17*  DEL=1.0
18*
19*  C   LOCATE MAXIMUM MAGNITUDE A(I,K) ON OR BELOW MAIN DIAGONAL
20*  DO 45 K=1,N
21*  IF(K-N) 12,30,30
22*  12  IMAX=K
23*  AMAX=ABS(A(K,K))
24*  KP1=K+1
25*  DO 20 I=KP1,N
26*  IF(AMAX-ABS(A(I,K))) 15,20,20
27*  15  IMAX=I

```

```

28*      AMAX=ABS(A(I,K))
29*      20  CONTINUE
30*
31*      C          INTERCHANGE ROWS IMAX AND K IF IMAX NOT EQUAL TO K
32*      IF(IMAX-K) 25,30,25
33*      25  DO 29 J=1,N
34*          ATMP=A(IMAX,J)
35*          A(IMAX,J)=A(K,J)
36*          A(K,J)=ATMP
37*          BTMP=B(IMAX,J)
38*          B(IMAX,J)=B(K,J)
39*      29  B(K,J)=BTMP
40*      DEL=-DEL
41*      30  CONTINUE
42*
43*      C          TEST FOR SINGULAR MATRIX
44*      IF(ABS(A(K,K))-EPS) 93,93,35
45*      35  DEL=A(K,K)*DEL
46*
47*      C          DIVIDE PIVOT ROW BY ITS MAIN DIAGONAL ELEMENT
48*      DIV=A(K,K)
49*      DO 38 J=1,N
50*          A(K,J)=A(K,J)/DIV
51*      38  B(K,J)=B(K,J)/DIV
52*
53*      C          REPLACE EACH ROW BY LINEAR COMBINATION WITH PIVOT ROW
54*      DO 43 I=1,N
55*          AMULT=A(I,K)
56*          IF(I-K) 39,43,39
57*      39  DO 42 J=1,N
58*          A(I,J)=A(I,J)-AMULT*A(K,J)
59*          B(I,J)=B(I,J)-AMULT*B(K,J)
60*      42  CONTINUE
61*      43  CONTINUE
62*      99  RETURN
63*      93  PRINT 113,K
64*          GOTO 99
65*      113 FORMAT(25H SINGULAR MATRIX FOR K =, I2)
66*      END

```

END OF COMPILATION: NO DIAGNOSTICS.

```

1*      SUBROUTINE GRAFO(P,IDENT,ID,XMAX,XORG,YMAX,YORG)
2*      C      THIS SUBROUTINE GIVES A PLOT OF THE ID POINTS WHOSE COORDIN
3*      C      PROVIDED IN THE ARRAY P.
4*      C      THE AXES ARE CENTERED IN (XORG,YORG) AND XMAX, YMAX ARE THE
5*      C      OF THE GRAPHIC.
6*      C      EACH POINT WILL BE PRINTED AS *,Q,X,..,A,B,C,D,E, OR F GI
7*      C      IDENTIFIER 0,1,2,3,4,5,6,7,8, OR 9 IN THE ARRAY IDENT.
8*      DIMENSION P(100,2),IDENT(100)
9*      DIMENSION P1(500,2),JS(130),IDENT1(500),AUX(500)
10*     AINTY=(YMAX-YORG)/50.0
11*     AINTX=(XMAX-XORG)/120.0
12*     JPOINT=1H*
13*     JBLANK=1H
14*     JONE=1HI
15*     JPLUS=1H+
16*     JMINUS=1H-
17*     JOO=1HQ
18*     JAX=1HX
19*     JBX=1H.
20*     JA=1HA
21*     JB=1HB
22*     JC=1HC
23*     JD=1HD
24*     JE=1HE
25*     JF=1HF
26*     XMIN=XORG
27*     YMIN=YORG
28*     X12=XMIN+12.0*AINTX
29*     X24=XMIN+24.0*AINTX
30*     X36=XMIN+36.0*AINTX
31*     X48=XMIN+48.0*AINTX
32*     X61=XMIN+60.0*AINTX
33*     X72=XMIN+72.0*AINTX
34*     X84=XMIN+84.0*AINTX
35*     X96=XMIN+96.0*AINTX
36*     X108=XMIN+108.0*AINTX
37*     DO 49 I=1, ID
38*     AUX(I)=P(I,2)
39*     P1(I,2)=YMIN
40*     49 CONTINUE
41*     DO 4900 IL=1, ID
42*     AY=YMIN
43*     NY=1
44*     DO 4901 I=1, ID
45*     IF(P(I,2)-AY)4901,4902,4902
46*     4902 AY=P(I,2)
47*     NY=I
48*     4901 CONTINUE
49*     P1(IL,2)=AY
50*     P1(IL,1)=P(NY,1)
51*     IDENT1(IL)=IDENT(NY)
52*     P(NY,2)=YMIN

```

```

55* 4900 CONTINUE
56*     J=1
57*     DO 4903 I=1, ID
58*         IF((P1(I,1).GT.XMAX).OR.(P1(I,1).LT.XMIN).OR.(P1(I,2).GT.YMAX)
59*           CGOTO 4903
60*         P1(J,1)=P1(I,1)
61*         P1(J,2)=P1(I,2)
62*         IDENT1(J)=IDENT1(I)
63*         J=J+1
64* 4903 CONTINUE
65*     J=J-1
66*     PRINT 1
67*     1  FORMAT(1H1)
68*     DO 4904 I=1, IZ1
69*         JS(I)=JBLANK
70* 4904 CONTINUE
71*     JS(9)=JONE
72*     IQ=1
73*     ILIN=1
74* 4905 IF(P1(IQ,2).LT.(YMAX-(ILIN-1)*AINTY)) GOTO 4915
75*     IF(IQ.GT.J) GOTO 4915
76*     KX=IFIX(((P1(IQ,1)-XMIN)/AINTX)+0.5)+9
77*     IKX=IDENT1(IQ)+1
78*     GO TO (4951,4950,4952,4953,4954,4955,4956,4957,4958,4959), IKX
79* 4950 JS(KX)=JQQ
80*     GOTO 4970
81* 4951 JS(KX)=JPOINT
82*     GOTO 4970
83* 4952 JS(KX)=JAX
84*     GOTO 4970
85* 4953 JS(KX)=JbX
86*     GOTO 4970
87* 4954 JS(KX)=JA
88*     GOTO 4970
89* 4955 JS(KX)=JB
90*     GOTO 4970
91* 4956 JS(KX)=JC
92*     GOTO 4970
93* 4957 JS(KX)=JD
94*     GOTO 4970
95* 4958 JS(KX)=JE
96*     GOTO 4970
97* 4959 JS(KX)=JF
98*     IQ=IQ+1
99*     IF(ILIN.GE.52) GO TO 4920
100*    GO TO 4905
101* 4920 CONTINUE
102*    PRINT 914, XORG, X12, X24, X36, X48, X61, X72, X84, X96, X108, XMAX
103*    914  FORMAT(11E12.3)
104*    DO 4921 I=1, ID
105*        P(I,2)=AUX(I)
106*        P1(I,1)=0.0
107*        P1(I,2)=0.0

```

```

106*      IDENT1(I)=0
107*      4921 CONTINUE
108*      PRINT 4940, A1, TX, AINTY
109*      4940 FORMAT(62X, 7HUNIT X=, E9.4/62X, 7HUNIT Y=, E9.4)
110*      PRINT 1
111*      RETURN
112*      4915 IF(ILIN.EQ.51) GOTO 4907
113*      IF(MOD(ILIN-1,5).EQ.0) GOTO 4908
114*      4906 PRINT 4910, (JS(L), L=1, 130)
115*      5005 FORMAT(I10, 4E15.4, 2I10)
116*      4910 FORMAT(130A1)
117*      4911 ILIN=ILIN+1
118*      DO 4930 I=1, 130
119*      JS(I)=JBLANK
120*      4930 CONTINUE
121*      JS(9)=JONE
122*      IF(ILIN.GE.52) GO TO 4920
123*      GO TO 4905
124*      4907 DO 4912 I1=9, 130
125*      IF((JS(I1).EQ.JBLANK).OR.(JS(I1).EQ.JONE)) JS(I1)=JMINUS
126*      4912 CONTINUE
127*      DO 4931 I2=9, 130, 12
128*      IF(JS(I2).EQ.JMINUS) JS(I2)=JPLUS
129*      4931 CONTINUE
130*      GO TO 4905
131*      4908 YAX=YMAX-(ILIN-1)*AINTY
132*      PRINT 913, YAX, (JS(L), L=9, 130)
133*      913  FORMAT(E6.2, 122A1)
134*      GO TO 4911
135*      END

```

END OF COMPILATION: NO DIAGNOSTICS.